



UNIVERSITÀ DI PARMA

UNIVERSITÀ DEGLI STUDI DI PARMA

DOTTORATO DI RICERCA IN
SCIENZA E TECNOLOGIA DEI MATERIALI

CICLO XXXI

Supramolecular and adaptable covalent
polyethylene networks

Coordinatore:

Prof. Enrico Dalcanale

Tutore:

Prof. Enrico Dalcanale

Dr. Maria Soliman

Dottorando: Arkadiusz Zych

Anni 2015/2018



سابك
SABIC

This work was supported by the Marie Skłodowska Curie project: SUPRAMolecular polyolefins as oxygen BARRIER materials (SUPRABARRIER), which is funded through the European Union Horizon 2020 Program (H2020-MSCA-ITN-2014) under the Grant Agreement No. 642929.

The financial support from SABIC is gratefully acknowledged.

List of abbreviations

¹H NMR	proton nuclear magnetic resonance
A	acceptor
AP	1-aminopyrene
BIF	barrier improvement factor
D	donor
Đ_M	dispersity of molecular weight
DBTDL	dibutyltin dilaurate
DCM	dichloromethane
DMSO	dimethyl sulfoxide
DMTA	dynamical mechanical thermal analysis
DSC	differential scanning calorimetry
EA	ethanolamine
EP	ethylene/propylene rubber
EVA	ethylene vinyl acetate
EVOH	ethylene vinyl alcohol
FT-IR	Fourier transformed infrared spectroscopy
HDI	hexamethylene diisocyanate
HDPE	high density polyethylene
HEMA	hydroxyethyl methacrylate
IE	fluorescence intensity of an excimer
IM	fluorescence intensity of a monomer

IPR-UPy	2-(6-isocyanatohexylaminocarbonylamino)-6-isopropyl-4[1H]pyrimidinone
LDPE	low density polyethylene
LLDPE	linear low density polyethylene
MAH	maleic anhydride
MIP	1-methylisocyanatopyrene
M_n	number average molecular weight
mol%	molar percentage
M_w	weight average molecular weight
NAPY	2,7-diamido-1,8-naphthyridine
-OH	hydroxy group
OP	oxygen permeability
PA	polyamide
PBT	polybutylene terephthalate
PE	polyethylene
PEX	crosslinked polyethylene
PP	polypropylene
REX	reactive extrusion
RH	relative humidity
ROMP	ring opening metathesis polymerization
RPM	revolutions per minute
RT	room temperature
SEC	size exclusion chromatography
TCE	tetrachloroethane
TGA	thermogravimetric analysis

T_m	melting temperature
TMSPEDA	N,N'-Bis[3-(trimethoxysilyl)propyl] ethylenediamine
T_β	β transition temperature
UHMWPE	ultra high molecular weight polyethylene
UPy	2-(6-isocyanatohexylaminocarbonylamino)-6-methyl-4[1H]pyrimidinone
UV	ultra violet
VLDPE	very low density polyethylene
WLF	Williams-Landel-Ferry
wt%	weight percentage
WVP	water vapor permeability
X_{cr}	degree of crystallinity

Table of contents

Summary	1
Chapter 1 Introduction	5
1.1 References	9
Chapter 2 Ureidopyrimidinone functionalized polyethylene	12
2.1 Introduction	13
2.2 Results and discussion	19
2.2.1 UPy grafting onto functionalized PE	19
2.2.2 Thermal stability of PEs grafted with UPy.	24
2.2.3 Rheological characterization.	28
2.2.4 Mechanical properties.	31
2.3 Conclusions	35
2.4 Experimental section	36
2.5 Appendix	41
2.6 References	54
Chapter 3 Pyrene functionalized polyethylene	63
3.1 Introduction	64
3.2 Results and discussion	67
3.2.1 AP reactive extrusion grafting onto PE-MAHs	67
3.2.2 PE-MAH-AP fluorescent characterization	70

3.3	Conclusions	73
3.4	Experimental section	74
3.5	Appendix	77
3.6	References	83
Chapter 4 Barrier properties of ureidopyrimidinone and pyrene functionalized polyethylene		86
4.1	Introduction	87
4.2	Results and discussion	92
4.2.1	Oxygen and water vapor permeability of PE-HEMA-UPy	93
4.2.2	Oxygen and water vapor permeability of PE-HEMA-MIP	97
4.3	Conclusions	100
4.4	Experimental section	101
4.5	Appendix	103
4.6	References	105
Chapter 5 Silyl ether polyethylene vitrimers		106
5.1	Introduction	107
5.2	Results and discussion	116
5.2.1	Crosslinking of PE-HEMA with TMSPEDA dynamic crosslinker <i>via</i> reactive extrusion.	116
5.2.2	Rheological characterization.	120
5.2.3	Mechanical properties.	121
5.3	Conclusions	125

5.4	Experimental section	126
5.5	Appendix	128
5.6	References	136
Chapter 6	Conclusions and outlook	141
	Acknowledgements	145
	Curriculum Vitae	146
	List of publications and patents	147

Summary

Polyethylene (PE) is the most widely used commodity thermoplastic due to its good solvent resistance, excellent flexibility, low cost and ease of processing. It finds application in common objects like plastic bags, packaging, automotive, medicine, aerospace and electronics.^{1,2} However, its use is limited by low melting point, stress cracking and poor wear resistance. To overcome those issues and expand its applications, crosslinking of polyethylene is used. Crosslinking forms a high molecular weight network, which improves impact strength, stress cracking resistance, creep and abrasion resistance without altering significantly tensile strength and density.^{3,4}

Despite the numerous advantages of crosslinked polyethylene (PEX) and its wide applications, recycling is a major drawback. Because of the crosslinking, PEX does not flow after melting and cannot be reprocessed like a thermoplastic. Most of the PEX waste is currently landfilled or incinerated which is a major problem both for the environment as well as for a recovery of valuable materials.^{5,6}

PE network that could be de-crosslinked at will or crosslinked using dynamic covalent crosslinkers would be easy to process and recycle while keeping benefits of PEX. The objective of this thesis is to explore properties and potential applications of PE crosslinked using physical or dynamic covalent crosslinkers.

Chapter 2 is focused on ureidopyrimidinone (UPy) functionalized polyethylene with enhanced mechanical properties. UPy was readily introduced into various PEs bearing hydroxy groups by solution grafting, affording physically crosslinked PE *via* supramolecular interactions. Utilizing low melting UPy where its methyl group is substituted with the isopropyl one (isopropyl UPy, IPR-UPy), reactive extrusion process was developed that allowed to significantly shorten the reaction time and eliminate the use of solvents and catalysts. Chemical structures were confirmed by Fourier transform infrared spectroscopy (FT-IR) and proton nuclear magnetic resonance (^1H NMR). Differential scanning calorimetry (DSC), rheology and dynamical mechanical thermal analysis (DMTA) were employed to investigate thermal stability of the obtained polymers and revealed that UPy functionalized PE can be safely processed using techniques like compression molding and extrusion below 150 °C. Introduction of UPy significantly improved mechanical properties and altered rheology showing that quadruple hydrogen bonding interactions are present both in the solid state and in the PE melt up to 150 °C after which UPy starts to degrade before it can dissociate.

The development of pyrene grafted polyethylene as a strain detector is described in Chapter 3. High density and very low density polyethylene-*graft*-maleic anhydride (HDPE-MAH and VLDPE-MAH respectively) functionalized with 1-aminopyrene (AP) were prepared *via* reactive extrusion. The resulting strain-reporting PE retains similar mechanical, thermal and rheological properties to that of the starting PE-MAH materials. Fluorescent emission spectroscopy revealed pronounced

changes in fluorescent behavior under stress due to the breakup of the pyrene excimers. For HDPE-MAH-AP this change was very sudden with a clear drop of excimer content (I_E/I_M) of around 50 % due to necking of the material stretched above 50 % strain. In contrast, VLDPE-MAH-AP showed no necking and a linear decrease of I_E/I_M ratio down to around 30 % when elongation up to 1100 % strain was reached while HDPE-MAH-AP broke after 200 % strain.

Oxygen and water vapor barrier properties of PE-HEMA functionalized with UPy (ureidopyrimidinone) or MIP (1-methylisocyanatopyrene) are investigated in Chapter 4. Functionalization of PE-HEMA1 with 2.2 mol% of UPy decreased OP (oxygen permeability) by about 30 % at 23 °C and 0 % RH (relative humidity) and about 25 % at 38 °C and 50 % RH and WVP (water vapor permeability) by about 25 %. When 1.2 mol% of MIP was introduced into PE-HEMA1, OP was decreased by about 35 % at 23 °C and 0 % RH and about 30 % at 38 °C and 50 % RH and WVP by about 40 %. Despite the achieved improvements the samples did not performed as well as the commercially available EVOH based multilayer structure used as a reference.

Synthesis and characterization of polyethylene silyl ether vitrimers is discussed in Chapter 5. PE was dynamically crosslinked directly *via* reactive extrusion using commercially available N,N'-Bis[3-(trimethoxysilyl)propyl] ethylenediamine (TMSPEDA). This fast and efficient process allowed to produce PE vitrimers without any synthetic effort or use of any solvent which makes it environmentally friendly and easy to upscale. Dynamic crosslinking transformed thermoplastic PE into an elastic solid with greatly improved melt strength as revealed by DMTA and rheology. Mechanical properties could be tuned by varying the amount of TMSPEDA crosslinker. All prepared

vitrimers were insoluble in xylene and were not affected by moisture, demonstrating crosslinked character and excellent solvent and hydrolysis resistance. Despite the crosslink nature dynamic silyl ether exchange enabled processability and recyclability of this system.

References

1. Kaminsky, W., *Polyolefins: 50 Years after Ziegler and Natta Ii*. Springer: 2013.
2. Vasile, C., *Handbook of Polyolefins*. CRC Press: 2000.
3. Ghosh, P., *Polymer Science and Technology*. Tata McGraw-Hill Education: 1990.
4. Platzer, N., *Encyclopedia of Polymer Science and Engineering*. Wiley: 1986.
5. Shang, L.; Wang, S.; Zhang, Y.; Zhang, Y. Pyrolyzed Wax from Recycled Cross-Linked Polyethylene as Warm Mix Asphalt (Wma) Additive for Sbs Modified Asphalt. *Constr. Build. Mater.* **2011**, *25*, 886-891.
6. Lee, H.-s.; Jeong, J. H.; Cho, H.-K.; Koo, C. M.; Hong, S. M.; Kim, H.; Lee, Y.-W. A Kinetic Study of the Decross-Linking of Cross-Linked Polyethylene in Supercritical Methanol. *Polym. Degrad. Stab.* **2008**, *93*, 2084-2088.

Chapter 1

Introduction

Polyethylene¹ (PE) is the most widely used commodity thermoplastic due to its good solvent resistance, excellent flexibility, low cost and ease of processing. It finds application in common objects like plastic bags, packaging automotive, medicine, aerospace and electronics.^{2,3} However, its use is limited by low melting point, stress cracking and poor wear resistance. To overcome those issues and expand its applications crosslinking of polyethylene is used. All types of polyethylene can be crosslinked including high density polyethylene (HDPE), low density polyethylene (LDPE), linear low density polyethylene (LLDPE) and ultra high molecular weight polyethylene (UHMWPE) however, branched structure is more suitable for crosslinking.⁴ Crosslinking forms a high molecular weight network, which improves impact strength, stress cracking resistance, creep and abrasion resistance without altering significantly tensile strength and density.⁵ Crosslinked polyethylene (PEX) is produced using either chemical or physical methods (Figure 1).

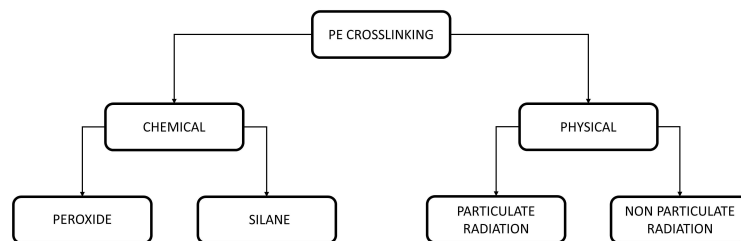


Figure 1. Methods of PE crosslinking

Chemical methods consist of peroxide initiated crosslinking or crosslinking *via* silane functionalization and hydrolysis. Peroxide process is based on the decomposition of a peroxide and the reaction of free radicals. The crosslinking occurs during the extrusion process in the molten state and is mainly used for the production of HDPE pipes.⁶⁻⁸ Silanes used for crosslinking contain vinyl groups for grafting onto PE backbone and alkoxy groups that can undergo hydrolysis and condensation forming crosslinks between the PE chains. In the first step PE containing silanes is produced either by high pressure copolymerization of ethylene with vinyl silane or by radical grafting. Subsequently, silane functionalized PE is processed with a suitable condensation catalyst like dibutyltin dilaurate (DBTDL) and can be extruded or injection molded before the crosslinking proceeds to completion. It is also possible to introduce the silane moieties and crosslink them in a one step process.⁹⁻¹¹

Physical methods typically do not require addition of any chemicals since free radicals are generated by high energy radiation. Crosslinks are created when two chains with free radicals meet together. Radiation induced crosslinking can be carried out using particulate or non-particulate radiations however, only non-particulate radiation sources are used for commercial crosslinking. Although microwave crosslinking is independent of the part thickness and can be used for parts of any size, only components containing polar groups are excitable in this field. Crosslinking of polyethylene using microwave radiation is very difficult and requires polar additives such as carbon black, peroxide, metallic powders etc.¹² Electron beam radiation is mainly used for thin wall products such as films and shrinkable insulating

parts because it can penetrate only up to few centimeters of thermoplastic polymers. The crosslinking of molded parts having thick walls results in a variable crosslink density.¹³ Crosslinking by UV radiation requires a use of photo-initiators such as benzophenone, and benzyl dimethyl ketal. The process is very slow and UV radiation penetrates only few millimeters therefore, UV light is suitable for crosslinking of thin parts only.¹⁴⁻¹⁶

PEX is currently commercially used in a broad range of applications such as civil engineering, electric and electronic fields, medicine and the packaging industry. One of the most important applications of PEX are hot water pipes for under floor or central heating and domestic or portable water piping systems. PEX pipes are an economic and lightweight alternative for copper and cement ones. Such material provides resistance to chemical and electrochemical corrosion, low encrustation tendency, long-term pressure resistance and noise dampening properties while being light, flexible, and easy to transport and install.¹⁷⁻²⁰ PEX finds also applications in the electrical cable industry. Crosslinking does not compromise the dielectric properties of polyethylene while providing good creep resistance. This allows for higher conductor operating temperature and reduces the risk of short circuit and required overload protection.²¹⁻²⁴ Polyethylene biomaterials remain the material of choice for artificial joint replacements like knee arthroplasty or artificial hip replacements. For that application, crosslinking of ultra high molecular weight polyethylene (UHMWPE) is utilized to minimize wear, particle generation and prolong the material lifetime.²⁵⁻²⁹ Specially molded articles such as containers made of crosslinked polyethylene provide improved solvent and creep resistance. Moreover, the increased dimensional

stability at elevated temperatures allows the article to come in contact with heated fluids.³⁰ Crosslinked polyethylene is used in packaging multi-layer film constructions to increase temperature resistance especially for hot filled or heat sterilization applications, heat seal strength, impact as well as tear and abuse resistance.³¹⁻³³

Despite the numerous advantages of PEX and its wide applications recycling is a major drawback. Because of the permanent covalent crosslinking, PEX does not flow after melting and cannot be reprocessed like a thermoplastic. Most of the PEX waste is currently landfilled or incinerated which is a major problem both for the environment as well as for a recovery of valuable materials.^{34,35}

The objective of this thesis is to explore properties and potential applications of PE crosslinked using reversible supramolecular or dynamic adaptable covalent crosslinkers. Such crosslinked PE would allow for easy processing and recycling keeping benefits of PEX. To achieve this aim, supramolecular polymer chemistry was employed. Non covalent interactions like pyrene π - π stacking and ureidopyrimidinone quadruple hydrogen bonding were incorporated into PE as physical crosslinks. Strength of those interactions gets weaker with increasing temperature which allows for thermoplastic like processing at elevated temperatures. Alternatively, covalent crosslinking based on dynamic reactions between trimethoxysilyl and hydroxy groups was employed to create silyl ether PE vitrimers. Those materials with dynamic crosslinks exhibit high dimensional stability and creep resistance at service temperatures, while maintaining processability at elevated temperatures.

1.1 References

1. Aaltonen, P.; Löfgren, B. Functionalization of Polyethylenes Via Metallocene/Methylaluminoxane Catalyst. *Eur. Polym. J.* **1997**, *33*, 1187-1190.
2. Kaminsky, W., *Polyolefins: 50 Years after Ziegler and Natta Ii*. Springer: 2013.
3. Vasile, C., *Handbook of Polyolefins*. CRC Press: 2000.
4. Anbarasan, R.; Babot, O.; Maillard, B. Crosslinking of High-Density Polyethylene in the Presence of Organic Peroxides. *J. Appl. Polym. Sci.* **2004**, *93*, 75-81.
5. Ghosh, P., *Polymer Science and Technology*. Tata McGraw-Hill Education: 1990.
6. Gedde, U.; Ifwarson, M. Molecular Structure and Morphology of Crosslinked Polyethylene in an Aged Hot-Water Pipe. *Polym. Eng. Sci.* **1990**, *30*, 202-210.
7. Sperling, L. H., *Introduction to Physical Polymer Science*. John Wiley & Sons: 2005.
8. Narkis, M.; Raiter, I.; Shkolnik, S.; Siegmantz, A.; Eyerer, P. Structure and Tensile Behavior of Irradiation and Peroxide-Crosslinked Polyethylenes. *J. Macromol. Sci., Phys.* **1987**, *26*, 37-58.
9. Shah, G. B.; Fuzail, M.; Anwar, J. Aspects of the Crosslinking of Polyethylene with Vinyl Silane. *J. Appl. Polym. Sci.* **2004**, *92*, 3796-3803.
10. Beltraán, M.; Mijangos, C. Silane Grafting and Moisture Crosslinking of Polypropylene. *Polym. Eng. Sci.* **2000**, *40*, 1534-1541.
11. Shieh, Y.-T.; Hsiao, K.-I. Thermal Properties of Silane-Grafted Water-Crosslinked Polyethylene. *J. Appl. Polym. Sci.* **1998**, *70*, 1075-1082.
12. Narkis, M.; Miltz, J. Chemically Crosslinked High-Density Polyethylene. *J. Appl. Polym. Sci.* **1969**, *13*, 713-720.
13. Badr, Y.; Ali, Z. I.; Zahran, A. H.; Khafagy, R. M. Characterization of Gamma Irradiated Polyethylene Films by Dsc and X-Ray Diffraction Techniques. *Polym. Int.* **2000**, *49*, 1555-1560.

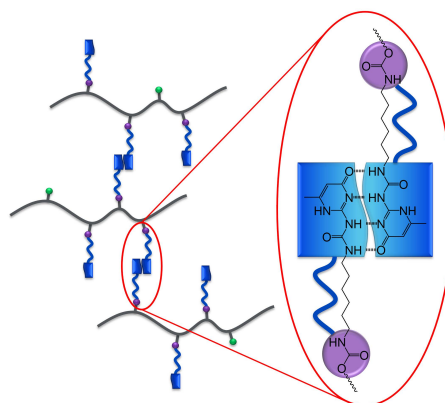
14. Mitsui, H.; Hosoi, F.; Ushirokawa, M. Effect of Double Bonds on the Γ -Radiation-Induced Crosslinking of Polyethylene. *J. Appl. Polym. Sci.* **1975**, *19*, 361-369.
15. Wu, Q.; Qu, B. Photoinitiating Characteristics of Benzophenone Derivatives as New Initiators in the Photocrosslinking of Polyethylene. *Polym. Eng. Sci.* **2001**, *41*, 1220-1226.
16. Ivanov, V. a. c. S., *Radiation Chemistry of Polymers*. Vsp: 1992.
17. Pakkanen, A.; Palmlof, M.; Oderkerk, J. Cross-Linked Polyethylene Pipe. US20110318516A1, 2011.
18. Viebke, J.; Elble, E.; Ifwarson, M.; Gedde, U. Degradation of Unstabilized Medium-Density Polyethylene Pipes in Hot-Water Applications. *Polym. Eng. Sci.* **1994**, *34*, 1354-1361.
19. Munier, C.; Gaillard-Devaux, E.; Tcharkhtchi, A.; Verdu, J. Durability of Cross-Linked Polyethylene Pipes under Pressure. *J. Mater. Sci.* **2002**, *37*, 4159-4163.
20. Viebke, J.; Gedde, U. Assessment of Lifetime of Hot-Water Polyethylene Pipes Based on Oxidation Induction Time Data. *Polym. Eng. Sci.* **1998**, *38*, 1244-1250.
21. Thue, W. A., *Electrical Power Cable Engineering*. CRC Press: 2016.
22. Priaroggia, P. G. Electric Cable. US3580987A, 1971.
23. Yamanouchi, S.; Inoue, Y.; Kondo, M. Cross-Linked Polyethylene-Insulated Cable. US4894284A, 1990.
24. Bartnikas, R.; Srivastava, K., *Power and Communication Cables*. McGraw-Hill Companies: 2000.
25. Kurtz, S. M., *Uhmwpe Biomaterials Handbook: Ultra High Molecular Weight Polyethylene in Total Joint Replacement and Medical Devices*. Academic Press: 2009.
26. Kurtz, S. M.; Muratoglu, O. K.; Evans, M.; Edidin, A. A. Advances in the Processing, Sterilization, and Crosslinking of Ultra-High Molecular Weight Polyethylene for Total Joint Arthroplasty. *Biomaterials* **1999**, *20*, 1659-1688.

27. McKellop, H.; Shen, F. W.; Lu, B.; Campbell, P.; Salovey, R. Development of an Extremely Wear-Resistant Ultra High Molecular Weight Polyethylene for Total Hip Replacements. *J. Orthop. Res.* **1999**, *17*, 157-167.
28. Dumbleton, J. H.; D'Antonio, J. A.; Manley, M. T.; Capello, W. N.; Wang, A. The Basis for a Second-Generation Highly Cross-Linked Uhmwpe. *Clin. Orthop. Relat. Res.* **2006**, *453*, 265-271.
29. Kurtz, S. M.; Villarraga, M. L.; Herr, M. P.; Bergström, J. S.; Rimnac, C. M.; Edidin, A. A. Thermomechanical Behavior of Virgin and Highly Crosslinked Ultra-High Molecular Weight Polyethylene Used in Total Joint Replacements. *Biomaterials* **2002**, *23*, 3681-3697.
30. Yagi, K.; Mantoku, H. Process for Preparation of Molecularly Oriented, Silane-Crosslinked Ultra-High-Molecular-Weight Polyethylene Molded Article. US4902460A, 1990.
31. Itaba, Y.; Izawa, M.; Saito, K.; Kondo, T. Heat-Sealable Crosslinked Oriented Polyethylene Film and Production Thereof. US5185203A, 1993.
32. Harbourne, D. A. Manufacture of Film from Partially Crosslinked Polyethylene. US 4226905A, 1980.
33. Doi, S.; Isaka, T.; Iida, S. Laminate Films and Sheets of Crosslinked Polyethylene Resins. US4351876A, 1982.
34. Shang, L.; Wang, S.; Zhang, Y.; Zhang, Y. Pyrolyzed Wax from Recycled Cross-Linked Polyethylene as Warm Mix Asphalt (Wma) Additive for Sbs Modified Asphalt. *Constr. Build. Mater.* **2011**, *25*, 886-891.
35. Lee, H.-s.; Jeong, J. H.; Cho, H.-K.; Koo, C. M.; Hong, S. M.; Kim, H.; Lee, Y.-W. A Kinetic Study of the Decross-Linking of Cross-Linked Polyethylene in Supercritical Methanol. *Polym. Degrad. Stab.* **2008**, *93*, 2084-2088.

Chapter 2

Ureidopyrimidinone functionalized polyethylene^a

Ureidopyrimidinone (UPy) was readily introduced into various PEs bearing hydroxy groups by solution grafting, affording physically crosslinked PE via supramolecular interactions. Utilizing low melting UPy where its methyl group is substituted with the isopropyl one (isopropyl



UPy, IPR-UPy), reactive extrusion process was developed allowing to significantly shorten the reaction time and eliminate the use of solvents and catalysts. Chemical structures were confirmed by Fourier transform infrared spectroscopy (FT-IR) and proton nuclear magnetic resonance (¹H NMR). Thermal stability revealed that UPy functionalized PE can be safely processed using techniques like compression molding and extrusion below 150 °C. Introduction of UPy moieties significantly improved mechanical properties and altered rheology showing that quadruple hydrogen bonding interactions are present both in the solid state and in the PE melt up to 150 °C after which UPy starts to degrade before it can dissociate.

^a The content of this chapter is covered by the patent application: Zych, J. Tellers, M. Soliman, R. Pinalli, J. Vachon, E. Dalcanale, Gas barrier film, 16POLY0166 and is being prepared to be submitted for publication: A. Zych, A. Verdelli, M. Soliman, R. Pinalli, J. Vachon, E. Dalcanale, Reactive extrusion of ureidopyrimidinone functionalized polyethylene with enhanced mechanical properties.

2.1 Introduction

Synthetic polymers have been extensively used for over a hundred years since the introduction of the first synthetic polymer by Leo Hendrik Baekeland. They are built from small organic molecules - monomers, covalently bonded into a long chain - polymer. Those conventional polymers have excellent mechanical properties but high melt viscosities due to the chain entanglements. Therefore, high temperatures and pressures are required for the processing of those polymers.

In 1878 Louise Henry proposed the idea of molecular polymerization by associative interactions and later Lehn and coworkers synthesized the first main-chain supramolecular polymer based on hydrogen bonding.¹ Supramolecular polymers are formed from building blocks of any size connected by reversible and highly directional non-covalent interactions, most commonly hydrogen bonds. Therefore, properties of such obtained materials depend on the strength, reversibility and directionality of those secondary interactions. Probably the biggest advantage of supramolecular polymers is the strong dependence of their melt viscosity on temperature allowing for good processability. Mechanism of the stress relaxation is based not only on reptation, like for conventional polymers, but also on breaking and recombination of supramolecular chains. Supramolecular polymers give rise to properties like self-healing,²⁻⁵ shape memory,⁶⁻⁹ stimuli responsiveness,¹⁰⁻¹² polymer blend compatibilization¹³⁻¹⁶ or enhanced mechanical properties.¹⁷⁻²⁰

Jean-Marie Lehn defined supramolecular chemistry as “a highly interdisciplinary field of science covering the chemical, physical, and biological features of chemical species of higher complexity, which are held together and organized by means of intermolecular (noncovalent) binding interactions”.²¹ Those noncovalent interactions can vary in type and strength, ranging from very weak dipole-dipole interactions, through hydrophobic interactions and hydrogen bonds, to very strong metal-ligand or ion-ion interactions with binding energies approaching covalent bonds.²² Hydrogen bonds are one of the most widely used weak interactions in supramolecular chemistry because of their directionality and versatile nature. The strength of a single hydrogen bond (1 - 40 kcal/mol)²³ is usually not strong enough to achieve a desired property which can be overcome by combining arrays of multiple hydrogen bonds.²⁴ The important aspect of linear multiple hydrogen bonding motifs is that their association constant depends not only on the number of hydrogen bonds but also on their arrangement. Looking at the possible triple hydrogen bonding motifs, ADA-DAD, AAD-DDA and AAA-DDD (A-acceptor, D-donor) arrays can be identified (Figure 1). The ADA-DAD array has the weakest association constant because of the repulsive A-A and D-D secondary interactions (red arrows). AAA-DDD array exhibit the strongest interaction thanks to solely attractive A-D secondary interactions (green arrows).²⁵

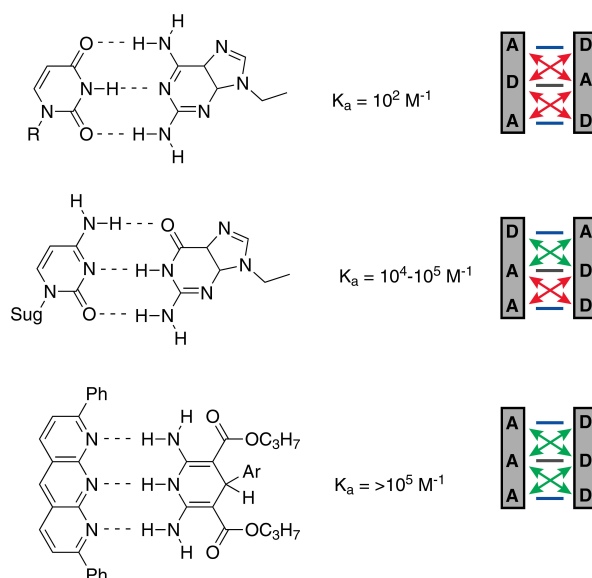


Figure 1. Influence of attractive and repulsive secondary interactions on the association constant of triple hydrogen bonding motifs.²⁵

The breakthrough in supramolecular polymer chemistry was the introduction of the quadruple hydrogen bonding unit UPy (ureidopyrimidinone) by Meijer and Sijbesma.²⁶ This self-complementary, hydrogen bonding system brings ease of synthesis and high dimerization constant of $6 \cdot 10^7 \text{ M}^{-1}$ and a lifetime of 0.1 s in chloroform.²⁷ It owes its high dimerization constant value to the almost planar DDAA motif with reduced number of repulsive secondary interactions.²⁸ The strength of UPy hydrogen bonding is highly dependent on a substituent on the 6-position of the pyrimidinone ring and its bulkiness (R group, Figure 2) as well as on a solvent and concentration. The tautomeric equilibrium can be shifted towards the self-complementary pyrimidin-4-ol exhibiting DADA array (Figure 2). Due to the increased number of secondary repulsive interactions the dimerization constant in chloroform is lowered to $9 \cdot 10^5 \text{ M}^{-1}$.

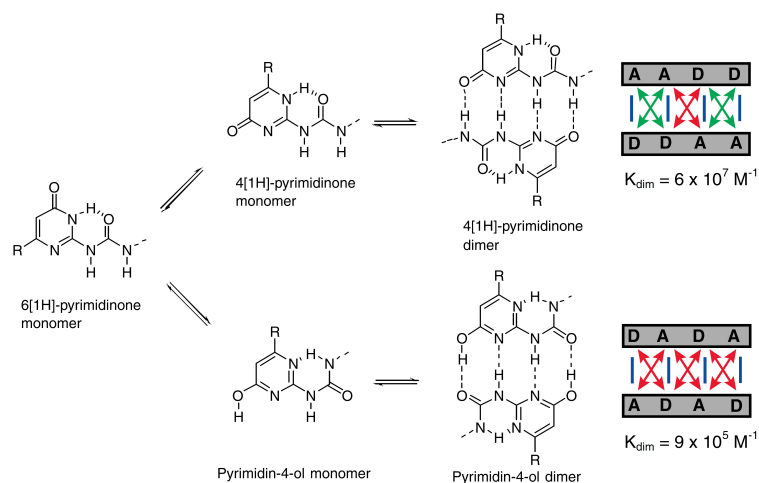


Figure 2. Tautomeric equilibria in the 2-ureido-pyrimidinone motif.²⁵

UPy can be readily obtained in a one step synthesis from commercially available methyl isocytosine and hexamethylene diisocyanate²⁶ and easily incorporated into polymers through versatile synthetic pathways. The isocyanate linker can efficiently react with a polymer bearing hydroxy or amino groups.²⁹⁻³² Amino terminated UPy have been synthesized as well and incorporated into polyurethane.³³ Another viable approach to introduce the UPy moiety is the reaction of carbonyldiimidazole activated isocytosine with amino groups.³⁴⁻³⁸ Celiz and Scherman used hydroxy terminated UPy as the initiator for the ring opening polymerization of caprolactone,³⁹ UPy methacrylate was copolymerized with hydroxyethyl methacrylate⁴⁰ and butyl acrylate⁴¹ by Lewis *et al.* and liquid UPy methacrylamide was copolymerized with various aliphatic and aromatic methacrylates by Heinzmann *et al.*⁴²

The use of complementary hydrogen bonding units in combination with polyolefins has been very limited. So far only UPy functionalized telechelic poly(ethylenebutylene),⁴³ UPy grafted polypropylene (PP),¹⁸ compatibilized

blends of isotactic PP functionalized with UPy and Ethylene/Propylene (EP) rubber functionalized with NAPY (2,7-diamido-1,8-naphthyridine),⁴⁴ and an olefin bearing UPy copolymerized with hexane¹⁷ have been reported. The introduction of such supramolecular groups often results in increased mechanical properties such as improved Young's modulus as well as better tensile and impact strength. As illustrated by these examples, there are a few challenges when it comes to incorporating such supramolecular units into polyolefins. For instance, the limited number and availability on a large scale of suitable functionalized polyolefins, the poor thermal stability of the supramolecular units as well as the lack of economical and easy to upscale production processes are key factors that limit the use of such polymers in real applications.

Traditionally, extruders are used to melt, homogenize and transport polymers for processes like film extrusion, film blowing, injection molding or blow molding. Reactive extrusion (REX) combines chemical reaction and the processing of the polymer into a one step process. In comparison to a batch process no large equipment is needed, use of solvents is avoided and residence time is significantly lowered. The ability of extruders to continuously create new thin surfaces can increase the degree of mixing and minimize temperature gradients within the polymer being processed, which solves heat and mass transfer problems that arise from high volumes and viscosities in batch processes. Additionally, REX allows to handle highly viscous materials without any solvents which substantially reduces energy usage and costs of raw materials and solvent recovery equipment.^{45, 46} Reactive extrusion of PE has been successfully employed for maleic anhydride

grafting,^{47, 48} silane grafting,^{49, 50} blending and blend compatibilization⁵¹⁻⁵⁴ and composites preparation⁵⁵⁻⁵⁷.

In this work, we demonstrate that by using the right supramolecular motif with the appropriate functionalized polyolefins and combining it with the reactive extrusion process, high scale production of processable materials with increased mechanical properties can be achieved. We synthesized and characterized functionalized PEs physically crosslinked *via* self-complementary quadruple hydrogen bonding of UPy (Scheme 1). Based on availability, three PEs containing up to 5 mol% of functional groups were used for UPy grafting in solution: polyethylene-*co*-2-hydroxyethyl methacrylate (PE-HEMA), polyethylene-*co*-vinyl acetate (EVA) and polyethylene-*graft*-maleic anhydride (PE-MAH). Moreover, low melting UPy where its methyl group is substituted with the isopropyl one (isopropyl UPy, IPR-UPy) was employed for reactive extrusion process, which significantly shortened the reaction time and eliminated the use of solvents and catalysts. The introduction of UPy and IPR-UPy dramatically influenced thermal, rheological and mechanical properties of those materials.

2.2 Results and discussion

2.2.1 UPy grafting onto functionalized PE

Since the isocyanate linker of UPy can readily react with hydroxy groups to form a carbamate, different polymers with pendant hydroxy groups were selected. While PE-HEMA copolymers already contain hydroxy groups and thus could be used directly, commercially available EVA and PE-MAH had to be further transformed. EVA was fully hydrolyzed into EVOH using a mixture of toluene and ethanol solution of potassium hydroxide (Figure appx 1), while PE-MAH was quantitatively functionalized with an excess of ethanolamine in xylene (Figure appx 2). Functional group content, melting temperatures (T_m), β transition temperatures (T_β), degrees of crystallinity (X_c) as well as number average molecular weights (M_n) and molecular weight distributions (\mathcal{D}_M) of the functionalized polyolefins are listed in Table 1.

UPy grafting onto functionalized PE involved typical reaction between the electrophilic isocyanate and nucleophilic hydroxy groups catalyzed by dibutyltin dilaurate (DBTDL) widely used in polyurethane production and organic synthesis.^{29, 58, 59} The solution grafting procedure consisted of dissolution of a functionalized polyolefin bearing hydroxy groups in toluene at 100 °C and subsequent addition of UPy and DBTDL catalyst (Scheme 1). The reactions were performed in a glass reactor with mechanical stirring and left overnight to proceed upon completion. Grafted polymers were recovered by precipitation in acetone and subsequent filtration.

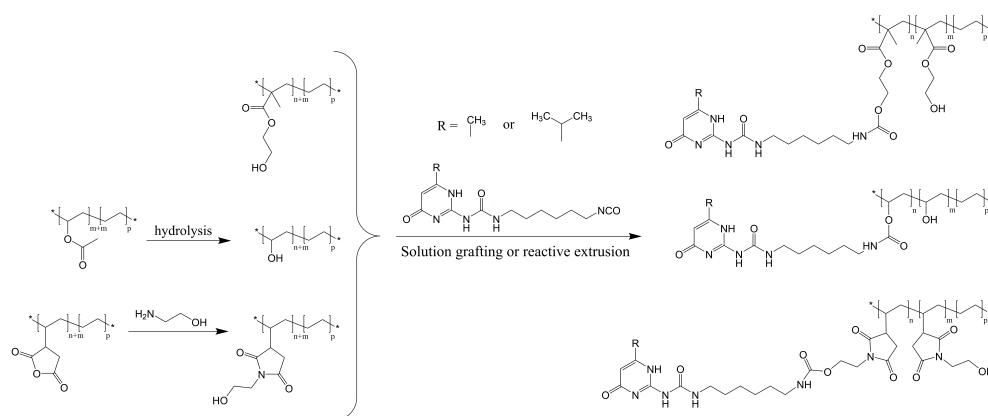
Table 1. Functional group content, melting temperatures (T_m), β transition temperatures (T_β), degrees of crystallinity (X_{cr}) as well as number average molecular weights (M_n) and molecular weight distributions (\mathcal{D}_M) of the functionalized polyolefins.

Polymer	Functional group content [mol%] ^a	T_m^b [°C]	T_β^c [°C]	X_{cr}^d [%]	M_n^e [g/mol]	\mathcal{D}_M^e
PE-HEMA1	4.4	99.6	7.1	12.2	4 000	4.2
PE-HEMA2	3.3	102.1	-2.1 ^f 68.9 ^f	20.1	5 700	2.6
EVA	3.0	99.1	-9.5 ^f 59.8 ^f	11.7	13 500	5.1
EVOH	3.0	110.4	31.5	23.5	10 800	4.6
PE-MAH	0.4	99.2	-16.4	9.3	2 500	2.4
PE-MAH-EA	0.4	99.8	-17.5	11.4	3 400	1.9

^aFunctional group content was calculated from ¹H NMR (120 °C, TCE-*d*₂). PE-MAH with higher functional group content was not available from Sigma-Aldrich. ^bMelting temperatures (T_m) were determined by DSC from the second heating scan. ^c β transition temperatures (T_β) were determined by DMTA from the maximum of $\tan \delta$. ^dDegrees of crystallinity (X_{cr}) were calculated dividing the melting enthalpy of 100 % crystalline PE (286.2 J/g)⁶⁰ by melting enthalpy of a polymer determined by DSC from the second heating scan. ^eMolecular weight and dispersity were determined by SEC in *o*DCB at 150 °C with respect to polyethylene standards. ^fTwo β transition temperatures were observed.

In order to avoid the use of a large quantity of solvents and catalyst as well as to make the production of UPy functionalized polyethylene viable on a large scale, the reactive extrusion process was envisioned. Low temperature of 120 °C was selected because of the concerns regarding thermal stability of UPy.⁶¹⁻⁶³ When UPy was extruded with PE-HEMA1 at 120 °C for 15 min, the final product contained white particles indicating that UPy did not react fully since it was extruded below its melting point (174 °C, Figure appx 3). When the temperature was raised above the melting point of UPy to 200 °C, the

product became brown indicating degradation which was confirmed by ^1H NMR (Figure appx 4). Based on those findings it became clear that a derivative of UPy that melts below the extrusion temperature is necessary. It has been demonstrated that when the methyl group of UPy is replaced with the isopropyl one (IPR-UPy) the melting temperature is lowered to $98\text{ }^\circ\text{C}$ which makes it liquid at the extrusion temperature of $120\text{ }^\circ\text{C}$.⁶³ When IPR-UPy was extruded with PE-HEMA2 at $120\text{ }^\circ\text{C}$ homogeneous and transparent PE-HEMA-IPR-UPy (polymer 2) was obtained without the need of DBTDL (Scheme 1). Reaction progress was followed by monitoring the melt viscosity measured by the extruder and a constant value was reached after around 15 min (Figure appx 5).



Scheme 1. UPy grafting on functionalized PE.

Full conversion of UPy (solution grafting) and IPR-UPy (reactive extrusion) was achieved which was confirmed by FT-IR (characteristic isocyanate band at $2275\text{-}2250\text{ cm}^{-1}$ was not detected, Figure appx 6). Polymer structure and degree of functionalization were determined by ^1H NMR, considering the integral of diagnostic peaks. There is a significant chemical

shift in the methylene signals of the HEMA units after reaction with isocyanate linker of UPy. For example, the degree of functionalization for polymer 1 (PE-HEMA1-UPy, Figure 3A) was calculated as a ratio of the integration of the peak 19, 20 (HEMA grafted with UPy) and peaks 28 and 29 (unreacted HEMA). The same approach was used for polymer 2 (PE-HEMA2-IPR-UPy, Figure 3B), polymer 3 (EVOH-UPy, Figure appx 1), and polymer 4 (PE-MAH-EA-UPy, Figure appx 2). It was not possible to use the characteristic UPy signals at low field: $-\text{NHC}(\text{CH}_3)=$, $-\text{CH}_2\text{NH}(\text{C}=\text{O})\text{NH}-$, $-\text{CH}_2\text{NH}(\text{C}=\text{O})\text{NH}-$ since they were very broad and hardly visible at 120 °C in TCE- d_2 . Table 2 summarizes the amount of hydroxy groups grafted, the amount and type of H-bonding motif used for grafting, melting temperatures (T_m), β transition temperatures (T_β) and degrees of crystallinity (X_{cr}), of functionalized polyolefins grafted with UPy (Figure appx 7 - Figure appx 10). Molecular weights of the functionalized polyolefins were not determined as these polymers are not suitable for SEC analysis due to the solubility issues.

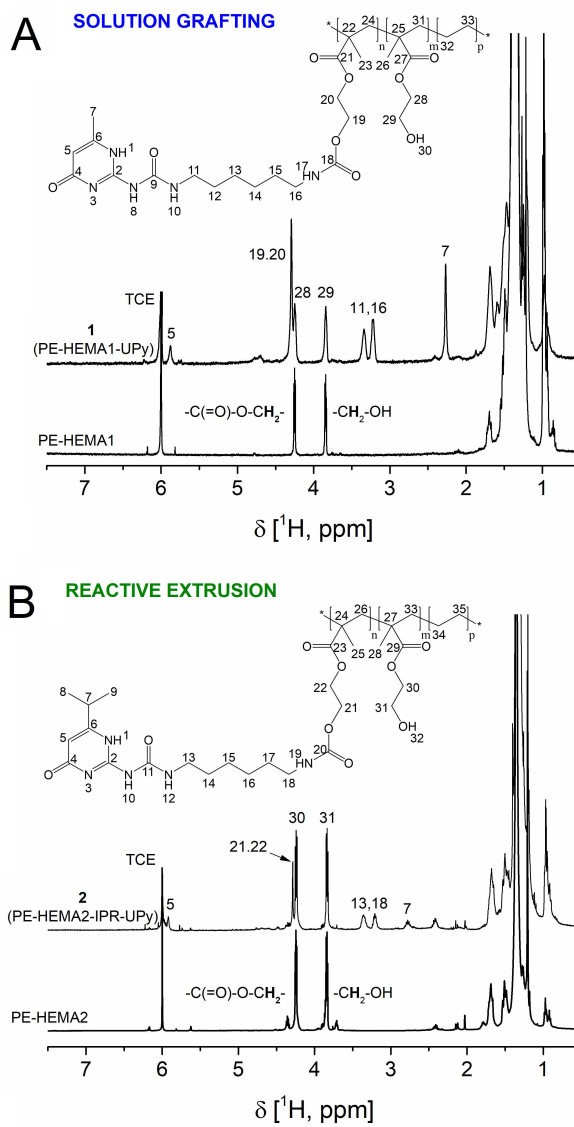


Figure 3. ^1H NMR spectra overlay of **A**: PE-HEMA1 and polymer 1 (PE-HEMA1-UPy), **B**: PE-HEMA2 and polymer 2 (PE-HEMA2-IPR-UPy) recorded at 120 °C in TCE- d_2 .

Table 2. Amount of hydroxy groups grafted, amount and type of H-bonding motif used for grafting, melting temperatures (T_m), β transition temperatures (T_β) and degrees of crystallinity (X_{cr}) of functionalized polyolefins grafted with UPy.

Polymer	-OH grafted ^a [%]	H-bonding motif		T_m^c [°C]	T_β^d [°C]	X_{cr}^e [%]	
		[mol%]	[1/chain] ^b				
1 (PE-HEMA1-UPy) ^f	50	UPy	2.2	2.4	97.7	18.6	11.0
2 (PE-HEMA2-IPR-UPy) ^g	33	IPR-UPy	1.1	2.0	101.5	12.3 ^h 68.9 ^h	17.7
3 (EVOH-UPy) ^f	80	UPy	2.4	11	99.5	26.0	7.1
4 (PE-MAH-EA-UPy) ^f	>99	UPy	0.4	0.5	94.7	-36.8	9.7

^aCalculated from ¹H NMR (120 °C, TCE-*d*₂). It was not possible to use the same PE-HEMA both for the solution and reactive extrusion grafting because of the limited availability of the material and timeline of the experiments. ^bNumber of UPy/chain was calculated based on the amount of -OH grafted and M_n of starting material. ^cMelting temperatures (T_m) were determined by DSC from the second heating scan. ^d β transition temperatures (T_β) were determined by DMTA from the maximum of $\tan \delta$. ^eDegrees of crystallinity (X_{cr}) were calculated dividing the melting enthalpy of 100 % crystalline PE (286.2 J/g)⁶⁰ by melting enthalpy of a polymer determined by DSC from the second heating scan. It can be noted ^fSynthesized in solution. ^gSynthesized *via* reactive extrusion. ^hTwo β transition temperatures were observed.

2.2.2 Thermal stability of PEs grafted with UPy.

As mentioned earlier, the thermal instability of polymers functionalized with UPy can limit the use of processing techniques like extrusion, injection molding, compression molding or thermoforming and consequently their applications. To the best of our knowledge there is no reported study investigating the thermal stability of UPy attached to a polymer chain. To investigate the thermal stability of PE-UPy polymers, DSC, rheology and TGA analysis were employed. As can be seen in Figure 4A, polymer 1

(PE-HEMA1-UPy) was subjected to heating cycles where the maximum temperature was increased by 10 °C after each cycle, starting from 120 °C. Until 150 °C, no change in the melting temperature of the polymer was observed. When the polymer was heated above 150 °C, the melting temperature started to shift toward lower values (marked with arrows). This behavior indicates thermal degradation of the polymer grafted with UPy that occurs at temperatures above 150 °C, which is in a good agreement with the UPy degradation temperature mentioned by van Beek *et al.*⁶² and 20 °C higher than the one mentioned by Botterhuis *et al.*⁶⁴ The same experiment was performed on UPy grafted EVOH (polymer 3, Figure appx 11), UPy grafted PE-MAH-EA (polymer 4, Figure appx 12) and compared to PE-HEMA1 that did not contain UPy. While no degradation was observed for PE-HEMA1, EVOH-UPy and PE-MAH-EA-UPy revealed very similar behavior with respect to PE-HEMA1-UPy, demonstrating that the thermal degradation can only be attributed to UPy and not to the polymer matrix.

This phenomenon was confirmed by rheology temperature sweep measurements which were performed on PE-HEMA1 and polymer 1 (PE-HEMA1-UPy) (Figure 4B). For PE-HEMA1, a typical decrease in storage modulus with increasing temperature was observed.^{65, 66} In contrast, for polymer 1, a short plateau followed by a rapid increase in storage modulus can be observed around 160-°C. This rapid increase was attributed to UPy degradation and subsequent covalent crosslinking between liberated isocyanate and hydroxy groups of functionalized polyolefins.⁶⁷ Similar observations arose for polymer 2 (Figure appx 14) as well as for polymer 3 and 4 (Figure appx 15 and Figure appx 16). Together, these measurements

confirm that PE grafted with UPy (polymer 1) or IPR-UPy (polymer 2) starts to degrade as low as 160 °C and the maximum safe processing temperature is confirmed to be 150 °C.

In contrast, TGA measurements showed that polymer 1 containing 2.2 mol% of UPy starts to degrade to volatile compounds around 300 °C (mass loss > 1 %) and corresponding PE-HEMA1 around 450 °C (Figure appx 17). These observations showcase that TGA alone cannot accurately assess thermal stability and structural degradation of polymeric materials. For reliable results it should be combined with other techniques such as NMR, DSC and rheology.

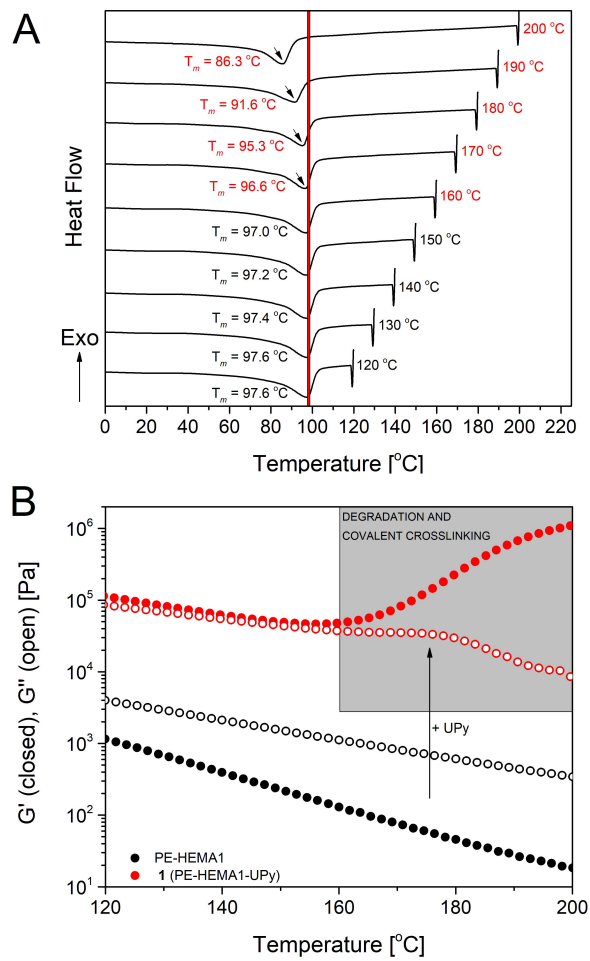


Figure 4. **A**: DSC heating curves of polymer 1 (PE-HEMA1-UPy). Maximal temperature was increased by 10 °C after each heating cycle, starting from 120 °C. **B**: Rheology temperature sweep curves of PE-HEMA1 and polymer 1, storage modulus (G') - closed circles, loss modulus (G'') - open circles.

2.2.3 Rheological characterization.

In order to explore properties of UPy functionalized PE in the melt, rheological analysis was employed. Frequency sweep showed pronounced effect of UPy hydrogen bonding on the flow of PE (Figure 5).

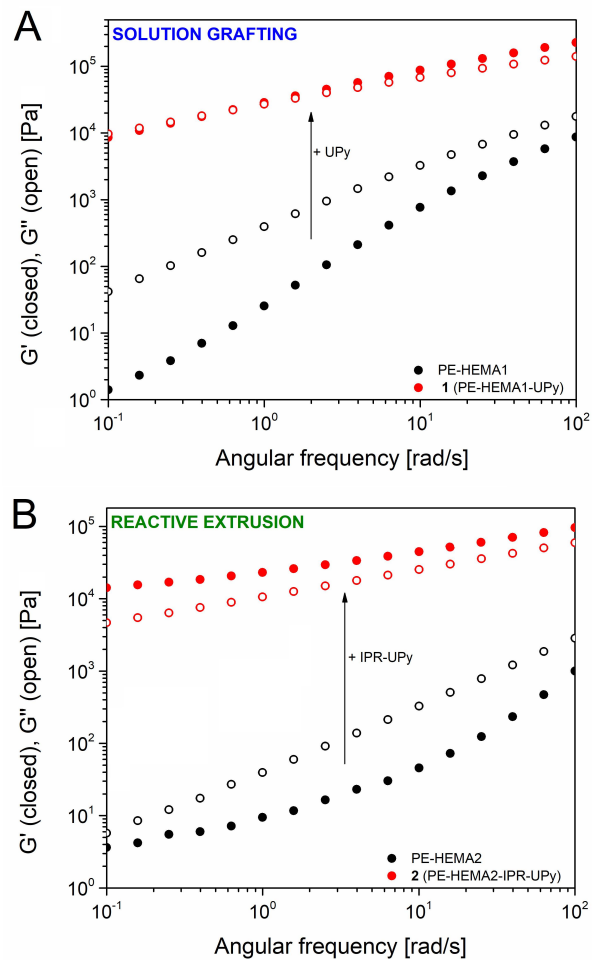


Figure 5. Rheology frequency sweep curves at 140 °C of **A**: PE-HEMA1 and **1** (PE-HEMA1-UPy), **B**: PE-HEMA2, and **2** (PE-HEMA2-IPR-UPy), storage modulus (G') - closed circles, loss modulus (G'') - open circles.

PE-HEMAs display a typical behavior of a low molecular weight polymer melt⁶⁸ with a strong frequency dependence. They have no crossover point between storage (G') and loss (G'') modulus and they are more viscous (G'' higher than G') than elastic (G' higher than G'') within the whole studied frequency range. When comparing PE-HEMA1 and polymer **1**, it can be observed that after the introduction of UPy, the material shows drastically different rheological behavior (Figure 5A). The crossover point appeared in between 0.1 and 1 rad/s and polymer **1** showed a more elastic behavior rather than viscous above 1 rad/s. This result shows that UPy hydrogen bonding increased the virtual molecular weight of the starting PE-HEMA1 even in the polymer melt at 140 °C.⁶⁶ Polymer **2**, obtained by reactive extrusion of PE-HEMA2 with IPR-UPy, behaved like an elastic solid (G' higher than G'') more than 30 °C above its melting point and was less frequency dependent than pristine PE-HEMA2 (Figure 5B) which is characteristic of crosslinked materials.^{69,70} The absence of crossover point for polymer **2** shows that overall it flows less than polymer **1** which can be caused by combination of different molecular weight, dispersity and HEMA content of the starting material as well as different amount of UPy grafted. In comparison with the PE-HEMA based polymers **1** and **2**, polymer **3** (EVOH-UPy) showed only a minimal frequency dependence (Figure appx 18) which indicates a highly crosslinked nature of this material. Finally, the introduction of UPy had also a great impact on PE-MAH-EA polymer flow behavior. While the pristine material showed very low viscosity hampering the measurement at lower frequencies, polymer **4** (PE-MAH-EA-UPy) was easily measured within the whole studied frequency range (Figure appx 19). This showcases the strength of UPy

interaction that increased the virtual molecular weight of this low molecular weight PE.

In general, supramolecular polymers combine mechanical properties of a high molecular weight polymer and easy melt processing thanks to a strong dependence of melt viscosity on temperature,⁷¹ which is clearly not observed in case of our UPy functionalized supramolecular PEs. It can be related to the relatively high molecular weight of polymers used in this study in comparison to usually used telechelic oligomers, the presence of multiple UPy units per chain and the apolar nature of PE that increases the strength of hydrogen bonding interactions.^{72,73}

Rheology temperature sweeps described in the thermal stability study section can be employed as well to determine the significant decrease in viscosity or storage modulus at a given temperature which can be attributed to a disassociation of UPy dimers. A clear dependence between the dissociation temperature and the polymer architecture was shown by Long *et al.* where polyethylene-*co*-propylene functionalized with UPy have a disassociation temperature of chain end functionalized material at around 80 °C, telechelic at around 120 °C and star shaped at around 160 °C.⁷⁴ Nojiri *et al.* claimed a disassociation temperature for UPy functionalized polypropylene at around 190 °C for the material compressed molded at 190 °C. Based on the UPy thermal stability study, a potential permanent covalent cross-link could have occurred to some extent, which can explain why no significant decrease in storage modulus was observed at temperatures as high as 230 °C. For our materials (Figure 4B) no significant drop in storage modulus was observed below 160 °C, which confirms that UPy association is

still present up to that temperature in the PE melt. At higher temperatures, a strong increase in storage modulus was observed which demonstrates that the previously mentioned permanent covalent cross-linking occurred before UPy had a chance to dissociate.

2.2.4 Mechanical properties.

Semicrystalline PE exhibits three characteristic temperature transitions.^{75, 76} γ transition is observed at around -130 °C, involving rotation of CH₂ groups in the amorphous and crystalline phases, and it is independent of the branching content as well as the degree of crystallinity and was not investigated in this study. β transition, occurring at higher temperatures, can be related to movements involving longer parts of the polymer chains and branch points. Finally, α transition is associated with a large movement of molecules that arise as the crystalline phase undergo melting. PE-HEMA copolymers exhibit also an additional transition around -60 °C that most likely results from hydrogen bonds breaking and reforming between hydroxy groups present in the HEMA units (-OH transition).⁷⁷ Grafting of PE-HEMAs with UPy moieties provides two opposed effects. Although quadruple hydrogen bonded crosslinks should reduce segmental mobility of PE chains increasing consequently the T_{β} ,⁴² the presence of bulky UPy groups further reduces crystallinity resulting in a decrease of the T_{β} . In fact, no drastic changes in T_{β} and no clear trend was observed when UPy moieties were grafted onto PE-HEMAs (Figure 6, Table 1, Table 2). A clear influence of quadruple hydrogen bonding was revealed after the α transition. While the

pristine PE-HEMA materials flowed after the melting (it was not possible to measure any modulus after the α transition),⁴² the introduction of UPy or IPR-UPy increased the virtual molecular weight by supramolecular crosslinking, resulting in a low but measurable storage modulus after melting. Additionally, this result can be used as an indirect measure of the melt strength which was significantly improved by the multiple hydrogen bonding interactions and is extremely important for processes like film blowing, blow molding, thermoforming and foaming.⁷⁰ The DMTA also confirmed the covalent cross-linking phenomenon at temperatures above 150 °C with a strong increase in modulus, again arising from UPy thermal degradation, both for PE-HEMA and EVOH materials (Figure 6, Figure appx 20). In contrast, the introduction of UPy to the low molecular weight PE-MAH-EA material only provided moderate improvement. Indeed, while PE-MAH-EA softened and failed around 70-80 °C, polymer **4** failed just around 15 °C later. This demonstrates that in case of polymer **4** not enough UPy was grafted to significantly increase the virtual molecular weight and create a supramolecular network (Figure appx 21).

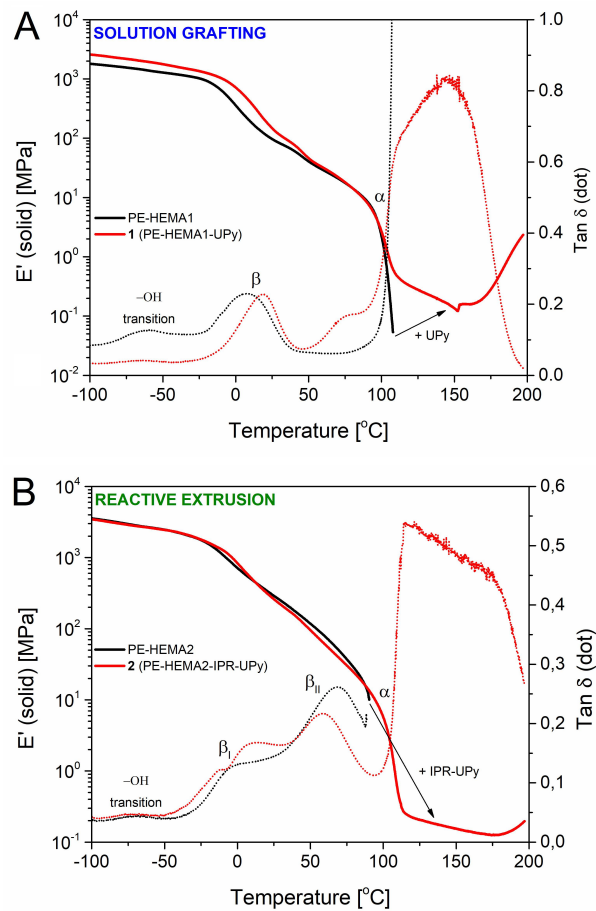


Figure 6. DMTA curves of **A**: PE-HEMA1 and polymer 1 (PE-HEMA1-UPy), **B**: PE-HEMA2, and polymer 2 (PE-HEMA2-IPR-UPy), storage modulus (E') - solid line, tangent delta ($\tan \delta$) - dot line.

PE-HEMAs exhibit tensile properties characteristic of a semicrystalline thermoplastic, presenting an initial elastic deformation before the neck is formed and subsequent cold drawing followed by strain hardening and fracture (Figure 7).⁷⁸ Multiple hydrogen bonds act like physical crosslinks, creating links between chains and long chain branches increasing the virtual molecular weight therefore, the introduction of UPy should lead to the

improved mechanical performance compared to the pristine materials. Indeed, increased toughness and ultimate tensile strength were achieved for all supramolecular polymers despite of the reduced crystallinity, which is particularly impressive. In details, polymer **1** was twice as tough and the ultimate strength was improved almost 2.5 times, maintaining similar strain at break and Young's modulus. It also showed more elastomer like characteristic, the cold drawing region was no longer observed and necking was immediately followed by the pronounced strain hardening.^{17, 79} Polymer **2**, made by reactive extrusion with IPR-UPy, showed even more significant improvements in toughness (3.5 times), ultimate tensile strength (around 70 %) and strain at break (almost 3 times) with respect to PE-HEMA2. Polymer **3** (EVOH-UPy) also displayed increased toughness and ultimate tensile strength without sacrificing strain at break (Figure appx 22). The low molecular weight of PE-MAH-EA, which is within the range of entanglement molecular weight (830-2600 g/mol),⁸⁰ led to a low ultimate tensile strength (<10 MPa) and a very low strain at break (~6 %) together with the absence of necking and strain hardening. For polymer **4**, the grafting of 0.4 mol% of UPy onto PE-MAH-EA doubled toughness and increased ultimate tensile strength to 11 MPa and strain at break to 10 % (Figure appx 23). This was particularly remarkable considering poor mechanical performance of the starting material.

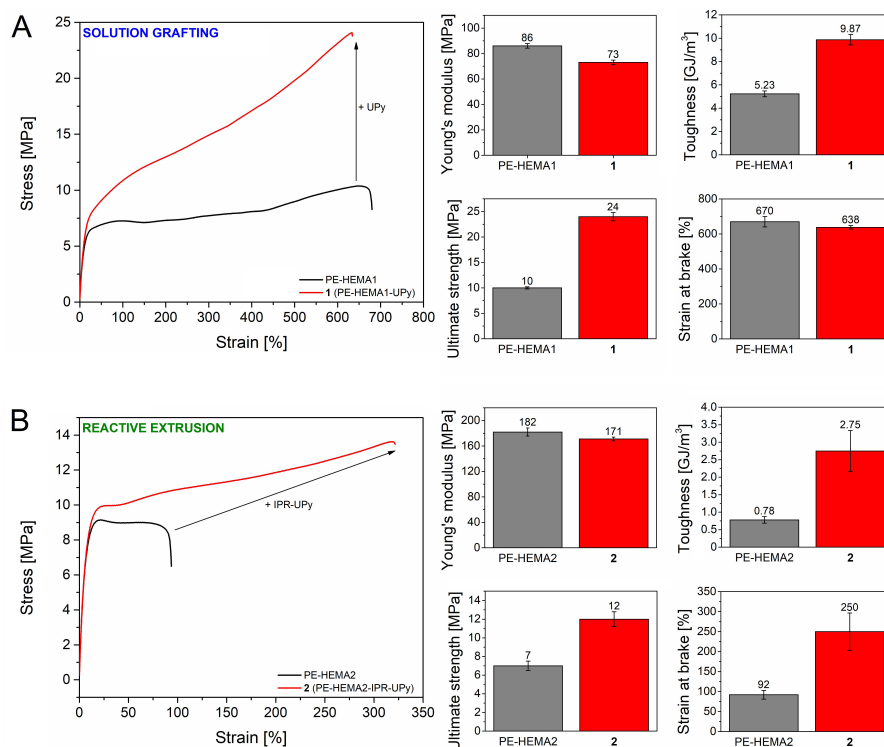


Figure 7. Representative stress-strain curves and Young's modulus, toughness, ultimate strength and strain at break of **A**: PE-HEMA1 and polymer 1 (PE-HEMA1-UPy), **B**: PE-HEMA2 and polymer 2 (PE-HEMA2-IPR-UPy).

2.3 Conclusions

UPy was readily introduced into various PEs bearing hydroxy groups by solution grafting, affording physically crosslinked PE *via* quadruple hydrogen bonding. By utilizing low melting IPR-UPy, it was possible to perform the grafting by reactive extrusion instead of solution grafting. This efficient process allowed to significantly shorten the reaction time and eliminate the use of solvents and catalysts. Incorporation of such supramolecular motifs into PE matrix changed the rheology of a typical

entangled thermoplastic melt to that of an elastic crosslinked system. DMTA measurements indicated significantly increased melt strength, which is extremely important for processes like film blowing, blow molding, thermoforming and foaming. Moreover, greatly improved toughness and ultimate tensile strength were achieved without sacrificing elongation at break or Young's modulus. Rheology, DMTA and DSC studies proved that UPy functionalized PEs degrade and crosslink above 150 °C and that TGA alone is not well suited to determine the true thermal stability, since it only shows the decomposition to volatile compounds. Identified thermal stability limit of those materials allowed for a safe processing, using techniques like compression molding and extrusion. Our work demonstrates an efficient way for physical crosslinking of PE *via* reactive extrusion utilizing IPR-UPy quadruple hydrogen bonding interactions that lead to improved mechanical properties. This process allows for easy upscaling and is applicable not only for PE but also for any thermoplastic bearing functional groups suitable for grafting below 150 °C.

2.4 Experimental section

Materials

Toluene, xylene, heptane, acetone, ethanol, 1,2-dichlorobenzene (*o*DCB), deuterated tetrachloroethene (TCE-*d*₂), deuterated dimethyl sulfoxide (DMSO-*d*₆), hexamethylene diisocyanate (HDI, 98 %), dibutyltin dilaurate (DBTDL, 95 %), ethanolamine (EA, 99 %), sodium hydroxide and 2-Amino-4-hydroxy-6-methylpyrimidine (methyl isocytosine, 98 %) were

purchased from Sigma-Aldrich. 2-(6-isocyanatohexylaminocarbonylamino)-6-methyl-4[1H]pyrimidinone (UPy) was synthesized according to the reported procedure.⁷² 2-(6-isocyanatohexylaminocarbonylamino)-6-isopropyl-4[1H]pyrimidinone (isopropyl-UPy, IPR-UPy, 95 %) was purchased from SupraPolix. Polyethylene-*co*-2-hydroxyethyl methacrylates (PE-HEMAs) were kindly provided by SABIC. Polyethylene-*co*-vinyl acetate (EVA, ELVAX 760A) was purchased from DuPont. Polyethylene-*graft*-maleic anhydride (PE-MAH) was purchased from Sigma-Aldrich. All materials were used as received unless otherwise stated.

Typical procedure for EVA hydrolysis

EVA (50.0 g) was dissolved in toluene (1000 mL) at 80 °C, under nitrogen atmosphere, in a glass reactor equipped with mechanical stirring (100 RPM). Subsequently, a solution of sodium hydroxide (3.0 g, 75.0 mmol) in ethanol (100 mL) was added and the reaction mixture was stirred at 80 °C for 24 h, under nitrogen atmosphere. The product was precipitated by pouring the reaction mixture into acetone, filtered, washed twice with acetone and dried at 60 °C under vacuum for 24 h. Full hydrolysis was confirmed by ¹H NMR (Figure appx 1).

Typical procedure for PE-MAH functionalization with ethanolamine

PE-MAH (50.0 g) was dissolved in xylene (1000 mL) at 140 °C in a glass reactor equipped with mechanical stirring (100 RPM) under nitrogen atmosphere. Subsequently, ethanolamine (2.9 g, 46.9 mmol) was added and the reaction mixture was stirred at 140 °C for 4 h, maintaining the nitrogen

atmosphere. The product was precipitated by pouring the reaction mixture into acetone, filtered, washed twice with acetone and dried at 60 °C under vacuum for 24 h. Full functionalization was confirmed by ¹H NMR (Figure appx 2).

Typical procedure for UPy grafting in solution

PE-HEMA1 (10.0 g) was dissolved in toluene (500 mL) at 100 °C in a glass reactor equipped with mechanical stirring (100 RPM) under nitrogen atmosphere. UPy (1.99 g, 6.78 mmol) and DBTDL (2 drops) were added and the reaction mixture was stirred at 100 °C for 24 h, maintaining the nitrogen atmosphere. The product was precipitated by pouring the reaction mixture into acetone, filtered, washed twice with acetone and dried at 60 °C under vacuum. (Figure 3A, Figure appx 1 and Figure appx 2)

Typical procedure of UPy grafting *via* reactive extrusion

PE-HEMA1 (7.00 g) and UPy (2.78 g, 9.48 mmol) were mixed in a metal cup and subsequently fed into a 15 mL twin crew micro extruder connected to a computer monitoring melt viscosity. The reaction mixture was processed under nitrogen, at 120 °C and the screw speed of 100 RPM for 15 min and a small sample was taken out by quickly opening the dye. The sample contained white particles indicating that UPy did not react fully at 120 °C which is below its melting point (174 °C, Figure appx 3). Subsequently, the temperature was raised above the melting point of UPy to 200 °C and the reaction mixture was processed for another 15 min. The product came out

brown suggesting degradation which was confirmed by $^1\text{H NMR}$ (Figure appx 4).

Typical procedure of IPR-UPy grafting *via* reactive extrusion

PE-HEMA2 (9.00 g) and IPR-UPy (1.00 g, 3.11 mmol) were mixed in a metal cup and subsequently fed into a 15 mL twin crew micro extruder connected to a computer monitoring melt viscosity. The reaction mixture was processed under nitrogen, at 120 °C and the screw speed of 100 RPM until the constant melt viscosity was reached (around 15 min, Figure 3B, Figure appx 5).

Measurements

$^1\text{H NMR}$ analysis was carried out either at room temperature or at 120 °C using deuterated tetrachloroethene ($\text{TCE-}d_2$), deuterated chloroform (CDCl_3) or deuterated dimethyl sulfoxide ($\text{DMSO-}d_6$) as the solvents and recorded in 5 mm tubes on a Varian Mercury spectrometer operating at frequencies of 400 MHz. Chemical shifts are reported in ppm and were determined by reference to the residual solvent peak.

Fourier transform infrared spectra (FT-IR) were obtained using a Varian 610-IR spectrometer at room temperature in attenuated total reflection (ATR) mode.

The molecular weight and dispersity were studied by size exclusion chromatography (SEC) measurements performed at 150 °C on a Polymer Char GPC-IR® built around an Agilent GC oven model 7890, equipped with an autosampler and the Integrated Detector IR4. *o*DCB was

used as an eluent at a flow rate of 1 mL/min. The SEC data were processed using Calculations Software GPC One®. The molecular weights were calculated with respect to polyethylene standards. Molecular weight of UPy functionalized polymers were not determined due to the solubility issues.

Melting temperatures (T_m) and enthalpies of the transition (ΔH_m) were measured by differential scanning calorimetry (DSC) using a DSC Q100 from TA Instruments. The measurements were carried out at a heating and cooling rate of 10 °C/min from -20 °C to 150 °C. The transitions were deduced from the second heating curves.

Thermogravimetric analysis (TGA) was performed in nitrogen atmosphere on Perkin Elmer Pyris 1 analyzer. Samples were heated to 100 °C at a heating rate of 10 °C/min and kept at that temperature for 15 min to get rid of potential traces of water. Subsequently, the temperature was raised to 800 °C at a heating rate of 10 °C/min and maintained for 15 min.

Tensile tests were performed with a Zwick Z100 tensile tester equipped with a 100 N load cell. The tests were performed on samples cut from 200 μ m films (ISO 527-2 type 5B). The samples were pre-stressed to 0.3 MPa, then loaded with a constant cross-head speed of 200 mm/min.

Dynamical mechanical thermal analysis (DMTA) was performed using TA Instruments Q800 in tensile mode. The strips were cut from 200 μ m films. Samples were measured from -100 to 200 °C with a heating speed of 3 °C/min and a fixed oscillation (amplitude 10 μ m, frequency 1 Hz).

Rheology was measured using TA Instruments DHR-2 equipped with a parallel plate geometry. Discs with diameter of 25 mm and thickness of 1 mm were compress molded at 140 °C. Temperature sweeps were measured

from 50 to 200 °C with a heating speed of 3 °C/min and a fixed oscillation (strain amplitude 0.4 %, frequency 1 Hz). Frequency sweeps were measured from 100 to 0.01 rad/s (strain amplitude of 0.4 %) at a temperature of 140 °C.

2.5 Appendix

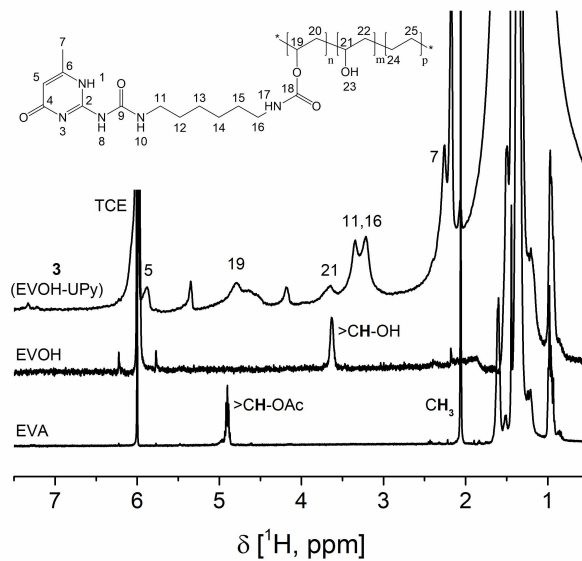


Figure appx 1. ¹H NMR spectra overlay of EVA, EVOH and 3 (EVOH-UPy) recorded at 120 °C in deuterated TCE.

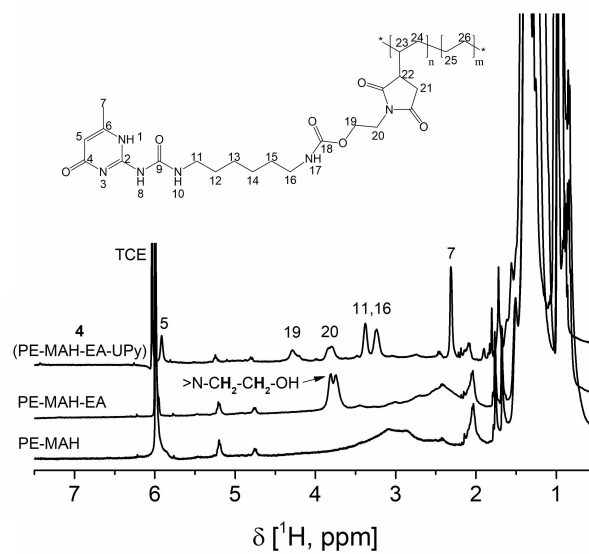


Figure appx 2. ^1H NMR spectra overlay of PE-MAH, PE-MAH-EA and 4 (PE-MAH-EA-UPy) recorded at 120 °C in deuterated TCE.

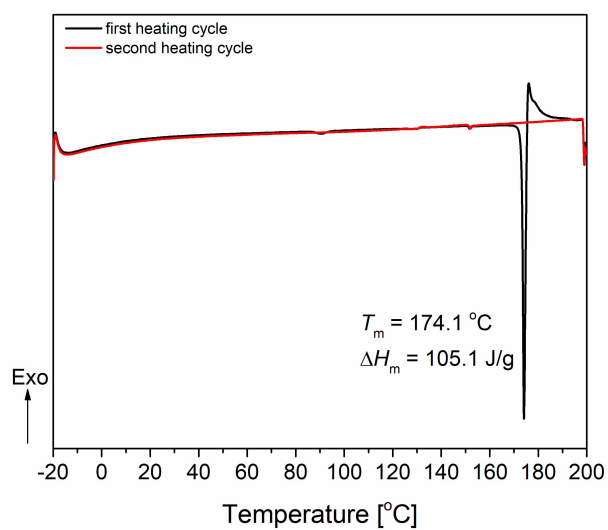


Figure appx 3. DSC first (black) and second (red) heating curve of UPy.

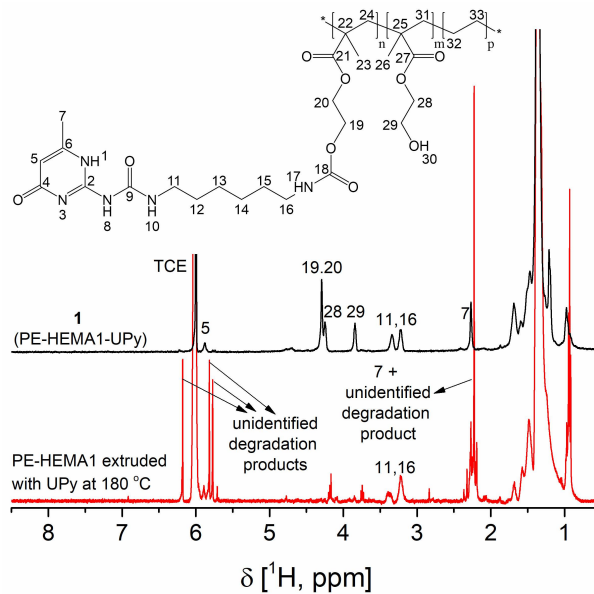


Figure appx 4. ^1H NMR spectra overlay of 1 (PE-HEMA1-UPy, black) and PE-HEMA1 extruded with UPy at 180 °C (red), recorded at 120 °C in deuterated TCE.

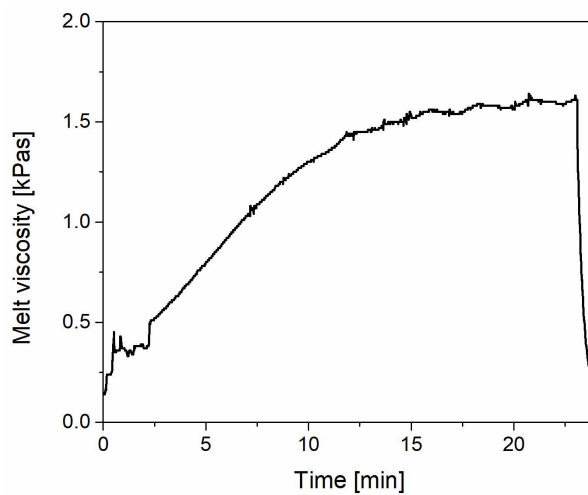


Figure appx 5. Representative melt viscosity changes recorded during the reactive extrusion of sample 2 (PE-HEMA2-IPR-UPy)

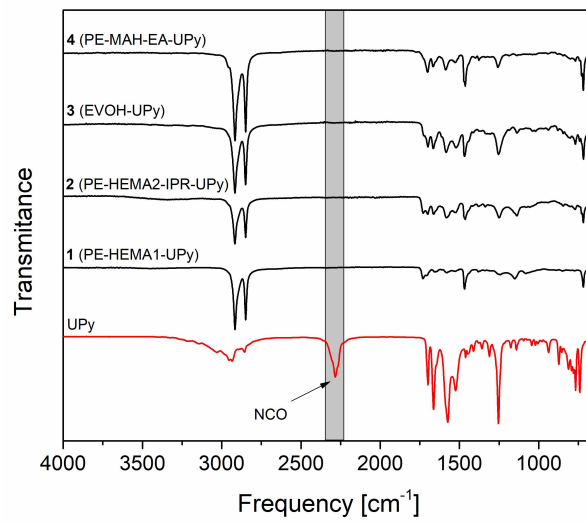


Figure appx 6. IR spectra overlay of UPy (red line) and functionalized polyolefins grafted with UPy or IPR-UPy (black lines).

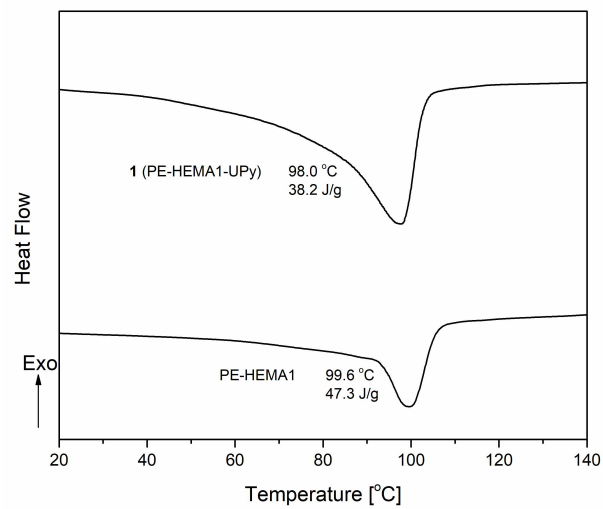


Figure appx 7. DSC second heating curves of PE-HEMA1 and 1 (PE-HEMA1-UPy).

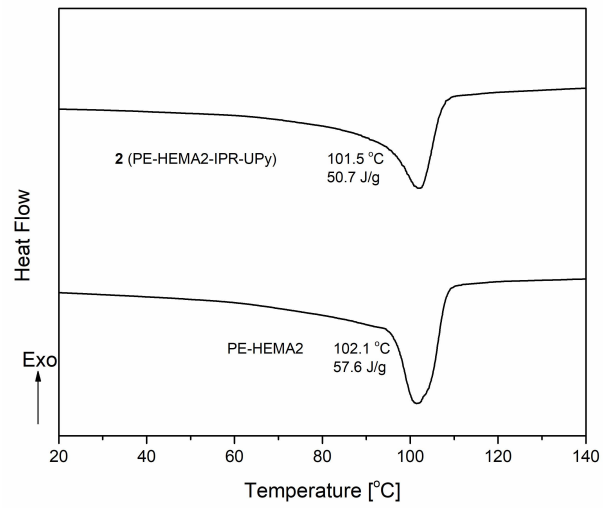


Figure appx 8. DSC second heating curves of PE-HEMA2, and 2 (PE-HEMA2-IPR-UPy).

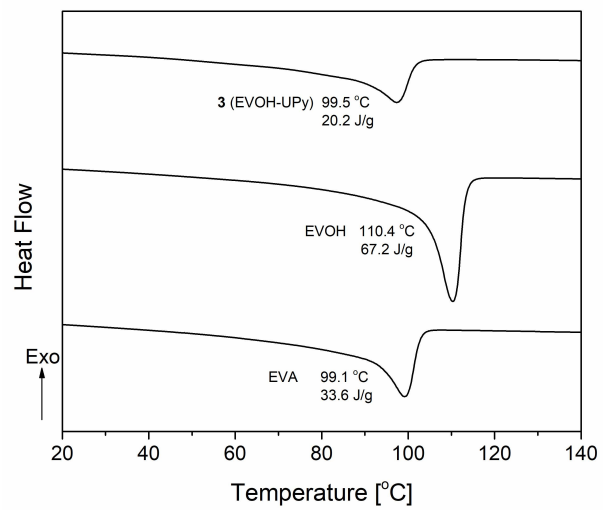


Figure appx 9. DSC second heating curves of EVA, EVOH and 3 (EVOH-UPy).

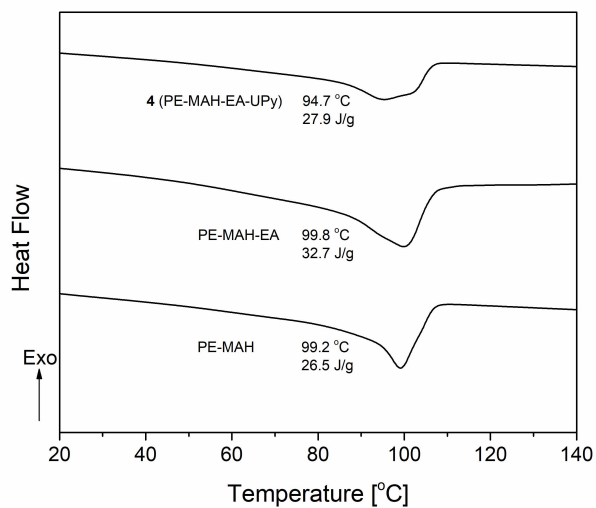


Figure appx 10. DSC second heating curves of PE-MAH, PE-MAH-EA and 4 (PE-MAH-EA-UPy).

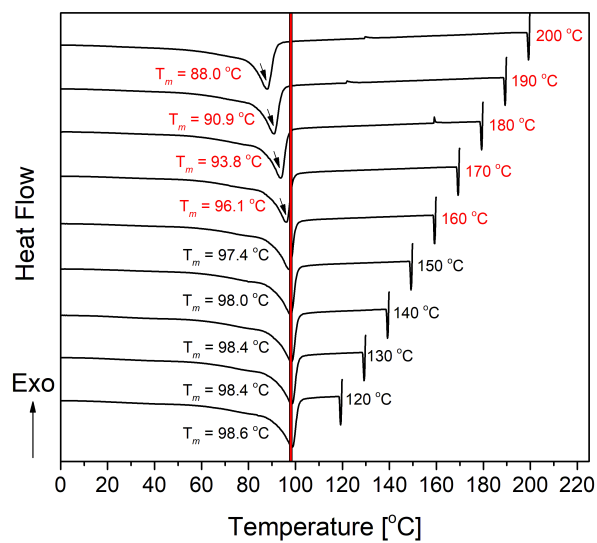


Figure appx 11. DSC heating curves of 3 (EVOH-UPy), maximal temperature was increased by 10 °C each time starting from 120 °C.

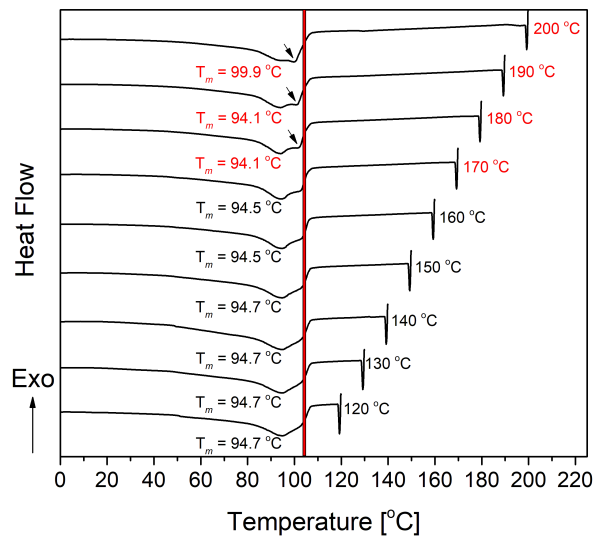


Figure appx 12. DSC heating curves of 4 (PE-MAH-EA-UPy) maximal temperature was increased by 10 °C each time starting from 120 °C.

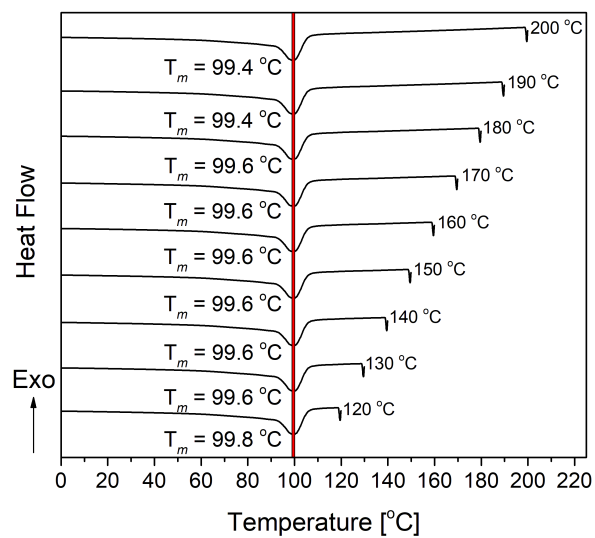


Figure appx 13. DSC heating curves of PE-HEMA1, maximal temperature was increased by 10 °C each time starting from 120 °C.

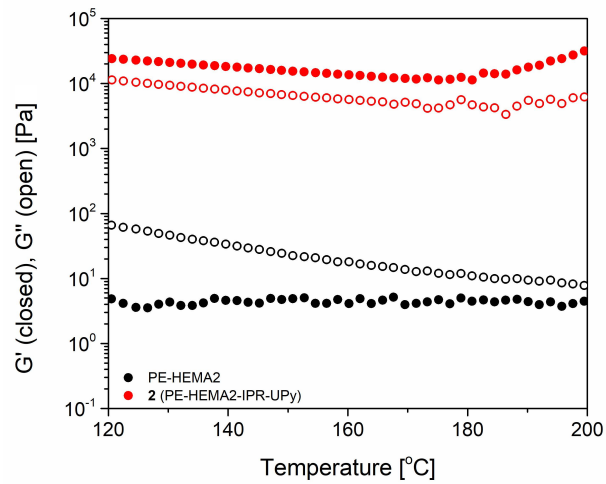


Figure appx 14. Rheology temperature sweep curves of PE-HEMA2 and **2** (PE-HEMA2-IPR-UPy), storage modulus (G') - closed circles, loss modulus (G'') - open circles.

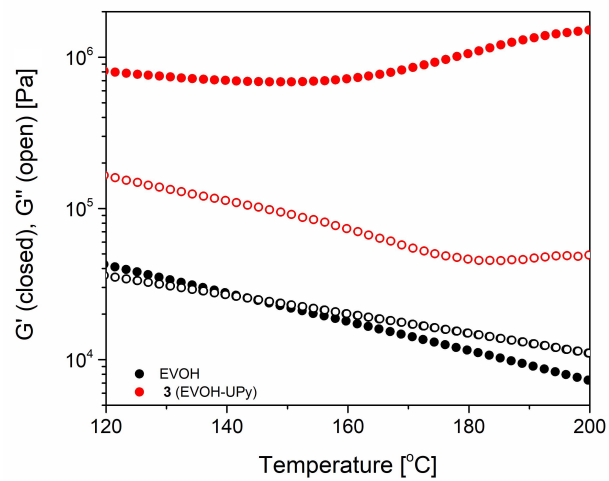


Figure appx 15. Rheology temperature sweep curves of EVOH and **3** (EVOH-UPy), storage modulus (G') - closed circles, loss modulus (G'') - open circles.

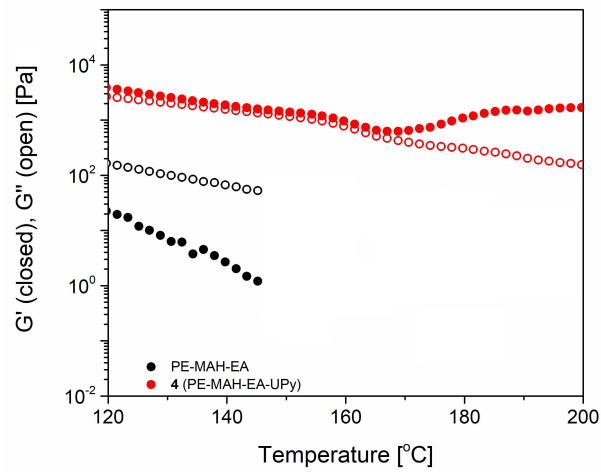


Figure appx 16. Rheology temperature sweep curves of PE-MAH-EA and 4 (PE-MAH-EA-UPy), storage modulus (G') - closed circles, loss modulus (G'') - open circles.

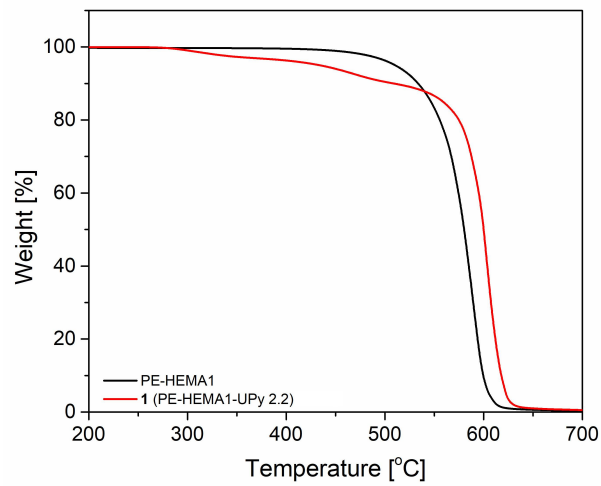


Figure appx 17. TGA curves of PE-HEMA1 and 1 (PE-HEMA1-UPy).

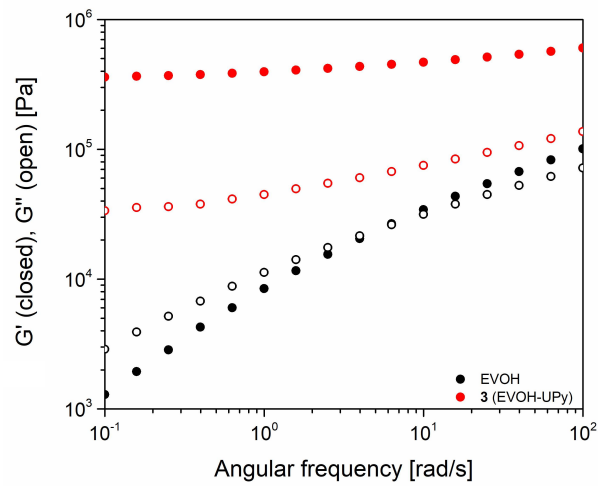


Figure appx 18. Rheology frequency sweep curves of EVOH and 3 (EVOH-UPy), storage modulus (G') - closed circles, loss modulus (G'') - open circles.

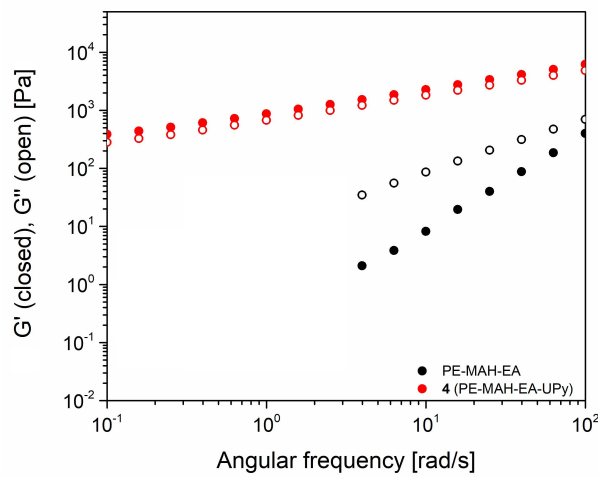


Figure appx 19. Rheology frequency sweep curves of PE-MAH-EA and 4 (PE-MAH-EA-UPy), storage modulus (G') - closed circles, loss modulus (G'') - open circles.

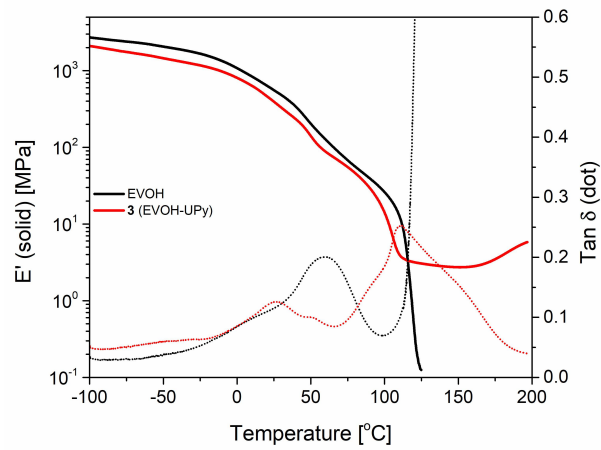


Figure appx 20. DMTA curves of EVOH and **3** (EVOH-UPy), storage modulus (E') - solid line, tangent delta ($\tan \delta$) - dot line.

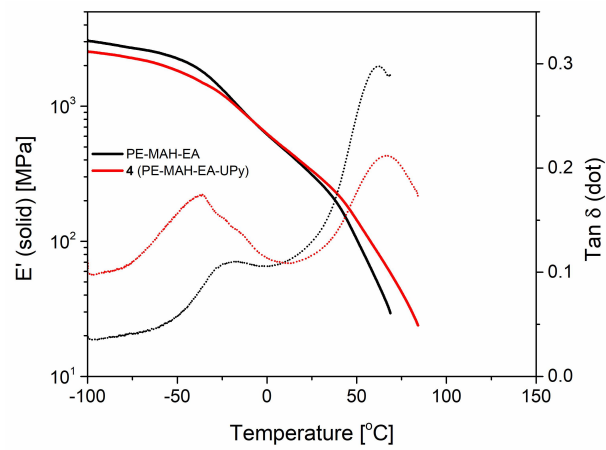


Figure appx 21. DMTA curves of PE-MAH-EA and **4** (PE-MAH-EA-UPy), storage modulus (E') - solid line, tangent delta ($\tan \delta$) - dot line.

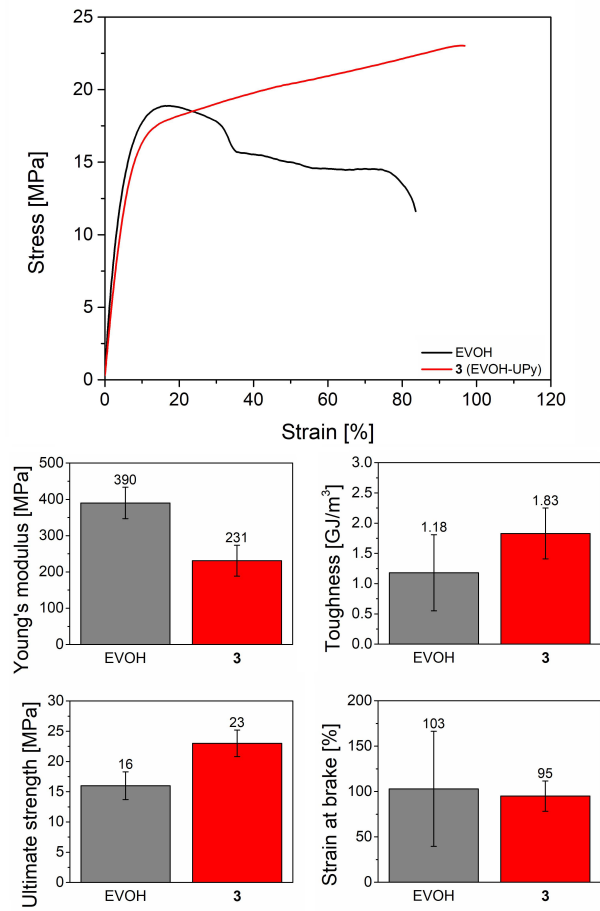


Figure appx 22. Representative stress-strain curves and Young's modulus, toughness, ultimate strength and strain at break of EVOH and 3 (EVOH-UPy).

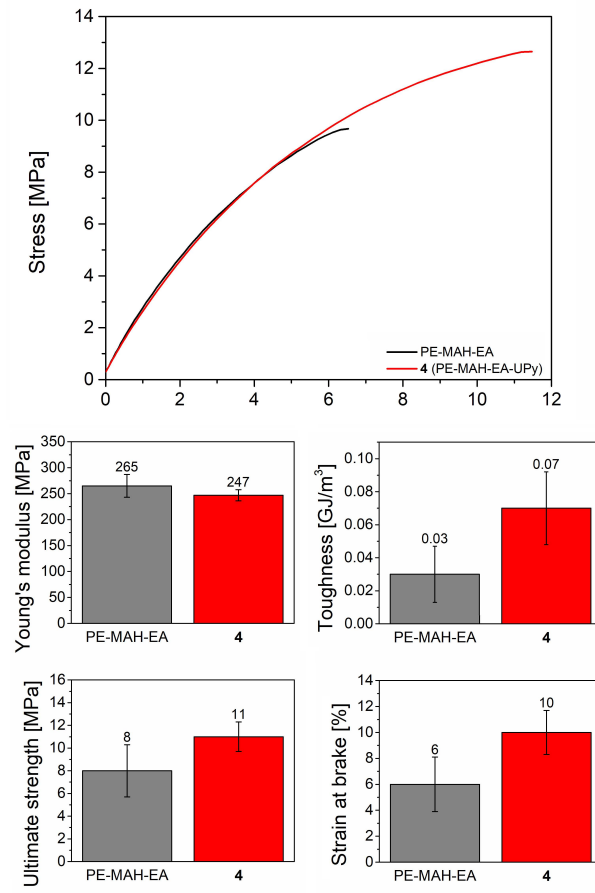


Figure appx 23. Representative stress-strain curves and Young's modulus, toughness, ultimate strength and strain at break of PE-MAH-EA and 4 (PE-MAH-EA-UPy).

2.6 References

1. Lehn, J. M. Perspectives in Supramolecular Chemistry - from Molecular Recognition Towards Molecular Information Processing and Self-Organization. *Angew. Chem. Int. Ed. Engl.* **1990**, *29*, 1304-1319.
2. Cordier, P.; Tournilhac, F.; Soulie-Ziakovic, C.; Leibler, L. Self-Healing and Thermoreversible Rubber from Supramolecular Assembly. *Nature* **2008**, *451*, 977-980.
3. Burattini, S.; Colquhoun, H. M.; Greenland, B. W.; Hayes, W. A Novel Self-Healing Supramolecular Polymer System. *Faraday Discuss.* **2009**, *143*, 251-264; discussion 265-275.
4. Chen, Y.; Kushner, A. M.; Williams, G. A.; Guan, Z. Multiphase Design of Autonomic Self-Healing Thermoplastic Elastomers. *Nat. Chem.* **2012**, *4*, 467-472.
5. Burattini, S.; Colquhoun, H. M.; Fox, J. D.; Friedmann, D.; Greenland, B. W.; Harris, P. J.; Hayes, W.; Mackay, M. E.; Rowan, S. J. A Self-Repairing, Supramolecular Polymer System: Healability as a Consequence of Donor-Acceptor π - π Stacking Interactions. *Chem. Commun.* **2009**, 6717-6719.
6. Chen, S.; Hu, J.; Yuen, C.-w.; Chan, L. Supramolecular Polyurethane Networks Containing Pyridine Moieties for Shape Memory Materials. *Mater. Lett.* **2009**, *63*, 1462-1464.
7. Yan, X.; Wang, F.; Zheng, B.; Huang, F. Stimuli-Responsive Supramolecular Polymeric Materials. *Chem. Soc. Rev.* **2012**, *41*, 6042-6065.
8. Ware, T.; Hearon, K.; Lonneck, A.; Wooley, K. L.; Maitland, D. J.; Voit, W. Triple-Shape Memory Polymers Based on Self-Complementary Hydrogen Bonding. *Macromolecules* **2012**, *45*, 1062-1069.
9. Li, J.; Viveros, J. A.; Wrue, M. H.; Anthamatten, M. Shape-Memory Effects in Polymer Networks Containing Reversibly Associating Side-Groups. *Adv. Mater.* **2007**, *19*, 2851-2855.

10. Beck, J. B.; Rowan, S. J. Multistimuli, Multiresponsive Metallo-Supramolecular Polymers. *J. Am. Chem. Soc.* **2003**, *125*, 13922-13923.
11. Gillies, E. R.; Jonsson, T. B.; Frechet, J. M. Stimuli-Responsive Supramolecular Assemblies of Linear-Dendritic Copolymers. *J. Am. Chem. Soc.* **2004**, *126*, 11936-11943.
12. Ding, Y.; Wang, P.; Tian, Y.-K.; Tian, Y.-J.; Wang, F. Formation of Stimuli-Responsive Supramolecular Polymeric Assemblies Via Orthogonal Metal-Ligand and Host-Guest Interactions. *Chem. Commun.* **2013**, *49*, 5951-5953.
13. Shokrollahi, P.; Mirzadeh, H.; Huck, W. T.; Scherman, O. A. Effect of Self-Complementary Motifs on Phase Compatibility and Material Properties in Blends of Supramolecular Polymers. *Polymer* **2010**, *51*, 6303-6312.
14. Chang, Y.-W.; Mishra, J. K.; Kim, S.-K.; Kim, D.-K. Effect of Supramolecular Hydrogen Bonded Network on the Properties of Maleated Ethylene Propylene Diene Rubber/Maleated High Density Polyethylene Blend Based Thermoplastic Elastomer. *Mater. Lett.* **2006**, *60*, 3118-3121.
15. Burattini, S.; Greenland, B. W.; Merino, D. H.; Weng, W.; Seppala, J.; Colquhoun, H. M.; Hayes, W.; Mackay, M. E.; Hamley, I. W.; Rowan, S. J. A Healable Supramolecular Polymer Blend Based on Aromatic Pi-Pi Stacking and Hydrogen-Bonding Interactions. *J. Am. Chem. Soc.* **2010**, *132*, 12051-12058.
16. Dionisio, M.; Ricci, L.; Pecchini, G.; Masseroni, D.; Ruggeri, G.; Cristofolini, L.; Rampazzo, E.; Dalcanale, E. Polymer Blending through Host-Guest Interactions. *Macromolecules* **2014**, *47*, 632-638.
17. Rieth, L. R.; Eaton, R. F.; Coates, G. W. Polymerization of Ureidopyrimidinone-Functionalized Olefins by Using Late-Transition Metal Ziegler-Natta Catalysts: Synthesis of Thermoplastic Elastomeric Polyolefins. *Angew. Chem. Int. Ed.* **2001**, *40*, 2153-2156.
18. Nojiri, S.; Yamada, H.; Kimata, S.; Ikeda, K.; Senda, T.; Bosman, A. W. Supramolecular Polypropylene with Self-Complementary Hydrogen Bonding System. *Polymer* **2016**, *87*, 308-315.

19. Kautz, H.; van Beek, D.; Sijbesma, R. P.; Meijer, E. Cooperative End-to-End and Lateral Hydrogen-Bonding Motifs in Supramolecular Thermoplastic Elastomers. *Macromolecules* **2006**, *39*, 4265-4267.
20. Tellers, J.; Canossa, S.; Pinalli, R.; Soliman, M.; Vachon, J.; Dalcanale, E. Dynamic Cross-Linking of Polyethylene Via Sextuple Hydrogen Bonding Array. *Macromolecules* **2018**, *51*, 7680-7691.
21. Lehn, J. M. Supramolecular Chemistry. *Science* **1993**, *260*, 1762-1763.
22. Goshe, A. J.; Steele, I. M.; Ceccarelli, C.; Rheingold, A. L.; Bosnich, B. Supramolecular Recognition: On the Kinetic Lability of Thermodynamically Stable Host-Guest Association Complexes. *Proc. Natl. Acad. Sci.* **2002**, *99*, 4823-4829.
23. Grabowski, S. J. Ab Initio Calculations on Conventional and Unconventional Hydrogen Bonds: Study of the Hydrogen Bond Strength. *J. Phys. Chem. A* **2001**, *105*, 10739-10746.
24. Sijbesma, R. P.; Meijer, E. W. Quadruple Hydrogen Bonded Systems. *Chem. Commun.* **2003**, 5-16.
25. Appel, W. P. J.; Nieuwenhuizen, M. M. L.; Meijer, E. W., *Multiple Hydrogen-Bonded Supramolecular Polymers*. Wiley: 2012.
26. Sijbesma, R. P.; Beijer, F. H.; Brunsveld, L.; Folmer, B. J.; Hirschberg, J. K.; Lange, R. F.; Lowe, J. K.; Meijer, E. Reversible Polymers Formed from Self-Complementary Monomers Using Quadruple Hydrogen Bonding. *Science* **1997**, *278*, 1601-1604.
27. Söntjens, S. H.; Sijbesma, R. P.; van Genderen, M. H.; Meijer, E. Stability and Lifetime of Quadruply Hydrogen Bonded 2-Ureido-4 [1 H]-Pyrimidinone Dimers. *J. Am. Chem. Soc.* **2000**, *122*, 7487-7493.
28. Beijer, F. H.; Sijbesma, R. P.; Kooijman, H.; Spek, A. L.; Meijer, E. Strong Dimerization of Ureidopyrimidones Via Quadruple Hydrogen Bonding. *J. Am. Chem. Soc.* **1998**, *120*, 6761-6769.

29. Britain, J.; Gemeinhardt, P. Catalysis of the Isocyanate-Hydroxyl Reaction. *J. Appl. Polym. Sci.* **1960**, *4*, 207-211.
30. Pannone, M. C.; Macosko, C. W. Kinetics of Isocyanate Amine Reactions. *J. Appl. Polym. Sci.* **1987**, *34*, 2409-2432.
31. Blank, W. J.; He, Z.; Hessel, E. T. Catalysis of the Isocyanate-Hydroxyl Reaction by Non-Tin Catalysts. *Prog. Org. Coat.* **1999**, *35*, 19-29.
32. Arnold, R.; Nelson, J.; Verbanc, J. Recent Advances in Isocyanate Chemistry. *Chem. Rev.* **1957**, *57*, 47-76.
33. Zhu, B.; Feng, Z.; Zheng, Z.; Wang, X. Thermoreversible Supramolecular Polyurethanes with Self-Complementary Quadruple Hydrogen-Bonded End Groups. *J. Appl. Polym. Sci.* **2012**, *123*, 1755-1763.
34. Scherz, L. F.; Costanzo, S.; Huang, Q.; Schlüter, A. D.; Vlassopoulos, D. Dendronized Polymers with Ureidopyrimidinone Groups: An Efficient Strategy to Tailor Intermolecular Interactions, Rheology, and Fracture. *Macromolecules* **2017**, *50*, 5176-5187.
35. Feldman, K. E.; Kade, M. J.; Meijer, E.; Hawker, C. J.; Kramer, E. J. Model Transient Networks from Strongly Hydrogen-Bonded Polymers. *Macromolecules* **2009**, *42*, 9072-9081.
36. Teunissen, A. J.; Paffen, T. F.; Ercolani, G.; de Greef, T. F.; Meijer, E. Regulating Competing Supramolecular Interactions Using Ligand Concentration. *J. Am. Chem. Soc.* **2016**, *138*, 6852-6860.
37. Bosman, A. W.; Janssen, H. M.; van Gemert, G. M. L.; Versteegen, R. M.; Meijer, E. W.; Sijbesma, R. P. Siloxane Polymers with Quadruple Hydrogen Bonding Units. WO2004052963, 2004.
38. Janssen, H. M.; van Gemert, G. M. L.; Meijer, E. W.; Bosman, A. W. Preparation of Supramolecular Polymers Containing Quadruple Hydrogen Bonding Units in the Polymer Backbone. WO2005042641 A1, 2005.

39. Celiz, A. D.; Scherman, O. A. Controlled Ring-Opening Polymerization Initiated Via Self-Complementary Hydrogen-Bonding Units. *Macromolecules* **2008**, *41*, 4115-4119.
40. Lewis, C. L.; Anthamatten, M. Synthesis, Swelling Behavior, and Viscoelastic Properties of Functional Poly(Hydroxyethyl Methacrylate) with Ureidopyrimidinone Side-Groups. *Soft Matter* **2013**, *9*, 4058-4066.
41. Lewis, C. L.; Stewart, K.; Anthamatten, M. The Influence of Hydrogen Bonding Side-Groups on Viscoelastic Behavior of Linear and Network Polymers. *Macromolecules* **2014**, *47*, 729-740.
42. Heinzmann, C.; Lamparth, I.; Rist, K.; Moszner, N.; Fiore, G. L.; Weder, C. Supramolecular Polymer Networks Made by Solvent-Free Copolymerization of a Liquid 2-Ureido-4[1h]-Pyrimidinone Methacrylamide. *Macromolecules* **2015**, *48*, 8128-8136.
43. Keizer, H. M.; van Kessel, R.; Sijbesma, R. P.; Meijer, E. Scale-up of the Synthesis of Ureidopyrimidinone Functionalized Telechelic Poly (Ethylenebutylene). *Polymer* **2003**, *44*, 5505-5511.
44. Nojiri, S.; Kimata, S.; Ikeda, K.; Senda, T.; Bosman, A. W.; Peeters, J. W.; Janssen, H. M. Novel Supramolecular Block Copolymer of Isotactic Polypropylene and Ethylene-Co-Propylene Connected by Complementary Quadruple Hydrogen Bonding System. *Macromolecules* **2017**, *50*, 5687-5694.
45. Tzoganakis, C. Reactive Extrusion of Polymers: A Review. *Adv. Polym. Tech.* **1989**, *9*, 321-330.
46. Raquez, J.-M.; Narayan, R.; Dubois, P. Recent Advances in Reactive Extrusion Processing of Biodegradable Polymer-Based Compositions. *Macromol. Mater. Eng.* **2008**, *293*, 447-470.
47. Ganzeveld, K. J.; Janssen, L. P. B. M. The Grafting of Maleic Anhydride on High Density Polyethylene in an Extruder. *Polym. Eng. Sci.* **1992**, *32*, 467-474.

48. Cartier, H.; Hu, G.-H. Styrene-Assisted Free Radical Grafting of Glycidyl Methacrylate onto Polyethylene in the Melt. *J. Polym. Sci., Part A: Polym. Chem.* **1998**, *36*, 2763-2774.
49. Garnier, L.; Duquesne, S.; Casetta, M.; Lewandowski, M.; Bourbigot, S. Melt Spinning of Silane–Water Cross-Linked Polyethylene–Octene through a Reactive Extrusion Process. *React. Funct. Polym.* **2010**, *70*, 775-783.
50. Sharif-Pakdaman, A.; Morshedian, J.; Jahani, Y. Influence of the Silane Grafting of Polyethylene on the Morphology, Barrier, Thermal, and Rheological Properties of High-Density Polyethylene/Organoclay Nanocomposites. *J. Appl. Polym. Sci.* **2012**, *125*, E305-E313.
51. Cheung, P.; Suwanda, D.; Balke, S. T. The Reactive Extrusion of Polyethylene/Polypropylene Blends. *Polym. Eng. Sci.* **1990**, *30*, 1063-1072.
52. Teh, J. W.; Rudin, A. Compatibilization of a Polystyrene-Polyethylene Blend through Reactive Processing in a Twin Screw Extruder. *Polym. Eng. Sci.* **1992**, *32*, 1678-1686.
53. Kelar, K.; Jurkowski, B. Preparation of Functionalised Low-Density Polyethylene by Reactive Extrusion and Its Blend with Polyamide 6. *Polymer* **2000**, *41*, 1055-1062.
54. Wang, S.; Yu, J.; Yu, J. Compatible Thermoplastic Starch/Polyethylene Blends by One-Step Reactive Extrusion. *Polym. Int.* **2005**, *54*, 279-285.
55. Wang, K. H.; Choi, M. H.; Koo, C. M.; Choi, Y. S.; Chung, I. J. Synthesis and Characterization of Maleated Polyethylene/Clay Nanocomposites. *Polymer* **2001**, *42*, 9819-9826.
56. Bengtsson, M.; Stark, N. M.; Oksman, K. Durability and Mechanical Properties of Silane Cross-Linked Wood Thermoplastic Composites. *Compos. Sci. Technol.* **2007**, *67*, 2728-2738.
57. Grubbström, G.; Holmgren, A.; Oksman, K. Silane-Crosslinking of Recycled Low-Density Polyethylene/Wood Composites. *Compos. Part. A: Appl. Sci. Manuf.* **2010**, *41*, 678-683.

58. Szycher, M., *Szycher's Handbook of Polyurethanes*. CRC press: 2012.
59. Hepburn, C., *Polyurethane Elastomers*. Springer: 1992.
60. Wunderlich, B.; Cormier, C. M. Heat of Fusion of Polyethylene. *J. Polym. Sci., Part A-2: Polym. Phys.* **1967**, *5*, 987-988.
61. Armstrong, G.; Buggy, M. Thermal Stability of a Ureidopyrimidinone Model Compound. *Mater. Sci. Eng., C* **2001**, *18*, 45-49.
62. van Beek, D.; Spiering, A.; Peters, G. W.; Te Nijenhuis, K.; Sijbesma, R. P. Unidirectional Dimerization and Stacking of Ureidopyrimidinone End Groups in Polycaprolactone Supramolecular Polymers. *Macromolecules* **2007**, *40*, 8464-8475.
63. van Gemert, G. M. L.; Janssen, H. M.; Meijer, E. W.; Bosman, A. W. Supramolecular Polymers from Low-Melting, Easily Processable Building Blocks. US14057893, 2015.
64. Botterhuis, N. E.; van Beek, D.; van Gemert, G. M.; Bosman, A. W.; Sijbesma, R. P. Self-Assembly and Morphology of Polydimethylsiloxane Supramolecular Thermoplastic Elastomers. *J. Polym. Sci., Part A: Polym. Chem.* **2008**, *46*, 3877-3885.
65. Kamykowski, G. W., *Handbook of Industrial Polyethylene and Technology: Definitive Guide to Manufacturing, Properties, Processing, Applications and Markets*. Wiley: 2017.
66. Osswald, T. A.; Rudolph, N., *Polymer Rheology: Fundamentals and Applications*. Hanser Publications: 2014.
67. Skuches, G.; Carleton, P. Correlation of Urea Structure with Thermal Stability in Model Compounds. *J. Appl. Polym. Sci.* **1984**, *29*, 3431-3443.
68. Cogswell, F. N., *Polymer Melt Rheology: A Guide for Industrial Practice*. Elsevier: 1981.
69. Deng, G.; Tang, C.; Li, F.; Jiang, H.; Chen, Y. Covalent Cross-Linked Polymer Gels with Reversible Sol– Gel Transition and Self-Healing Properties. *Macromolecules* **2010**, *43*, 1191-1194.

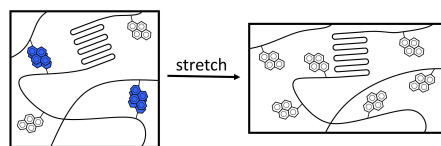
70. Zhou, Y.; Goossens, J. G.; Sijbesma, R. P.; Heuts, J. P. Poly (Butylene Terephthalate)/Glycerol-Based Vitrimers Via Solid-State Polymerization. *Macromolecules* **2017**, *50*, 6742-6751.
71. Bosman, A. W.; Sijbesma, R. P.; Meijer, E. Supramolecular Polymers at Work. *Mater. Today* **2004**, *7*, 34-39.
72. Folmer, B. J.; Sijbesma, R.; Versteegen, R.; van der Rijt, J.; Meijer, E. Supramolecular Polymer Materials: Chain Extension of Telechelic Polymers Using a Reactive Hydrogen-Bonding Synthron. *Adv. Mater.* **2000**, *12*, 874-878.
73. Seiffert, S.; Kumacheva, E.; Okay, O.; Anthamatten, M.; Chau, M.; Dankers, P. Y.; Greenland, B. W.; Hayes, W.; Li, P.; Liu, R., *Supramolecular Polymer Networks and Gels*. Springer: 2016.
74. Elkins, C. L.; Viswanathan, K.; Long, T. E. Synthesis and Characterization of Star-Shaped Poly (Ethylene-Co-Propylene) Polymers Bearing Terminal Self-Complementary Multiple Hydrogen-Bonding Sites. *Macromolecules* **2006**, *39*, 3132-3139.
75. Sauer, J.; Woodward, A. Transitions in Polymers by Nuclear Magnetic Resonance and Dynamic Mechanical Methods. *Rev. Mod. Phys.* **1960**, *32*, 88.
76. Martín, S.; Vega, J. F.; Expósito, M. T.; Flores, A.; Martínez-Salazar, J. A Three-Phase Microstructural Model to Explain the Mechanical Relaxations of Branched Polyethylene: A Dsc, Waxd and Dmta Combined Study. *Colloid. Polym. Sci.* **2011**, *289*, 257-268.
77. Pathmanathan, K.; Johari, G. Dielectric and Conductivity Relaxations in Poly (Hema) and of Water in Its Hydrogel. *J. Polym. Sci., Part B: Polym. Phys.* **1990**, *28*, 675-689.
78. Xu, M.-m.; Huang, G.-y.; Feng, S.-s.; McShane, G. J.; Stronge, W. J. Static and Dynamic Properties of Semi-Crystalline Polyethylene. *Polymers* **2016**, *8*, 77.
79. Elkins, C. L.; Park, T.; McKee, M. G.; Long, T. E. Synthesis and Characterization of Poly (2-Ethylhexyl Methacrylate) Copolymers Containing

- Pendant, Self-Complementary Multiple-Hydrogen-Bonding Sites. *J. Polym. Sci., Part A: Polym. Chem.* **2005**, *43*, 4618-4631.
80. Litvinov, V.; Ries, M.; Baughman, T.; Henke, A.; Matloka, P. Chain Entanglements in Polyethylene Melts. Why Is It Studied Again? *Macromolecules* **2013**, *46*, 541-547.

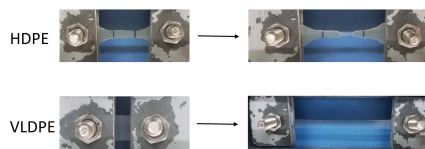
Chapter 3

Pyrene functionalized polyethylene^a

High density and very low density polyethylene-graft-maleic anhydride (HDPE-MAH and VLDPE-MAH respectively) functionalized with 1-aminopyrene (AP) were prepared via reactive extrusion. Covalent attachment of AP was confirmed by lack of residual free AP



= PE = pyrene = pyrene excimer



after extraction with dichloromethane. Differential scanning calorimetry (DSC), tensile test, dynamical mechanical thermal analysis (DMTA) and rheology were employed to investigate the influence of AP incorporation on thermal, mechanical and rheological properties when grafted on both HD and VLDPE-MAHs. Fluorescent emission spectroscopy revealed pronounced changes in fluorescent behavior under stress due to the breakup of the pyrene excimers. For HDPE-MAH-AP this change was very sudden with a clear drop of excimer content (I_E/I_M) of around 50 % due to necking of the material stretched above 50 % strain. In contrast, VLDPE-MAH-AP showed no necking and a linear decrease of I_E/I_M ratio down to around 30 % when elongation up to 1100 % strain was reached while HDPE-MAH-AP broke after 200 % strain.

^a The content of this chapter has been submitted for publication to *Eur. Pol. J.*: A. Zych, A. Verdelli, M. Soliman, R. Pinalli, A. Pedrini, J. Vachon, E. Dalcanale, Strain-reporting pyrene-grafted polyethylene.

3.1 Introduction

The monitoring of strain in polymeric materials is of great importance to prevent premature failure like stress fracture or fatigue.¹ Polyethylene (PE) is the most widely used commodity thermoplastics due to its good solvent resistance, excellent flexibility, low cost and ease of processing, thanks to which it finds application in automotive, medicine, aerospace and electronic industries.^{2, 3} Despite the wide use, PE suffers from premature failure like stress cracking of pipes,⁴⁻⁶ cables^{7, 8} and storage tanks⁹ as well as of laboratory supplies and implants for medical applications, which could be prevented by suitable monitoring. One of the most promising tools for strain detection in polymers is fluorescent emission spectroscopy.¹ This noninvasive method allows for a real time *in situ* analysis and it is based on a mechanochromic polymer containing a fluorophore showing changes in fluorescence in response to a mechanical stimulus.^{10, 11} Changes in fluorescence during deformation can be induced by an altered aggregation or alignment of the fluorophore, typically transition from an excimer to a monomer due to the separation of the aggregates^{11, 12} or aggregation-induced emission phenomena.^{13, 14} Fluorophores are typically dispersed in the bulk of the appropriate polymer matrix by means of solution or melt blending. The polymer chains remain structurally unaltered and the obtained material is generally biphasic unless the used dye is fully soluble in the polymer.¹⁰ During the lifetime of the material, the dye usually migrates from the core to the surface and will alter the fluorescence properties of the material. To circumvent that problem, efforts are being put into the preparation of

mechanochromic polymers with fluorophores covalently attached to the macromolecular chains. This method allows to obtain a material with homogeneously distributed fluorophore molecules preventing its diffusion, leaching and segregation. However, the need of appropriate functional groups on both macromolecules and fluorophores limits its applications.^{1, 10} Even more demanding is the grafting procedure, which must be as simple and cheap as possible, particularly for commodity polymers.

Despite the extensive research on mechanochromic polymers in recent years, PE with covalently attached fluorophores remains mainly unexplored as PE lacks proper functionality allowing such grafting. The group of Weder and Crenshaw published reports on mechanochromic blends of PE and cyano-oligo(*p*-phenylene vinylene).^{15, 16} The mechanical deformation of those materials led to a pronounced change in photoluminescent characteristics and when the strain reached 500 %, the monomer to excimer emission ratios I_M/I_E were increased by a factor of up to 10 (Figure 1A and B). Kunzelman *et al.* reported on self-assessing polymer blends based on poly(ethylene terephthalate glycol) and linear low density polyethylene (LLDPE) with a cyano-substituted oligo(*p*-phenylene vinylene) obtained by melt-processing and subsequent quenching below T_g (Figure 1C).¹⁷ Ruggeri *et al.* reported on two perylene tetracarboxylic acid bis-imides containing linear or branched alkyl chains dispersed in LLDPE at low loadings by melt processing (Figure 1D).¹⁸ To the best of our knowledge, strain detection in polyethylene with covalently attached fluorophores is unprecedented. Brown *et al.* investigated selectivity and efficiency of pyrene attachment to polyethylene

films by bombardment with MeV-range protons; however, the potential of this material as strain detector was not explored.¹⁹

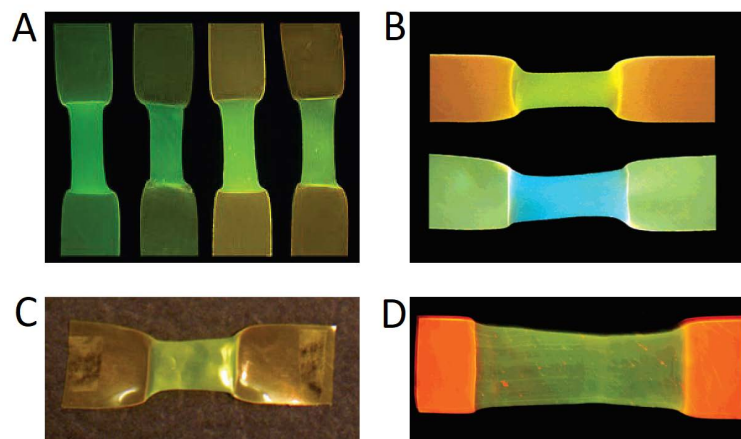


Figure 1. **A:** Picture of HDPE films containing 0.1, 0.2, 0.4, or 0.8 wt% of bis(R-cyano-4-octadecyloxy-styryl)-2,5-dimethoxybenzene deformed to around 400 % draw ratio.¹⁵ **B:** Picture of LLDPE films containing 0.18 wt% of 1,4-bis(R-cyano-4-methoxystyryl)-2,5-dimethoxybenzene (top) and 0.20 wt% of 1,4-bis(R-cyano-4-methoxystyryl) benzene (bottom) stretched at room temperature to a draw ratio of 500 %. The pictures were taken under excitation with UV light of a wavelength of 365 nm.¹⁶ **C:** Picture of LLDPE film containing 1 wt% of bis(R-cyano-4-octadecyloxy-styryl)-2,5-dimethoxybenzene stretched to a draw ratio of around 300 %.¹⁷ **D:** Picture of LDPE film containing 0.1 wt% of N,N'-bis-(2'-ethylhexyl)perylene-3,4,9,10-tetracarboxyldiimide film stretched to a draw ratio of around 400 % under excitation with UV light of a wavelength of 366 nm.¹⁸

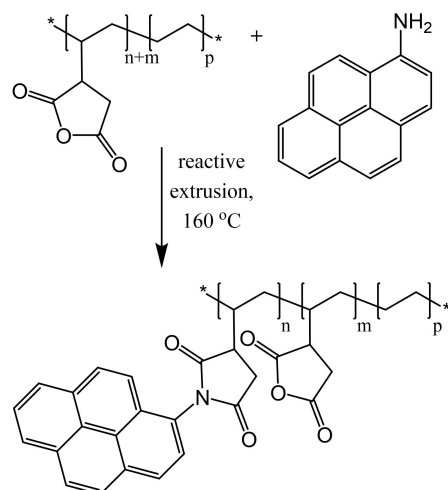
Herein, we describe a strain-reporting polymer based on polyethylene-*graft*-maleic anhydride (PE-MAH) with covalently attached pyrene as a fluorophore, produced directly *via* reactive extrusion. Both HDPE-MAH and VLDPE-MAH were functionalized with 1-aminopyrene (AP) and their changes in fluorescence as a response to stress were investigated. The thermal, rheological and mechanical properties of both

pyrene functionalized polymers were also tested in comparison with those of the pristine samples.

3.2 Results and discussion

3.2.1 AP reactive extrusion grafting onto PE-MAHs

1-Aminopyrene (AP) was used as a fluorophore of choice thanks to pyrene's clear and well-separated monomer and excimer emissions both in solution and in the solid state, long singlet monomer excited state fluorescence life time, high luminescence quantum yield as well as chemical and thermal robustness.^{20,21} For the synthesis of pyrene functionalized PE, two types of polyethylene grafted with maleic anhydride were selected: highly crystalline, stiff HDPE and more elastic VLDPE with low crystallinity (Table 1). To graft AP onto PE-MAHs a reaction between amino group of AP and maleic anhydride forming a robust maleimide was used (Scheme 1).²²⁻²⁵ The reactions were performed at 160 °C in a corotating twin-screw micro extruder allowing to eliminate the use of solvents.



Scheme 1. AP reactive extrusion grafting onto PE-MAHs.

Increasing amount of AP was introduced ranging from 0.01 to 1 % leaving always the excess of MAH to achieve complete grafting, which was confirmed by extraction with DCM as no free AP could be detected by ^1H NMR (Figure appx 3 and Figure appx 4). The covalent attachment of AP to polyethylene backbone prevents leaching, ensuring a long-term stability.²⁶⁻²⁸ Incorporation of AP within the studied range did not influence significantly thermal properties of PE-MAHs as indicated by DSC measurements (Figure appx 5 and Figure appx 6). AP content, melting temperatures (T_m), degrees of crystallinity (X_{cr}) as well as number average molecular weights (M_n) and molecular weight distributions (\mathcal{D}_M) of the samples are listed in Table 1.

Table 1. MAH and AP content, melting temperatures (T_m), degrees of crystallinity (X_{cr}) as well as number average molecular weights (M_n) and the molecular weight distributions (\mathcal{D}_M) of PE-MAHs and corresponding PE-MAH-APs.^a

Polymer	MAH ^b [mol%]	AP [wt%]	T_m ^c [°C]	X_{cr} ^d [%]	M_n ^e [g/mol]	\mathcal{D}_M ^e
HDPE-MAH	0.7	-	125.7	53.9	6 000	3.7
1 (HDPE-MAH-AP)	-	0.01	127.7	42.6	-	-
2 (HDPE-MAH-AP)	-	0.1	128.2	42.2	-	-
3 (HDPE-MAH-AP)	-	1	127.9	42.3	-	-
VLDPE-MAH	1.2	-	76.6	3.8	4 500	5.3
4 (VLDPE-MAH-AP)	-	0.01	73.4	4.1	-	-
5 (VLDPE-MAH-AP)	-	0.1	73.6	3.7	-	-
6 (VLDPE-MAH-AP)	-	1	73.6	3.4	-	-

^a Conditions: reactive extrusion grafting was carried in a 15 mL twin crew micro extruder for 10 min at 160 °C and a screw speed of 100 RPM. ^b MAH content was calculated from the ¹H NMR (120 °C, TCE-*d*₂).

^c Melting temperatures (T_m) were determined by DSC from the second heating scan. ^d Degrees of crystallinity (X_{cr}) were calculated dividing the melting enthalpy of 100 % crystalline PE (286.2 J/g)²⁹ by melting enthalpy of a polymer determined by DSC from the second heating scan. ^e Molecular weight and dispersity were determined by SEC in *o*DCB at 150 °C with respect to polyethylene standards.

Tensile test, DMTA and rheology were employed to investigate the impact of AP on mechanical performance and flow behavior of PE-MAH-APs. Tensile and DMTA curves before and after introduction of 1 % of AP were almost identical as well as rheology frequency sweeps, proving that mechanical properties and flow behavior remained unaltered (Figure appx 7 - Figure appx 12).

3.2.2 PE-MAH-AP fluorescent characterization

To investigate the amount of excimer present in PE-MAHs containing different amount of AP, fluorescence emission spectra were recorded (Figure 2). Samples containing low amount of pyrene (0.01 to 0.1 %) exhibit a low excimer formation ($I_E/I_M < 0.1$) and only when the pyrene content was increased to 1 % a pronounced broad peak around 465 nm was observed confirming the excimer formation in PE matrix. Interestingly HDPE-MAH-AP materials contain more excimer than VLDPE-MAH-AP ones. Since grafted AP is present solely in the amorphous phase (no significant decrease in melting point or degree of crystallinity after AP grafting was observed),³⁰ which is less abundant in HDPE than VLDPE, pyrene groups in HDPE are more concentrated leading to increased excimer formation.

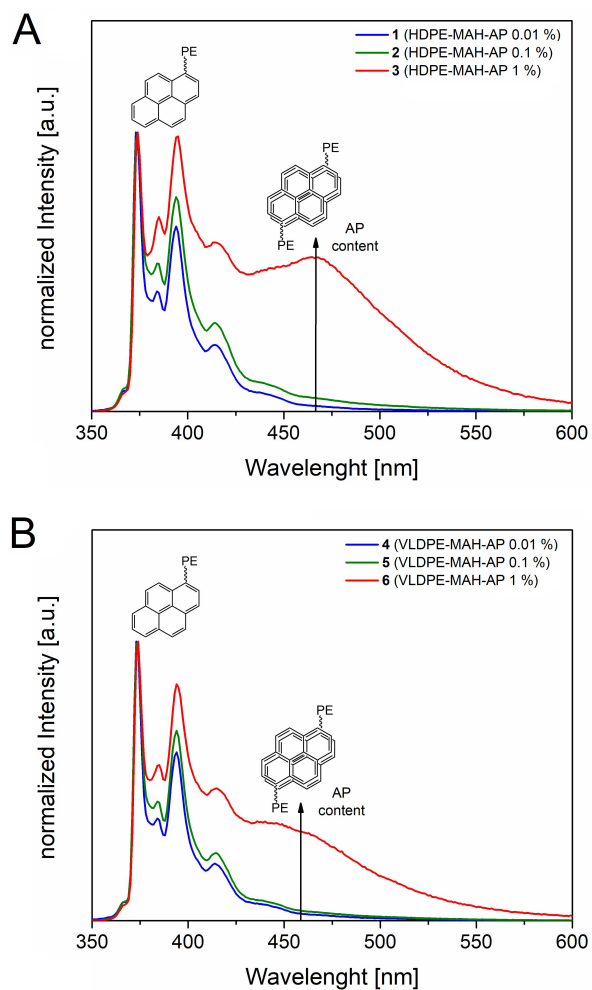


Figure 2. Normalized fluorescence spectra of **A**: HDPE samples grafted with AP (polymer **1**, **2** and **3**) and **B**: VLDPE samples grafted with AP (polymer **4**, **5** and **6**).

Samples grafted with 1 % of AP, therefore containing the highest amount of excimer, were selected to investigate the fluorescent behavior under stress. Specimens for testing were prepared by compression molding, mounted in a metal frame between clamps and subjected to stretching with 5 mm increments. After each stretching step, the frame containing the sample was placed in the spectrofluorimeter and the emission spectrum was

recorded. As expected, stress induced plastic deformation broke the excimers which manifested itself in the decrease of the I_E/I_M ratio. Due to the different tensile properties of HDPE-MAH and VLDPE-MAH, a different fluorescent behavior under stress was observed. Polymer **3** (HDPE-MAH-AP 1 %) showed necking after 50 % strain and a clear drop of around 50 % of I_E/I_M ratio was observed when the emission spectrum was collected from the neck area (Figure 3A). Samples of polymer **3** failed when the strain exceeded 200 %. In contrast, polymer **6** (VLDPE-MAH-AP 1 %) showed no necking and a linear decrease of I_E/I_M ratio with elongation down to around 30 % for 1100 % strain was observed, which is the maximum elongation the device can allow (Figure 3B). The linear relationship between the extension ratio and excimer content of polymer **6** (VLDPE-MAH-AP 1 %) can be used as a calibration line for the construction of a strain-reporting polyethylene sensor.

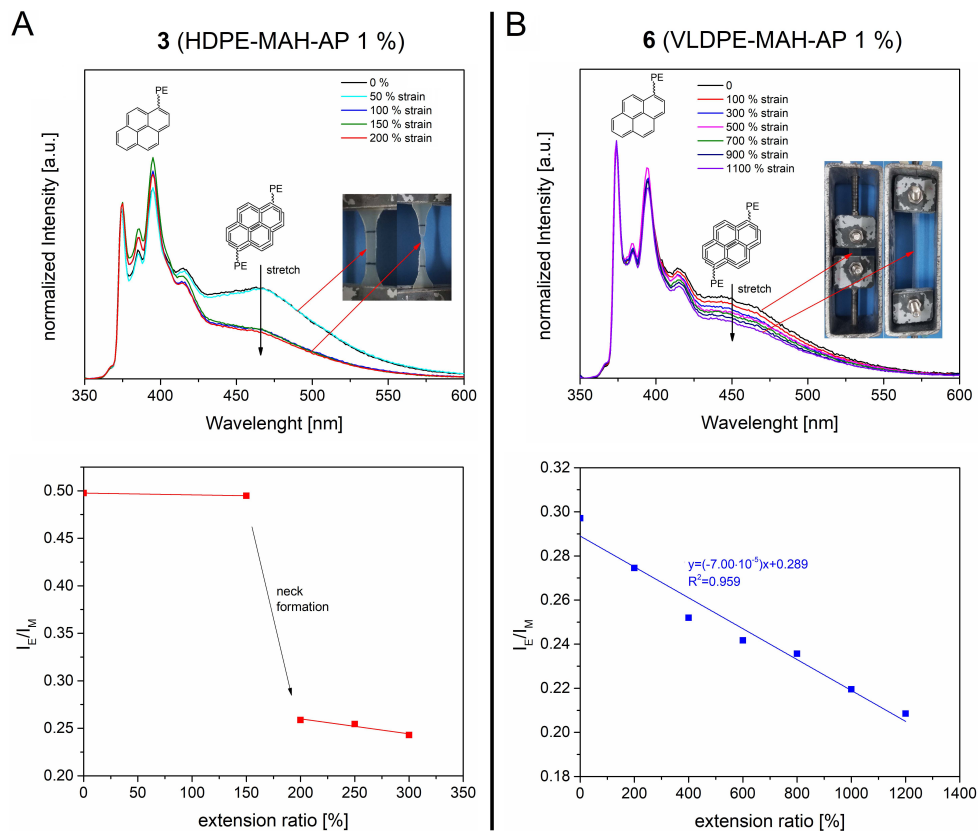


Figure 3. Fluorescent behavior under stress of **A**: polymer **3** (HDPE-MAH-AP 1 %) and **B**: polymer **6** (VLDPE-MAH-AP 1 %).

3.3 Conclusions

Reactive extrusion was successfully employed as an efficient and practical method to covalently functionalize PE-MAHs with increasing amounts of AP (from 0.01 to 1 %). The resulting strain-reporting PE retains similar mechanical, thermal and rheological properties to that of the starting PE-MAH materials. Both polymers **3** (HDPE-MAH-AP 1 %) and **6** (VLDPE-MAH-AP 1 %) showed pronounced fluorescence changes under

stress which could be correlated to their different tensile properties. Around 50 % drop of the excimer content (I_E/I_M) in polymer **3** was observed when the elongation exceeded 50 % which could be related to a neck formation. In contrast, polymer **6** showed no necking and a linear decrease of the excimer content (I_E/I_M) with elongation up to 1100 %. The results demonstrate a significant potential for the development of a strain-reporting PE directly *via* reactive extrusion. This solution is applicable not only for PE but also for any thermoplastic bearing maleic anhydride units.

3.4 Experimental section

Materials

Chloroform, dichloromethane (DCM) 1,2-dichlorobenzene (*o*DCB), deuterated chloroform ($CDCl_3$), deuterated tetrachloroethene ($TCE-d_2$) and 1-aminopyrene (AP, 97 %) were purchased from Sigma-Aldrich. High density polyethylene-*graft*-maleic anhydride (HDPE-MAH) was kindly provided by SABIC. Very low density polyethylene-*graft*-maleic anhydride (VLDPE-MAH) was purchased from YPAREX. All materials were used as received unless otherwise stated.

Typical procedure for pyrene reactive extrusion grafting onto polyethylene-*graft*-maleic anhydride (PE-MAH)

VLDPE-MAH (9.9 g) and AP (0.1 g, 0.46 mmol) were mixed in a metal cup and subsequently fed into a 15 mL corotating twin-crew micro extruder. The reaction mixture was processed for 10 min at 160 °C and a screw speed of

100 RPM after which the discharge valve was opened. The amount of grated AP was determined from the weight ratio of the polymer and AP fed into the extruder. Extraction experiments proved that all AP has reacted (see below) and ^1H NMR showed the resonances of grafted pyrene at AP concentration of 1 % (and Figure appx 2).

Typical procedure for PE-MAH-AP extraction with DCM

A piece of PE-MAH-AP polymer (around 200 mg) was placed in a vial and 5 mL of DCM was added. The vial was closed and left at RT for 24 h. Subsequently, DCM was evaporated, the vial was washed with 0.5 mL of CDCl_3 and ^1H NMR of the solution was recorded to detect if any free AP was present (Figure appx 3 and Figure appx 4).

Measurements

^1H NMR analysis was carried out either at room temperature or at 120 °C using deuterated chloroform (CDCl_3) or deuterated tetrachloroethene ($\text{TCE-}d_2$) as solvents and recorded in 5 mm tubes on a Varian Mercury spectrometer operating at frequencies of 400 MHz. Chemical shifts are reported in ppm versus tetramethylsilane and were determined by reference to the residual solvent signal.

The molecular weight and dispersity were studied by size exclusion chromatography (SEC) measurements performed at 150 °C on a Polymer Char GPC-IR[®] built around an Agilent GC oven model 7890, equipped with an autosampler and the Integrated Detector IR4. *o*DCB was used as an eluent at a flow rate of 1 mL/min. The SEC data were processed

using Calculations Software GPC One®. The molecular weights were calculated with respect to polyethylene standards.

Melting temperatures (T_m) and enthalpies of the transition (ΔH_m) were measured by differential scanning calorimetry (DSC) using a DSC Q100 from TA Instruments. The measurements were carried out at a heating and cooling rate of 10 °C/min from -20 °C to 150 °C. The transitions were deduced from the second heating curves (Figure appx 5 and Figure appx 6).

Fluorescence emission spectra were measured in a solid state (film thickness around 100 μm) on a Horiba Jobin Yvon Fluoromax-3 spectrofluorometer equipped with a xenon arc lamp as a light source using excitation wavelength of 320 nm.

Tensile tests were performed with a Zwick Z100 tensile tester equipped with a 100 N load cell. The tests were performed on injection molded tensile bars. The samples were pre-stressed to 0.3 MPa, then loaded with a constant cross-head speed of 50 mm/min (Figure appx 7 and Figure appx 8).

Rheology was measured using TA Instruments DHR-2 equipped with a parallel plate geometry. Discs with diameter of 25 mm and thickness of 1 mm were injection molded at 160 °C. Frequency sweeps were measured from 100 to 0.1 rad/s (strain amplitude of 0.4 %) at a temperature of 160 °C (Figure appx 9 and Figure appx 10).

Dynamical mechanical thermal analysis (DMTA) was measured using TA Instruments Q800 in tensile mode. The specimens were compression molded at 160 °C. Samples were measured from -100 to 200 °C with a heating speed of 3 °C/min and a fixed oscillation (amplitude 10 μm , frequency 1 Hz, Figure appx 11 and Figure appx 12).

3.5 Appendix

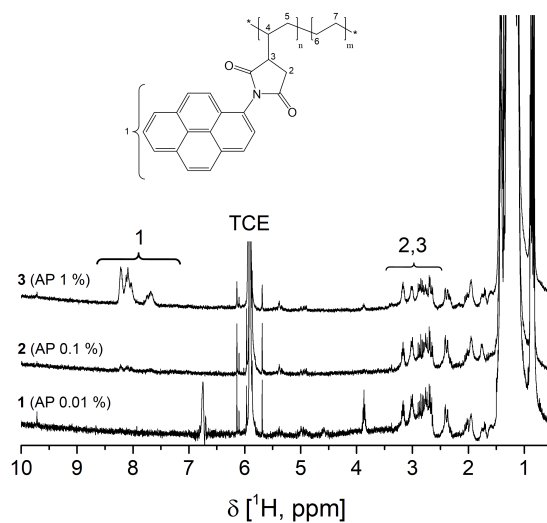


Figure appx 1. ^1H NMR spectra overlay of HDPE-MAH and 1, 2 and 3 (HDPE-MAH-AP) recorded at 120 °C in deuterated TCE.

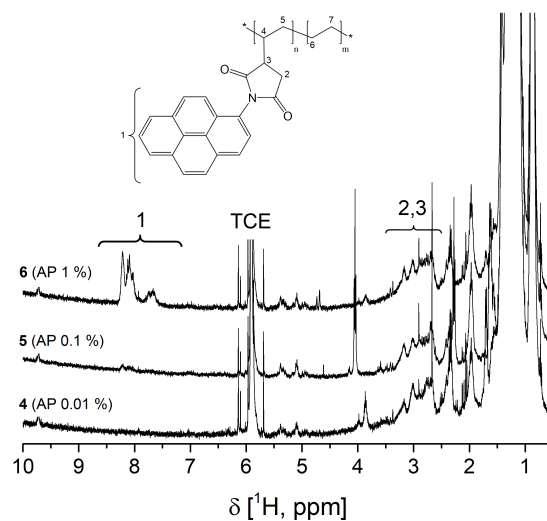


Figure appx 2. ^1H NMR spectra overlay of VLDPE MAH and 4, 5 and 6 (VLDPE-MAH-AP) recorded at 120 °C in deuterated TCE.

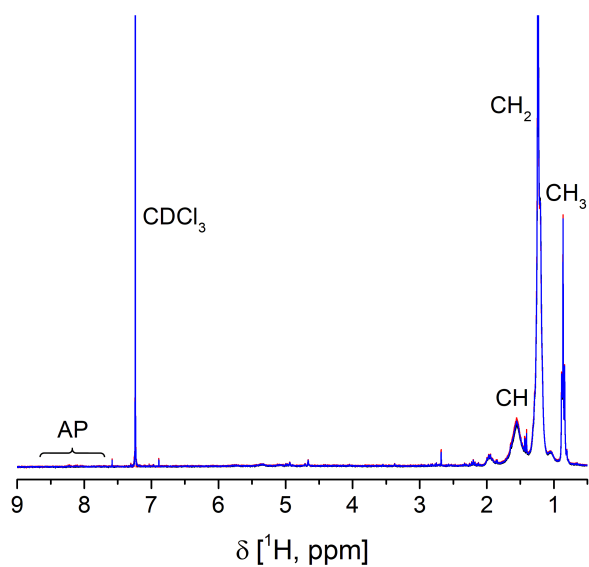


Figure appx 3. ^1H NMR spectra overlay after extraction of **1**, **2** and **3** (HDPE-MAH-AP) with DCM recorded at RT in CDCl_3 .

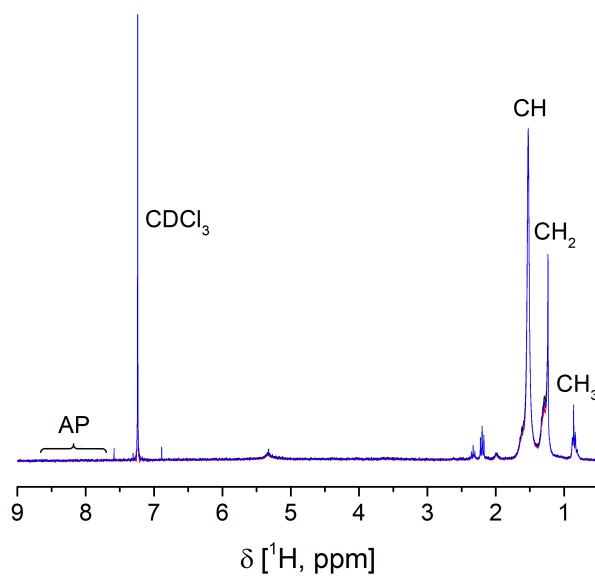


Figure appx 4. ^1H NMR spectra overlay after extraction of **4**, **5** and **6** (VLDPE-MAH-AP) with DCM recorded at RT in CDCl_3 .

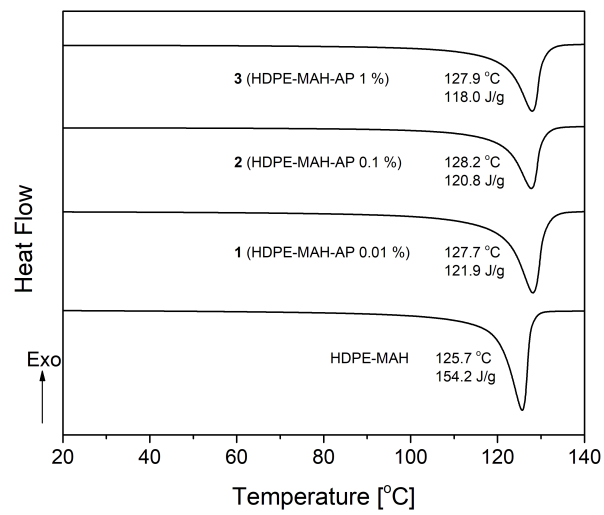


Figure appx 5. DSC second heating curves of HDPE-MAH and 1, 2 and 3 (HDPE-MAH-AP).

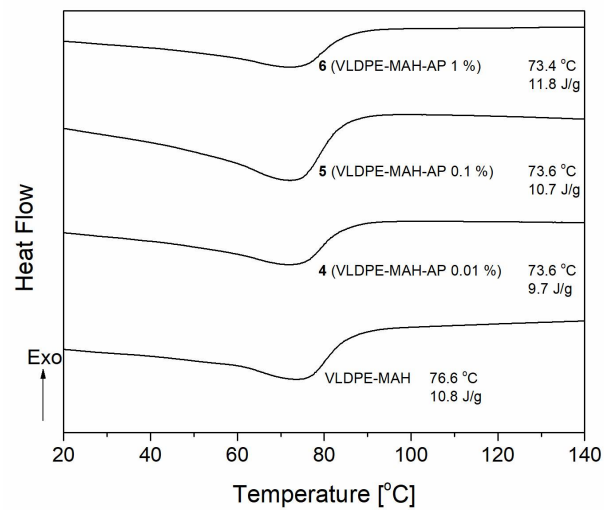


Figure appx 6. DSC second heating curves of VLDPE-MAH and 4, 5 and 6 (VLDPE-MAH-AP).

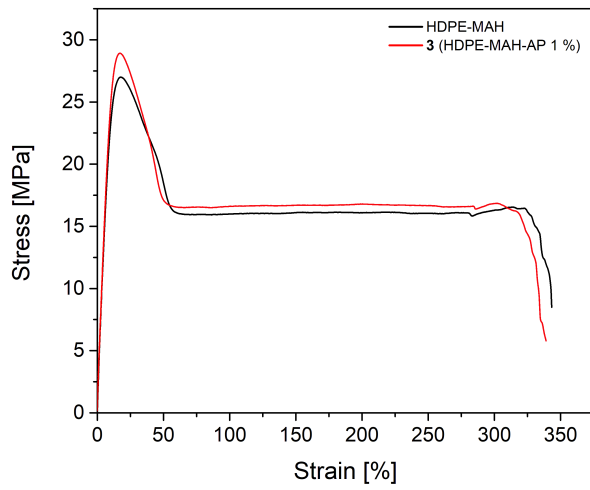


Figure appx 7. Representative stress-strain curves of HDPE-MAH and **3** (HDPE-MAH AP %).

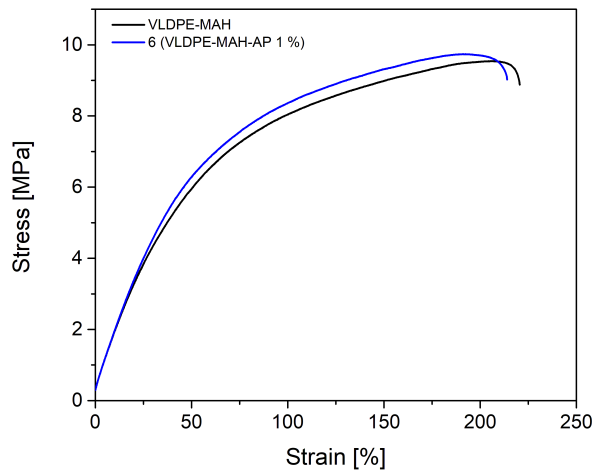


Figure appx 8. Representative stress-strain curves of VLDPE-MAH and **6** (VLDPE-MAH-AP 1 %).

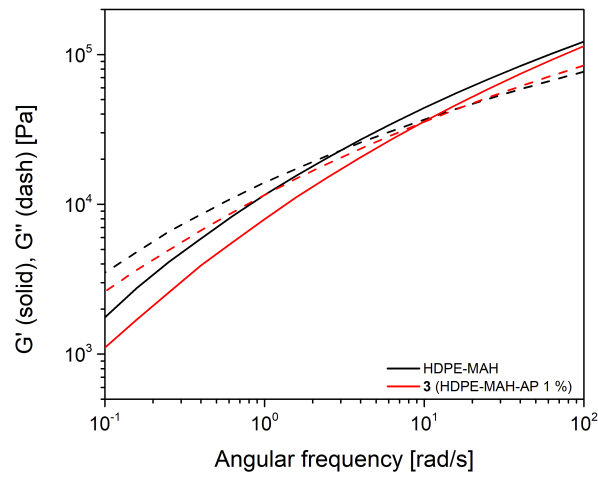


Figure appx 9. Rheology frequency sweep curves of HDPE-MAH and 3 (HDPE-MAH-AP 1 %), storage modulus (G') - solid line, loss modulus (G'') - dash line.

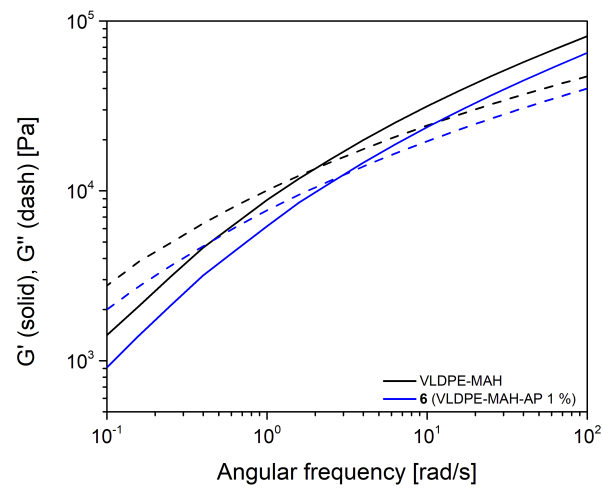


Figure appx 10. Rheology frequency sweep curves of VLDPE-MAH and 6 (VLDPE-MAH-AP 1 %), storage modulus (G') - solid line, loss modulus (G'') - dash line.

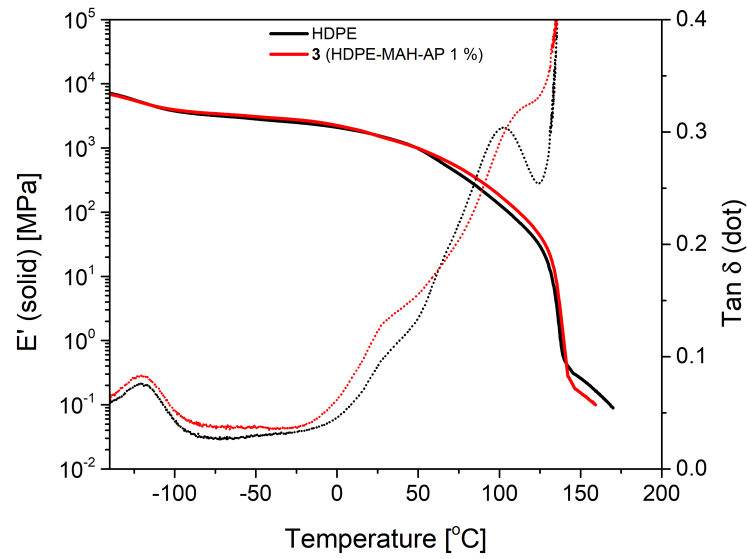


Figure appx 11. DMTA curves of HDPE-MAH and 3 (HDPE-MAH-AP 1 %), storage modulus (E') - solid line, tangent delta (tan δ) - dot line.

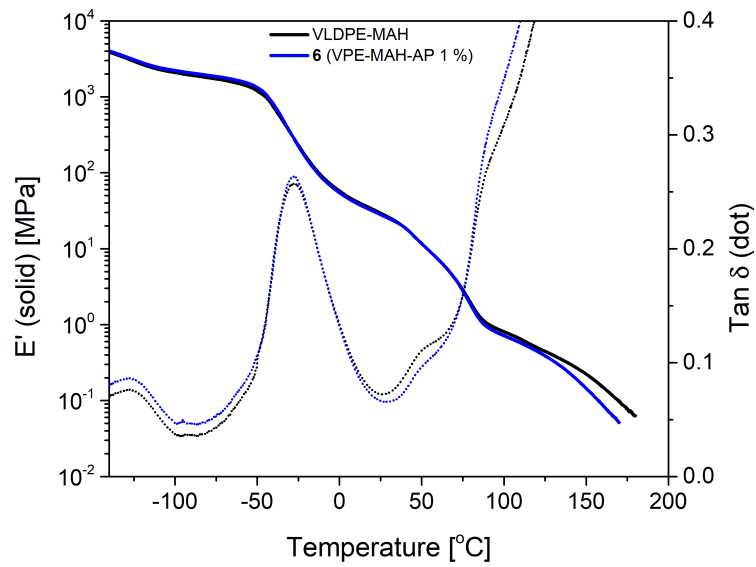


Figure appx 12. DMTA curves of VLDPE-MAH and 6 (VLDPE-MAH-AP 1 %), storage modulus (E') - solid line, tangent delta (tan δ) - dot line.

3.6 References

1. Roberts, D. R. T.; Holder, S. J. Mechanochromic Systems for the Detection of Stress, Strain and Deformation in Polymeric Materials. *J. Mater. Chem.* **2011**, *21*, 8256-8268.
2. Kaminsky, W., *Polyolefins: 50 Years after Ziegler and Natta II*. Springer: 2013.
3. Vasile, C., *Handbook of Polyolefins*. CRC Press: 2000.
4. Bohm, L. L.; Enderle, H. F.; Fleißner, M. High-Density Polyethylene Pipe Resins. *Adv. Mater.* **1992**, *4*, 234-238.
5. Hamouda, H. B. H.; Simoes-betbeder, M.; Grillon, F.; Blouet, P.; Billon, N.; Piques, R. Creep Damage Mechanisms in Polyethylene Gas Pipes. *Polymer* **2001**, *42*, 5425-5437.
6. Lustiger, A.; Markham, R. L. Importance of Tie Molecules in Preventing Polyethylene Fracture under Long-Term Loading Conditions. *Polymer* **1983**, *24*, 1647-1654.
7. Minnema, L.; Barneveld, H.; Rinkel, P. An Investigation into the Mechanism of Water Treeing in Polyethylene High-Voltage Cables. *IEEE Trans. Electr. Insul.* **1980**, *EI-15*, 461-472.
8. Shimizu, N.; Nagata, T.; Horii, K.; Fukushima, K.; Nagao, M.; Kosaki, M. Thermal Contraction and Cracking of Extruded Polyethylene Electrical Insulation at Cryogenic Temperatures. *Cryogenics* **1986**, *26*, 459-466.
9. Tekkanat, B.; McKinney, B. L.; Behm, D. Environmental Stress Cracking Resistance of Blow Moded Poly (Ethylene Terephthalate) Containers. *Polym. Eng. Sci.* **1992**, *32*, 393-399.
10. Ciardelli, F.; Ruggeri, G.; Pucci, A. Dye-Containing Polymers: Methods for Preparation of Mechanochromic Materials. *Chem. Soc. Rev.* **2013**, *42*, 857-870.
11. Haehnel, A. P.; Sagara, Y.; Simon, Y. C.; Weder, C., *Mechanochemistry in Polymers with Supramolecular Mechanophores*. Springer: 2015.

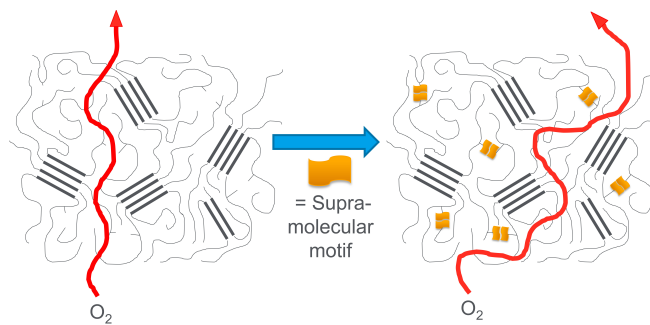
12. Löwe, C.; Weder, C. Oligo(P-Phenylene Vinylene) Excimers as Molecular Probes: Deformation-Induced Color Changes in Photoluminescent Polymer Blends. *Adv. Mater.* **2002**, *14*, 1625-1629.
13. Chi, Z.; Zhang, X.; Xu, B.; Zhou, X.; Ma, C.; Zhang, Y.; Liu, S.; Xu, J. Recent Advances in Organic Mechanofluorochromic Materials. *Chem. Soc. Rev.* **2012**, *41*, 3878-3896.
14. Li, W.; Huang, D.; Wang, J.; Shen, W.; Chen, L.; Yang, S.; Zhu, M.; Tang, B.; Liang, G.; Xu, Z. A Novel Stimuli-Responsive Fluorescent Elastomer Based on an Aie Mechanism. *Polym. Chem.* **2015**, *6*, 8194-8202.
15. Crenshaw, B. R.; Weder, C. Deformation-Induced Color Changes in Melt-Processed Photoluminescent Polymer Blends. *Chem. Mater.* **2003**, *15*, 4717-4724.
16. Crenshaw, B. R.; Burnworth, M.; Khariwala, D.; Hiltner, A.; Mather, P. T.; Simha, R.; Weder, C. Deformation-Induced Color Changes in Mechanochromic Polyethylene Blends. *Macromolecules* **2007**, *40*, 2400-2408.
17. Kunzleman, J.; Crenshaw, B. R.; Kinami, M.; Weder, C. Self-Assembly and Dispersion of Chromogenic Molecules: A Versatile and General Approach for Self-Assessing Polymers. *Macromol. Rapid Commun.* **2006**, *27*, 1981-1987.
18. Donati, F.; Pucci, A.; Cappelli, C.; Mennucci, B.; Ruggeri, G. Modulation of the Optical Response of Polyethylene Films Containing Luminescent Perylene Chromophores. *J. Phys. Chem. B* **2008**, *112*, 3668-3679.
19. Brown, G. O.; Guardala, N. A.; Price, J. L.; Weiss, R. G. Selectivity and Efficiency of Pyrene Attachment to Polyethylene Films by Bombardment with Mev-Range Protons. *J. Phys. Chem. B* **2002**, *106*, 3375-3382.
20. Winnik, F. M. Photophysics of Preassociated Pyrenes in Aqueous Polymer Solutions and in Other Organized Media. *Chem. Rev.* **1993**, *93*, 587-614.
21. Basu, B. Optical Oxygen Sensor Coating Based on the Fluorescence Quenching of a New Pyrene Derivative. *Sens. Actuators B Chem.* **2005**, *104*, 15-22.

22. Coleman, L.; Bork, J.; Dunn, H. Notes. Reaction of Primary Aliphatic Amines with Maleic Anhydride. *J. Org. Chem.* **1959**, *24*, 135-136.
23. Hu, G. H.; Lindt, J. T. Amidification of Poly(Styrene-Co-Maleic Anhydride) with Amines in Tetrahydrofuran Solution: A Kinetic Study. *Polym. Bull.* **1992**, *29*, 357-363.
24. Vermeesch, I.; Groeninckx, G. Chemical Modification of Poly(Styrene-Co-Maleic Anhydride) with Primaryn-Alkylamines by Reactive Extrusion. *J. Appl. Polym. Sci.* **1994**, *53*, 1365-1373.
25. Trivedi, B., *Maleic Anhydride*. Springer Science & Business Media: 2013.
26. Basu, B. J.; Anandan, C.; Rajam, K. S. Study of the Mechanism of Degradation of Pyrene-Based Pressure Sensitive Paints. *Sens. Actuators B Chem.* **2003**, *94*, 257-266.
27. Basu, B. J.; Rajam, K. S. Comparison of the Oxygen Sensor Performance of Some Pyrene Derivatives in Silicone Polymer Matrix. *Sens. Actuators B Chem.* **2004**, *99*, 459-467.
28. Le Sant, Y.; Mérienne, M. C. Surface Pressure Measurements by Using Pressure-Sensitive Paints. *Aerospace Sci. Tech.* **2005**, *9*, 285-299.
29. Wunderlich, B.; Cormier, C. M. Heat of Fusion of Polyethylene. *J. Polym. Sci., Part A-2: Polym. Phys.* **1967**, *5*, 987-988.
30. Rutkowski, S.; Zych, A.; Przybysz, M.; Bouyahyi, M.; Sowinski, P.; Koevoets, R.; Haponiuk, J.; Graf, R.; Hansen, M. R.; Jasinska-Walc, L.; Duchateau, R. Toward Polyethylene–Polyester Block and Graft Copolymers with Tunable Polarity. *Macromolecules* **2016**, *50*, 107-122.

Chapter 4

Barrier properties of ureidopyrimidinone and pyrene functionalized polyethylene^a

UPy or MIP supramolecular motifs were introduced into PE-HEMA copolymers by solution grafting. The incorporation was confirmed by NMR



spectroscopy. Oxygen (OP) and water vapor (WVP) permeabilities of those materials were measured and compared to that of LDPE and polyethylene/polyamide/ethylene vinyl alcohol (PE/PA/EVOH) multilayer structure to investigate the influence of UPy quadruple hydrogen bonding and MIP π - π stacking on oxygen and water vapor barrier properties. Functionalization of PE-HEMA1 with 2.2 mol% of UPy decreased OP by about 30 % at 23 °C and 0 % RH, and about 25 % at 38 °C and 50 % RH while WVP by about 25 %. When 1.2 mol% of MIP was introduced into PE-HEMA1, OP was decreased by about 35 % at 23 °C and 0 % RH, and about 30 % at 38 °C and 50 % RH while WVP by about 40 %.

^a The content of this chapter is covered by the patent application: Zych, J. Tellers, M. Soliman, R. Pinalli, J. Vachon, E. Dalcanale, Gas barrier film, 16POLY0166.

4.1 Introduction

Currently, the world is using 28 million tons of plastics for food packaging and 6.8 million tons for healthcare applications including cosmetics, hygienic, packaging and components. The most common polymers used in food packaging have performed well with regard to chemical and heat resistance. For instance, PE offers not only a good processability but also an excellent water vapor barrier, which is required for many water-sensitive food products such as dried food products. However, this type of plastic is not appropriate for oxidation-sensitive food products due to its low oxygen barrier property (Table 1). Concerning PP, it is often used for a variety of food products ranging from cold-chain to heat-treated food products, including microwaveable products available in either flexible or rigid plastic packaging. Similarly to PE, due to its poor oxygen barrier properties, PP is very often used in multilayers with high-oxygen-barrier polymers such as ethylene vinyl alcohol (EVOH) for oxygen-sensitive food products like apple products, meat products, soup, baby food, ketchup, and cooked rice.¹ However, multilayer films have a major drawback, they are very difficult to recycle.² Therefore, there is a strong need of developing new modified polyolefins with improved oxygen barrier that could be used as a single layer material for food packaging enabling the recycling.

Barrier properties of ureidopyrimidinone and pyrene functionalized polyethylene

Table 1. Oxygen and water vapor permeability values of some commodity polymers.³

Polymer	O ₂ Permeability	H ₂ O Permeability
	[cm ³ (O ₂)·mm/ (m ² ·24h)]	[g(H ₂ O)·mm/ (m ² ·24h)]
Polyethylene (PE)	50 - 200	0.5 - 2
Polypropylene (PP)	50 - 100	0.2 - 0.4
Polystyrene (PS)	100 - 150	1 - 4
Polyvinyl chloride (PVC)	2 - 8	1 - 2
Polyvinyl alcohol (PVOH)	0.02 (dry)	30
Ethylene vinyl alcohol (EVOH)	0.001 - 0.01 (dry)	1 - 3
Polyvinylidene chloride (PVDC)	0.01 - 0.3	0.1
Polyethylene terephthalate (PET)	1 - 5	0.5 - 2
Polyamide (PA)	0.1 - 1 (dry)	0.5 - 10

Gas barrier properties of polymers are controlled by typical mass transfer phenomena: permeation, absorption, and diffusion (Figure 1). Permeation is the ability of permeants to penetrate and pass through an entire material in response to a difference in partial pressure. Diffusion is the movement of a diffusant in a medium caused by a concentration difference acting as a driving force. Absorption and its counterpart desorption measure the affinity of a given substance for two media with which it comes into contact. Permeation is driven by the chemical potential caused by gradient of concentration or partial pressure and is determined by solubility (relationship between concentration in the solid and in the gas following Henry's law) and diffusion (rate aspect of mass transfer from Fick's first law).

The permeability (P) relates the diffusion coefficient and solubility according to eq (1).

$$P = DS = \frac{qL}{At\Delta p} \quad (1)$$

Where P: Permeability, D: Diffusion, S: Solubility, q: quantity of permeant transferred by unit of area, L: film thickness, t: time; A: area of the film, Δp : partial pressure difference.⁴

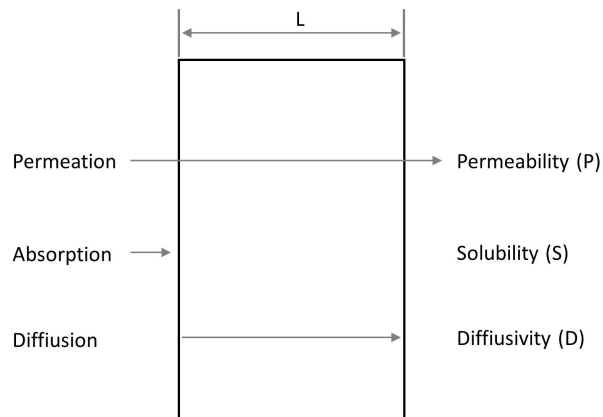


Figure 1. Mass transfer phenomena and their characteristic coefficients.

It is known that barrier properties of PE are affected by crystallinity. When crystallinity increases, density increases and thus permeability decreases. This is related to the increased tortuous path brought by the crystalline phase that is virtually impermeable to a gas (Figure 2). The presence of more space and voids within the amorphous phase makes amorphous polymers more permeable. HDPE (X_c up to 85 %) has thus a higher gas barrier compared to LD/LLDPE (X_c between 30 to 55 %).

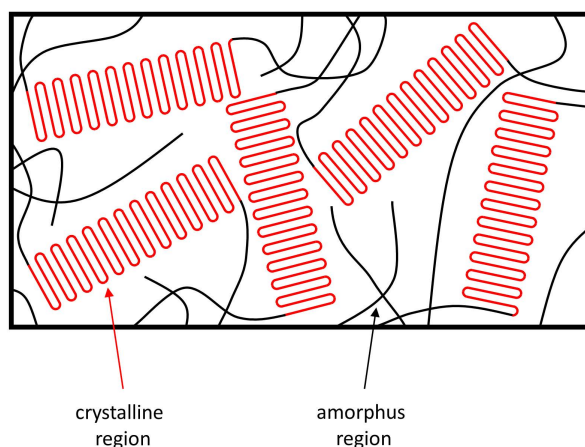


Figure 2. Schematic representation of amorphous and crystalline regions within a polymer.

The influence of the degree of crystallinity of PE on oxygen permeability, solubility and diffusivity is shown in Figure 3.⁵ While solubility decreases less than a factor 10 with increasing X_c , the diffusivity decreases a factor of a few hundreds, which shows that diffusivity is the main factor driving oxygen permeability for PE. Moreover, this effect is especially evident when it comes to higher degrees of crystallinity (> 60 %). When crystallinity is in between 20 and 60 %, a minimal change of permeation factors is noticed. However, a major step change occurs at $X_c \sim 60$ %. For X_c between 60 and 80 %, a factor of a few hundred decrease of P is seen in this 20 % range of crystallinity. At a higher crystallinity, the crystal structure changes from discontinuous to continuous crystal domains which effectively prevent the diffusion of gas molecules (Figure 4).⁶

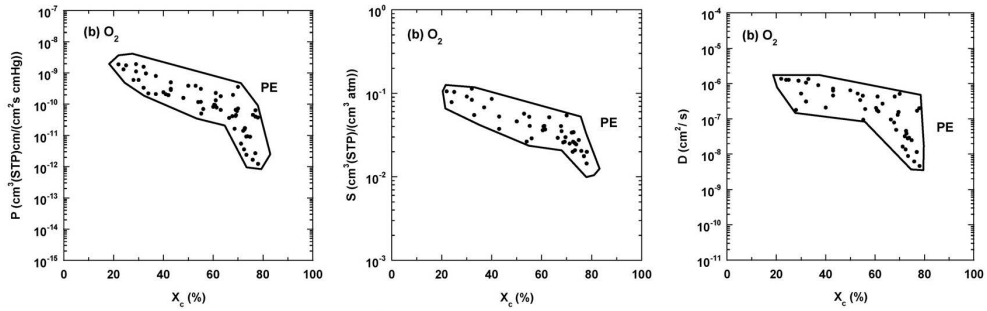


Figure 3. Oxygen permeability (P , left), solubility (S , middle) and diffusivity (D , right) as a function of the degree of crystallinity (X_c) of polyethylene.⁵

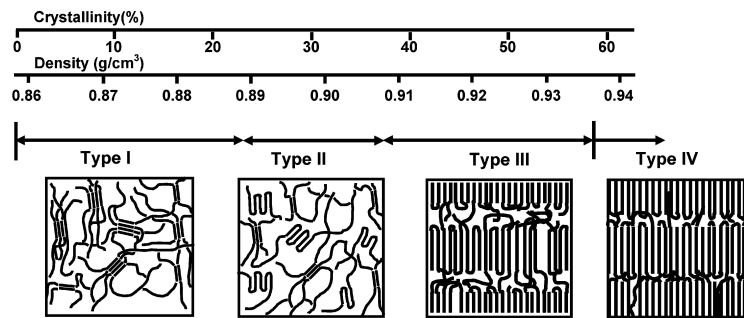


Figure 4. Change of polymer morphology (ethylene - octene copolymers) depending on its degree of crystallinity.⁶

Since the crystalline phase of PE is virtually impermeable towards gas molecules, it is the amorphous phase that has to be modified to improve the barrier properties. One of the possible approaches is to enhance cohesive interactions between PE chains in the amorphous phase utilizing supramolecular interaction like π - π stacking (pyrene) or multiple hydrogen bonding (UPy). Here we report the effect of the introduction of UPy and pyrene moieties into a PE matrix on the oxygen/water barrier properties of the resulting materials.

4.2 Results and discussion

Low density polyethylene (LDPE) and a commercial EVOH based multilayer structure (PE/PA/EVOH) made of polyethylene (PE), polyamide (PA) and ethylene-*co*-vinyl alcohol (EVOH) were selected as benchmarks for modified polyethylene samples. Oxygen and water vapor permeability were measured at least twice for each sample to ensure reliable results.

As expected, PE/PA/EVOH commercial multilayer structure shows a very good performance both in terms of oxygen and water vapor permeability. It combines good oxygen barrier properties of EVOH protected from moisture with LDPE outer layers ensuring sufficient water vapor barrier. Water vapor permeability (WVP) is just slightly higher than that of LDPE and oxygen permeability (OP) is reduced around 350 times. Despite being a bit more sensitive to increased humidity and temperature, PE/PA/EVOH keeps low OP of 1.3 at 38 °C and 50 % RH (Table 2 and Table 3).

Table 2. Oxygen Permeability results of benchmark samples.

Polymer	Temperature [°C]	Humidity [%]	O ₂ Permeability [cm ³ (O ₂)-mm/ (m ² -24h)]
PE/PA/EVOH	23	0	0.3
	38	50	1.3
LDPE	23	0	107
	38	50	244

Table 3. Water vapor permeability results of benchmark samples.

Polymer	Temperature [°C]	Humidity [%]	H ₂ O
			Permeability [g(H ₂ O)·mm/ (m ² ·24h)]
PE/PA/EVOH	23	85	0.08
LDPE	23	85	0.06

4.2.1 Oxygen and water vapor permeability of PE-HEMA-UPy

The functionalization of PE-HEMA with UPy moieties in solution and the relative characterization of the obtained PE-HEMA-UPy samples were described in Chapter 2. OP and WVP results of PE-HEMA1 containing 4.4 mol% of HEMA and corresponding samples functionalized with 0.5 and 2.2 mol% of UPy (Table 4) are presented below in Table 5 and Table 6 and visualized in Figure 5.

Barrier properties of ureidopyrimidinone and pyrene functionalized polyethylene

Table 4. PE-HEMA-UPy samples used for permeability measurements.^a

Polymer	-OH ^b [mol%] ^a	UPy ^b [mol%]	<i>T_m</i> ^c [°C]	<i>X_c</i> ^d [%]	<i>M_n</i> ^d [g/mol]	<i>Đ_M</i> ^d
PE-HEMA1	4.4	-	99,6	12,2	4 000	4,2
PE-HEMA1-UPy 0.5	3,9	0,5	97,5	10,4	-	-
PE-HEMA1-UPy 2.2	2,2	2,2	97,7	11,0	-	-

^a Conditions: reactions were carried out under nitrogen in a glass reactor equipped with a mechanical stirrer set to 100 RPM at 100 °C for 24 h. 500 mL of toluene and 2 drops of DBTDL catalyst were used for 10 g of starting polymer. ^b Calculated from ¹H NMR (120 °C, TCE-*d*₂). ^c Melting temperatures (*T_m*) were determined by DSC from the second heating scan. ^d Degrees of crystallinity (*X_c*) were calculated dividing the melting enthalpy of 100 % crystalline PE (286.2 J/g)⁷ by melting enthalpy of a polymer determined by DSC from the second heating scan. ^e Molecular weight and dispersity were determined by SEC in *o*DCB at 150 °C with respect to polyethylene standards.

Table 5. Oxygen permeability results of PE-HEMA-UPy samples.^a

Polymer	UPy ^b [mol%]	Temperature [°C]	Humidity [%]	O ₂ Permeability	
				[cm ³ (O ₂)·mm/ (m ² ·24h)]	BIF ^c
PE-HEMA1	-	23	0	107	-
		38	50	297	-
PE-HEMA1 0.5	0.5	23	0	93	1.15
		38	50	264	1.12
PE-HEMA1 2.2	2.2	23	0	77	1.39
		38	50	230	1.29

^a Samples were prepared by compression molding, thickness around 100 μm. ^b Calculated from ¹H NMR (120 °C, TCE *d*₂). ^c BIF (barrier improvement factor) was calculated by dividing the permeability of a reference material by the permeability of the modified one.

Table 6. Water vapor permeability results of PE-HEMA-UPy samples.^a

Polymer	UPy ^b [mol%]	Temperature [°C]	Humidity [%]	H ₂ O Permeability	
				[g(H ₂ O)·mm/ (m ² ·24h)]	BIF ^c
PE-HEMA1		23	85	0.53	-
PE-HEMA1 0.5	0.5	23	85	0.49	1.08
PE-HEMA1 2.2	2.2	23	85	0.45	1.18

^aSamples were prepared by compression molding, thickness around 100 μm. ^bCalculated from ¹H NMR (120 °C, TCE-*d*₂). ^cBIF (barrier improvement factor) was calculated by dividing the permeability of a reference material by the permeability of the modified one.

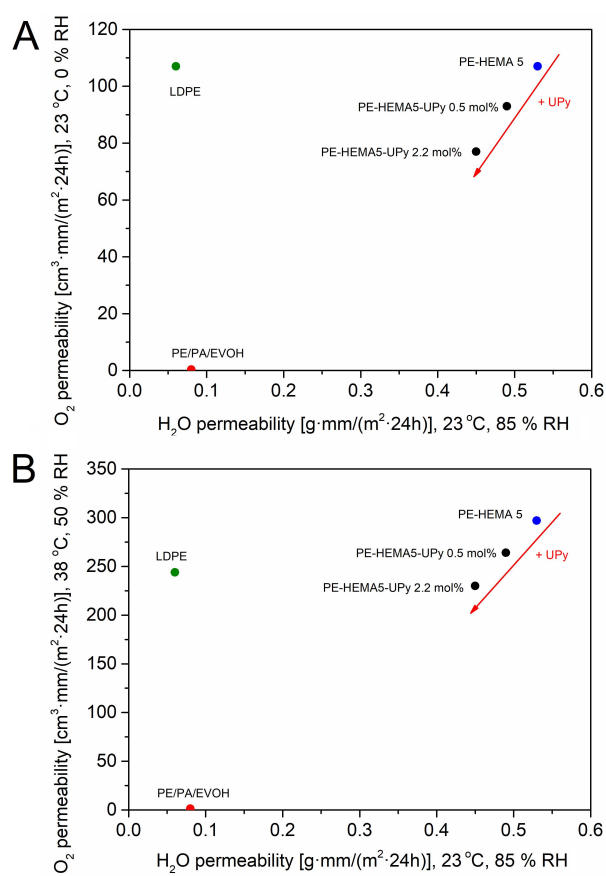


Figure 5. Permeability results of PE-HEMA1-UPy samples, **A**: OP at 23 °C and 0 % RH, **B**: OP at 38 °C and 50 % RH.

PE-HEMA1 has around 5 times higher WVP than LDPE due to the presence of hydrophilic HEMA comonomer (increased water solubility) and decreased crystallinity (increased diffusivity). Surprisingly, it does not show a decreased OP at 23 °C and 0 % RH as EVOH does and has a comparable oxygen barrier to LDPE. That outcome can be caused by two conflicting effects: decreased solubility of non-polar oxygen caused by the presence of hydrophilic HEMA lowers OP, while the increased diffusivity by the decreased crystallinity rises OP. At higher temperature and humidity PE-HEMA1 performs worse than LDPE since hydrogen bonding of HEMA gets weaker and the amorphous phase become more mobile.

The introduction of 0.2 and 2.2 mol% of UPy gradually decreased OP and WVP. This result proves that the quadruple hydrogen bonding of UPy is insensitive to humidity unlike the hydrogen bonds between hydroxy groups of HEMA, and increases the cohesive interactions between the polymer chains more efficiently. By the introduction of 2.2 mol% of UPy into PE HEMA1, OP was decreased about 30 % at 23 °C and 0 % RH (BIF = 1.39) and about 25 % at 38 °C and 50 % RH (BIF = 1.29). However, the PE-HEMA-UPy samples did not perform better than the commercial solution. Although higher amount of UPy could potentially further improve the oxygen and water vapor barrier, samples with such a high UPy content would be very difficult to process, if not impossible, which is impractical for any packaging applications.

4.2.2 Oxygen and water vapor permeability of PE-HEMA-MIP

PE-HEMA1 containing 4.4 mol% of HEMA and PE-HEMA3 containing 0.8 mol% of HEMA were functionalized with methylisocyanatopyrene (MIP) using the same procedure as for UPy solution grafting. PE-HEMA1 was functionalized with 1.2 mol% of MIP and PE-HEMA3 with 0.6 mol% (Table 7). OP and WVP results of PE-HEMA-MIP samples are presented below in Table 8 and Table 9 and visualized in Figure 6.

Table 7. PE-HEMA-MIP samples used for permeability measurements.^a

Polymer	-OH ^b [mol%] ^a	MIP [mol%]	T_m ^c [°C]	X_c ^d [%]	M_n ^e [g/mol]	\bar{M}_w ^e
PE-HEMA3	0.8	-	109.0	19.5	16 200	3.9
PE-HEMA1	4.4	-	99.6	12.2	4 000	4.2
PE-HEMA3-MIP	0.2	0.6	108.3	16.0	-	-
PE-HEMA1-MIP	3.2	1.2	98.2	10.6	-	-

^a Conditions: reactions were carried out under nitrogen in a round bottom flask with magnetic stirrer set to 100 RPM at 100 °C for 24 h. 100 mL of toluene and 1 drop of DBTDL catalyst were used for 2 g of starting polymer. ^b Calculated from ¹H NMR (120 °C, TCE-*d*₂). ^c Melting temperatures (T_m) were determined by DSC from the second heating scan. ^d Degrees of crystallinity (X_c) were calculated dividing the melting enthalpy of 100 % crystalline PE (286.2 J/g)⁷ by melting enthalpy of a polymer determined by DSC from the second heating scan. ^e Molecular weight and dispersity were determined by SEC in *o*DCB at 150 °C with respect to polyethylene standards.

Barrier properties of ureidopyrimidinone and pyrene functionalized polyethylene

Table 8. Oxygen permeability results of PE-HEMA-MIP samples compared to those of their precursors.^a

Polymer	MIP ^b [mol%]	Temperature [°C]	Humidity [%]	O ₂ Permeability	
				[cm ³ (O ₂)·mm/ (m ² ·24h)]	BIF ^c
PE-HEMA3	-	23	0	118	-
		38	50	262	-
PE-HEMA3-MIP	0.6	23	0	87	1.36
		38	50	233	1.12
PE-HEMA1	-	23	0	107	-
		38	50	297	-
PE-HEMA1-MIP	1.2	23	0	67	1.60
		38	50	212	1.40

^aSamples were prepared by compression molding, thickness around 100 μm . ^bCalculated from ¹H NMR (120 °C, TCE-*d*₂). ^cBIF (barrier improvement factor) was calculated by dividing the permeability of a reference material by the permeability of the modified one.

Table 9. Water vapor permeability results of PE-HEMA-MIP samples compared to those of their precursors.^a

Polymer	MIP ^b [mol%]	Temperature [°C]	Humidity [%]	H ₂ O	
				Permeability [g(H ₂ O)·mm/ (m ² ·24h)]	BIF ^c
PE-HEMA3	-	23	85	0.08	-
PE-HEMA3-MIP	0.6	23	85	0.12	0.66
PE-HEMA1	-	23	85	0.53	-
PE-HEMA1-MIP	1.2	23	85	0.32	1.66

^aSamples were prepared by compression molding, thickness around 100 μm . ^bCalculated from ¹H NMR (120 °C, TCE-*d*₂). ^cBIF (barrier improvement factor) was calculated by dividing the permeability of a reference material by the permeability of the modified one.

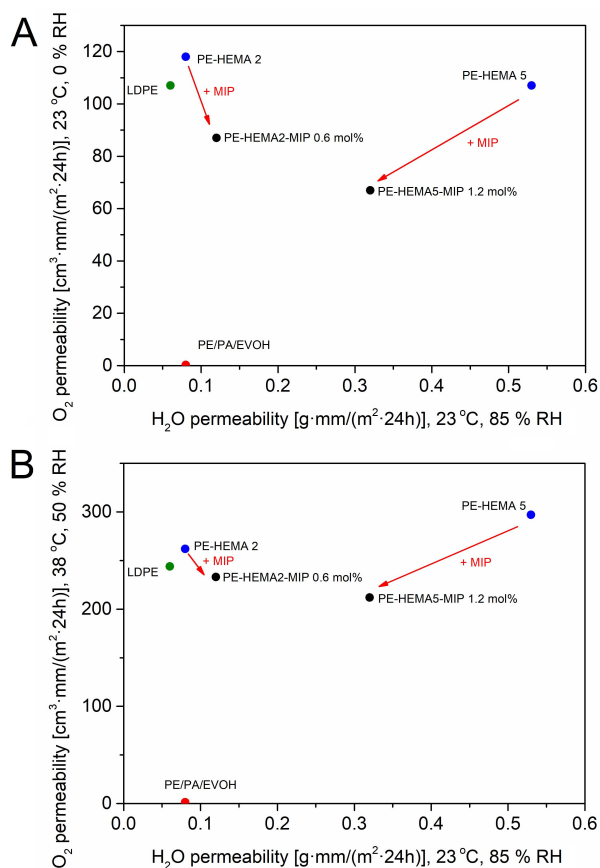


Figure 6. Permeability results of PE-HEMA-MIP samples, **A**: OP at 23 °C and 0 % RH, **B**: OP at 38 °C and 50 % RH.

PE-HEMA3 with the low HEMA content of 0.8 mol% has a similar barrier performance to LDPE. When HEMA content is increased to 4.4 mol% in PE-HEMA1, it shows a slightly lower OP but a much higher WVP. This behavior can be explained by looking separately at the solubility and diffusivity factors that are affected by the increased HEMA content. Both for oxygen and water vapor barrier, a high HEMA content leads to a more amorphous material, and as a consequence, a higher diffusivity. In case of oxygen, a high HEMA content means a lower solubility, which then

compensate to some extent the increased. However, for water vapor the opposite effect is present where higher affinity to water of polar HEMA units increase solubility leading to increased WVP.

Both polymers functionalized with MIP show decreased OP, which is more significant for PE-HEMA1-MIP containing more MIP (1.2 mol%). It shows that the MIP π - π stacking increases cohesive interactions between the PE-HEMA chains (decreased diffusivity) improving the oxygen barrier. Moreover, PE-HEMA1-MIP shows also decreased WVP because MIP decreases the polarity of PE-HEMA (decreased solubility). Even though OP was decreased around 35 % (BIF = 1.66) in case of PE-HEMA1 functionalized with 1.2 mol% of MIP, results are still far from the performance of the commercial multilayer.

4.3 Conclusions

PE-HEMA samples were functionalized with UPy or MIP. Oxygen and water vapor permeability of those materials were measured at different temperatures and humidity. Both UPy quadruple hydrogen bonding and MIP π - π stacking were able to improve oxygen and water vapor barrier. Functionalization of PE-HEMA1 with 2.2 mol% of UPy decreased OP by about 30 % at 23 °C and 0 % RH, and about 25 % at 38 °C and 50 % RH while WVP by about 25 %. When 1.2 mol% of MIP was introduced into PE-HEMA1, OP was decreased by about 35 % at 23 °C and 0 % RH, and about 30 % at 38 °C 50 % RH while WVP by about 40 %. Despite the achieved improvements the samples performed worse than commercial multilayer solution. The poor

performance can be explained by decreased crystallinity when polyethylene is functionalized. As a consequence, diffusivity through more amorphous polyethylene is increased compromising both oxygen and water vapor barrier properties. This effect is only partially compensated by the increase cohesive interactions between the PE-HEMA chains thanks to the water insensitive hydrogen bonding of UPy or π - π interactions of MIP.

4.4 Experimental section

Materials

Toluene, acetone, dichloromethane (DCM) deuterated tetrachloroethene (TCE- d_2), trimethylamine (99.5 %), triphosgene (98 %), hexamethylene diisocyanate (HDI, 98 %), dibutyltin dilaurate (DBTDL, 95 %) and 2-Amino-4-hydroxy-6-methylpyrimidine (methyl isocytosine, 98 %) were purchased from Sigma-Aldrich. 2-(6-isocyanatohexylaminocarbonylamino)-6-methyl-4[1H]pyrimidinone (UPy) was synthesized according to the reported procedure.⁸ 1-methylisocyanatopyrene (MIP) was synthesized according to the reported procedure.⁹ Polyethylene-*co*-2-hydroxyethyl methacrylate (PE-HEMA) was kindly provided by SABIC. All materials were used as received unless otherwise stated.

Typical procedure for UPy grafting in solution

PE-HEMA (10.0 g) was dissolved in toluene (500 mL) at 100 °C in a glass reactor equipped with mechanical stirring (100 RPM) under nitrogen atmosphere. Subsequently, desired amount of UPy and DBTDL (2 drops)

were added and the reaction mixture was stirred at 100 °C for 24 h, maintaining the nitrogen atmosphere. The product was precipitated by pouring the reaction mixture into acetone, filtered, washed twice with acetone and dried at 60 °C under vacuum.

Typical procedure for MIP grafting in solution

PE-HEMA (10.0 g) was dissolved in toluene (500 mL) at 100 °C in a round bottom flask with magnetic stirring (100 RPM) under nitrogen atmosphere. Subsequently, desired amount of MIP and DBTDL (2 drops) were added and the reaction mixture was stirred at 100 °C for 24 h, maintaining the nitrogen atmosphere. The product was precipitated by pouring the reaction mixture into acetone, filtered, washed twice with acetone and dried at 60 °C under vacuum (Figure appx 3 and Figure appx 4).

Typical procedure for compression molding

Appropriate molds were filled with the polymer powder and placed between the plates of the compression molding machine for 5 min at 140 °C. After that, force of 500 kN was applied for 10 min followed by cooling at a rate of 15 °C /min until a temperature of 40 °C was reached while maintaining the applied force.

Measurements

Oxygen and water transmissions were measured on at least two compressed molded films for each sample and the average was calculated. Oxygen transmission rates were determined at 23 °C, 0 % relative humidity

(R.H.) and at 38 °C, 50 % R.H. according to ISO 15105-2. Water transmission rates were determined at 23 °C, 80 % R.H. according to ISO 15106-3 standard. The thickness of films was around 100 μm (Figure appx 1 and Figure appx 2).

4.5 Appendix

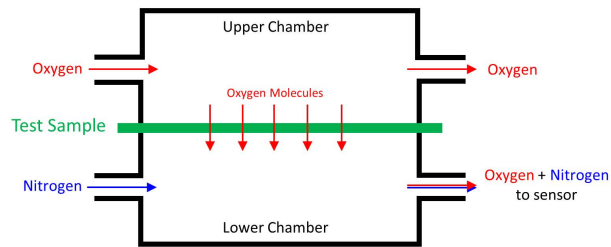


Figure appx 1. Schematic representation of oxygen permeability tester.

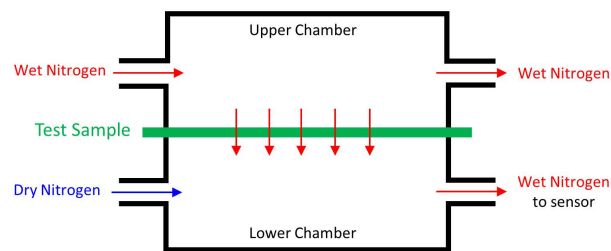


Figure appx 2. Schematic representation of water vapor permeability tester.

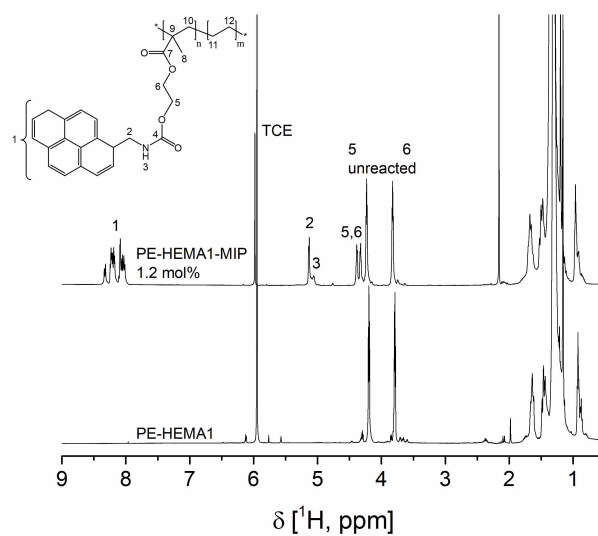


Figure appx 3. ¹H NMR spectra overlay of PE-HEMA1 and PE-HEMA1-MIP 1.2 mol% recorded at 120 °C in deuterated TCE.

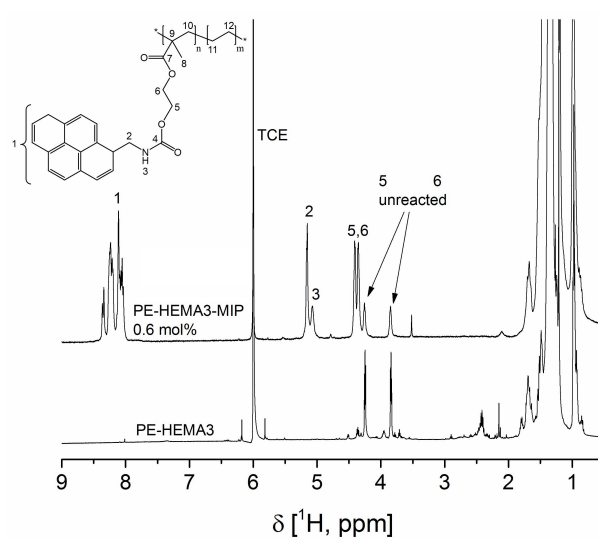


Figure appx 4. ¹H NMR spectra overlay of PE-HEMA3 and PE-HEMA3-MIP 0.6 mol% recorded at 120 °C in deuterated TCE.

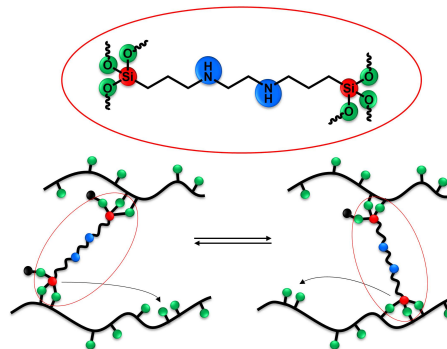
4.6 References

1. Kim, Y. T.; Min, B.; Kim, K. W., *General Characteristics of Packaging Materials for Food System*. Elsevier: 2014.
2. Fávares, S. L.; Freitas, A. R.; Ganzerli, T. A.; Pereira, A. G. B.; Cardozo, A. L.; Baron, O.; Muniz, E. C.; Giroto, E. M.; Radovanovic, E. Pet and Aluminum Recycling from Multilayer Food Packaging Using Supercritical Ethanol. *J. Supercrit. Fluid.* **2013**, *75*, 138-143.
3. Lange, J.; Wyser, Y. Recent Innovations in Barrier Technologies for Plastic Packaging? A Review. *Packag. Technol. Sci.* **2003**, *16*, 149-158.
4. Han, J. H.; Scanlon, M. G., *Mass Transfer of Gas and Solute through Packaging Materials*. Elsevier: 2014.
5. Kanehashi, S.; Kusakabe, A.; Sato, S.; Nagai, K. Analysis of Permeability; Solubility and Diffusivity of Carbon Dioxide; Oxygen; and Nitrogen in Crystalline and Liquid Crystalline Polymers. *J. Membr. Sci.* **2010**, *365*, 40-51.
6. Wang, H. P.; Khariwala, D. U.; Cheung, W.; Chum, S. P.; Hiltner, A.; Baer, E. Characterization of Some New Olefinic Block Copolymers. *Macromolecules* **2007**, *40*, 2852-2862.
7. Wunderlich, B.; Cormier, C. M. Heat of Fusion of Polyethylene. *J. Polym. Sci., Part A-2: Polym. Phys.* **1967**, *5*, 987-988.
8. Folmer, B. J.; Sijbesma, R.; Versteegen, R.; van der Rijt, J.; Meijer, E. Supramolecular Polymer Materials: Chain Extension of Telechelic Polymers Using a Reactive Hydrogen-Bonding Synthone. *Adv. Mater.* **2000**, *12*, 874-878.
9. Biedermann, F.; Appel, E. A.; del Barrio, J. s.; Gruending, T.; Barner-Kowollik, C.; Scherman, O. A. Postpolymerization Modification of Hydroxyl-Functionalized Polymers with Isocyanates. *Macromolecules* **2011**, *44*, 4828-4835.

Chapter 5

Silyl ether polyethylene vitrimers^a

Functionalized polyethylene bearing pendant hydroxy groups was dynamically crosslinked directly via reactive extrusion using commercially available *N,N'*-Bis[3-(trimethoxysilyl)propyl] ethylenediamine (TMSPEDA). This fast and efficient process allowed to produce PE vitrimers without any synthetic effort or use of any solvent which makes it environmentally friendly and easy to upscale. The dynamic crosslinking transformed thermoplastic PE into an elastic solid with greatly improved melt strength as revealed by DMTA and rheology analysis. Mechanical properties could be tuned by varying the amount of TMSPEDA crosslinker. All prepared vitrimers were insoluble in xylene and were not affected by moisture, demonstrating crosslinked character and excellent solvent and hydrolysis resistance which is of great importance for industrial applications. Despite the crosslink nature of the material, the dynamic silyl ether exchange enabled processability and recyclability of this system using industrially relevant techniques like injection and compression molding.



^a The content of this chapter is being prepared to be covered by the patent application: Zych, J. Tellers, M. Soliman, R. Pinalli, J. Vachon, E. Dalcanale, Silyl ether vitrimers, and to be submitted for publication: A. Zych, M. Soliman, R. Pinalli, J. Vachon, E. Dalcanale, Reactive extrusion of polyethylene vitrimers based on silyl ether exchange.

5.1 Introduction

The world of polymers is generally divided into thermoplastics and thermosets with each of them having unique properties and applications. Thermoplastics can be easily processed using industrial processes like extrusion, injection molding or blow molding. However, their applications are limited by high creep, poor abrasion and solvent resistance. Those drawbacks are not present in thermosets but the crosslinking reduces their ability to flow. Therefore, they cannot be processed like thermoplastics and have to be polymerized in a mold to give them a desired shape. Moreover, reprocessing and recycling of those materials are very difficult, if not impossible.

Vitrimers form a new class of materials that at service temperatures behave like permanently crosslinked ones but flow at elevated temperatures. They are crosslinked using exchangeable covalent bonds, which enables them to change topology, maintaining constant number of chemical bonds and crosslinks. The exchange reactions speed up with temperature making processing possible. The shape of the final object is then fixed by freezing the exchange reaction^{1, 2} through quenching below a glass transition or *via* crystallization.^{3,4}

When an amorphous polymer is heated, it undergoes the glass transition (T_g). Above the T_g , the polymer softens and its viscosity decreases by several orders of magnitude following a non-Arrhenius, Williams-Landel-Ferry (WLF) law (Figure 1A).⁵⁻⁷ Vitrimers additionally undergo a second transition called topology freezing transition (T_v) coming

from the network cross-link exchange reactions.² When bond exchange becomes faster than material deformation, the network can rearrange its topology, resulting in a flow and the transition from viscoelastic solid to viscoelastic liquid occurs. If the vitrimer has T_g lower than T_v (Figure 1B) when heated from a temperature below T_g to a temperature between T_g and T_v , it will undergo a transition from the glassy to the rubbery state and will behave like an elastomer, since the exchange reactions are very slow. When heated above T_v , the exchange reactions become fast enough to transform the elastomer to a viscoelastic liquid whose flow behavior is controlled by the cross-link exchange kinetics following Arrhenius law. If a fast exchange reaction is incorporated into a rigid polymer matrix having a T_g higher than the expected T_v (Figure 1C), topology freezing transition is only theoretical since the network is not frozen by the exchange reactions kinetics, but by the lack of segmental motions associated with the glass transition.^{4, 8} At temperatures below T_g no segmental motion is present so no exchange reactions can occur and the network is fixed. When the material is heated above the T_g , segmental motion is slowly initiated while the exchange reactions are already fast. Network rearrangement is controlled by segmental motions (diffusion control) that results in a WLF viscosity behavior. Upon further heating, network rearrangement becomes dominated by the exchange reactions, which follows the Arrhenius law.

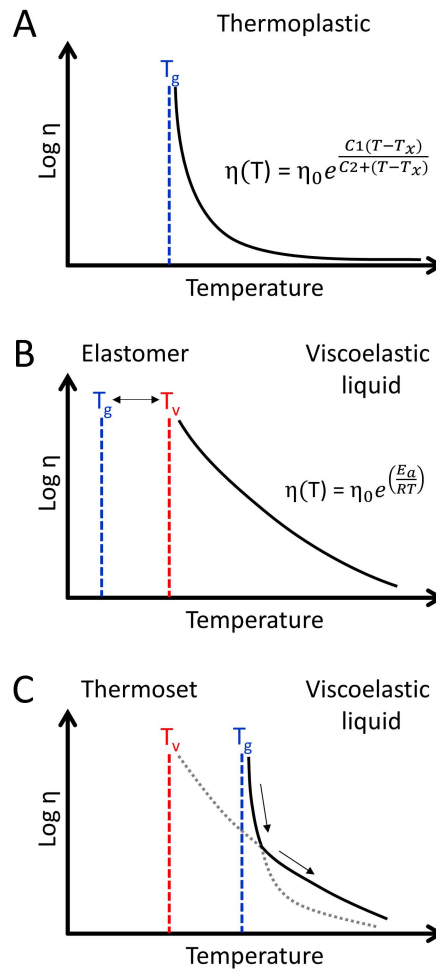


Figure 1. Representation of the viscoelastic behavior of **A:** thermoplastic, **B:** vitrimer with T_g lower than T_v , **C:** vitrimer with T_g higher than the theoretical T_v .⁴

The first vitrimer based on a transesterification reaction in the epoxy system catalyzed by zinc acetate was designed by Leibler *et al.* in 2011 (Figure 2).¹ The exchange reaction kinetics of those transesterification-based vitrimers could be simply tuned by changing the amount and nature of the catalyst.²

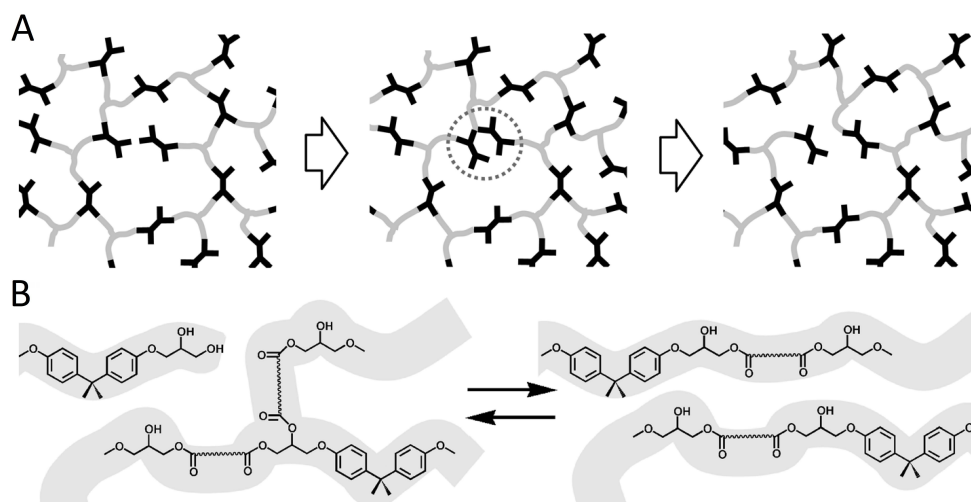


Figure 2. Exchange process *via* transesterification in hydroxy-ester networks.¹

Since the pioneering work of the Liebler's group, several vitrimers based on versatile associative exchange chemistries were developed. An interesting system based on transesterification was published by Zhou *et al.*⁹ They prepared a new type of semicrystalline vitrimer by incorporating glycerol and zinc transesterification catalyst into the amorphous phase of poly(butylene terephthalate) (PBT) using bulk pre-polymerization followed by solid-state polymerization (Figure 3). A near quantitative incorporation of glycerol was achieved while maintaining the crystallization characteristics of normal PBT. A wide range of thermal, rheological and mechanical properties were obtained by changing the cross-link density. Those semicrystalline vitrimers could be recycled multiple times by compression molding without a substantial loss in dynamic mechanical and thermal properties.⁹

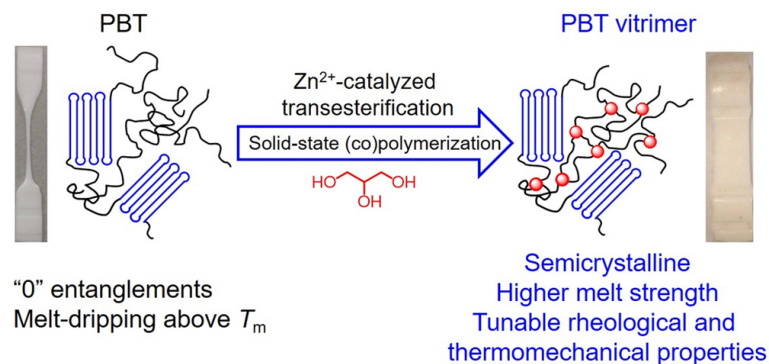


Figure 3. Synthesis of Poly(butylene terephthalate)/Glycerol-based vitrimers by solid-state polymerization.⁹

Similar PBT vitrimer system was prepared by Demongeot *et al.*¹⁰ by reactive extrusion. The resulting polymers are not soluble in tetrachloroethane; however, in contrast to the radiation cross-linked PBT, they were processable and could be reshaped and recycled.

Du Prez *et al.* explored catalyst-free transamination of vinylogous urethanes as an exchange reaction for vitrimers.³ Poly(vinylogous urethane) networks with a storage modulus of around 2.4 GPa and a glass transition temperature above 80 °C were prepared by bulk polymerization of cyclohexane dimethanol bisacetoacetate, *m*-xylylene diamine, and tris(2-aminoethyl)amine (Figure 4). The samples were insoluble even at elevated temperature and a rubbery plateau was observed by DMTA. Stress relaxation and creep experiments revealed a viscoelastic liquid behavior. Relaxation times as short as 85 s at 170 °C were achieved without any catalyst. The networks were recyclable up to four times by consecutive grinding and compression molding with no significant mechanical or chemical

degradation.³ The exchange reactions can be either accelerated using Brønsted or Lewis acid additives or inhibited by adding a base to the polymer matrix.¹¹

Stukenbroeker *et al.* utilized vinylogous urethane exchange to synthesize elastomeric vitrimers *via* the crosslinking of a polydimethylsiloxane bearing pendant amino groups with a bis-vinylogous urethane crosslinker.¹² The elastic properties of this material can be tuned across a wide range of moduli by varying the crosslink density. Reshaping and recycling is possible at 100 °C. Masking the residual free amines with methyl acetoacetate suppressed the stress relaxation leading to a material with the properties of a conventional elastomer.¹²

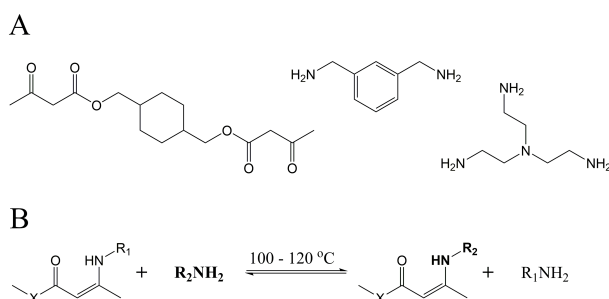


Figure 4. **A:** Monomers used for vitrimer preparation. A small excess of amines was used in order to keep residual free amines in the cross-linked material. **B:** Schematic representation of transamination in vinylogous urethanes.³

Cromwell *et al.* created dynamic polycyclooctene network by ring opening metathesis polymerization (ROMP) of cyclooctane with dihydroxycyclooctene and subsequent crosslinking using a boronic ester (Figure 5). The introduction of neighboring amino groups within the crosslinker led to malleability and self-healing properties, demonstrating a direct link between diboronic ester exchange kinetics and rate of self-healing.¹³

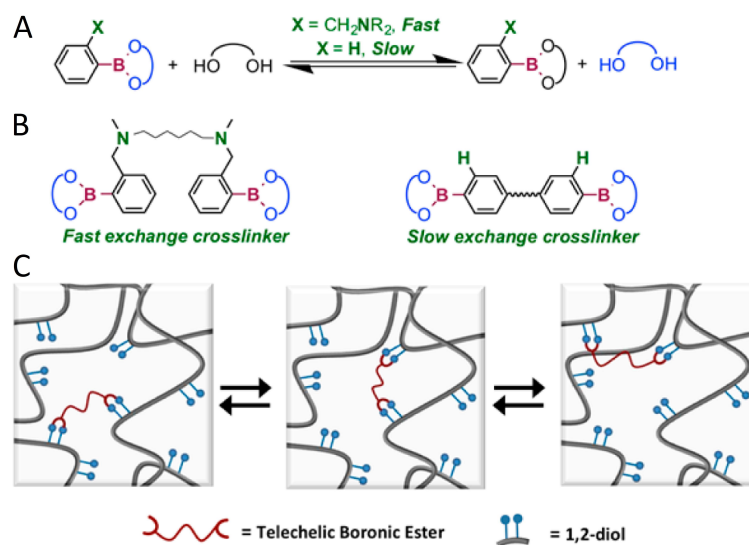


Figure 5. **A:** Tuning neighboring group to control the exchange kinetics of boronic ester. **B:** Design of diboronic ester crosslinkers with tunable exchange kinetics. **C:** Dynamic exchange of boronic ester cross-linkers affords dynamic materials.¹³

Boronic ester chemistry for vitrimer synthesis was explored by Röttger *et al.* as well.¹⁴ They discovered that dioxaborolanes undergo a rapid metathesis reaction at moderate temperatures without the need of a catalyst. Dioxaborolane metathesis allowed for the synthesis of vitrimers from widely used polymers. Methyl methacrylate and styrene were copolymerized with methacrylate functionalized phenylboronic ester while polyethylene was grafted with maleimide functionalized phenylboronic ester. Subsequent crosslinking with phenyldiboronic ester led to vitrimers with improved melt strength, dimensional stability at elevated temperatures, solvent resistance and environmental stress cracking resistance while being processable and recyclable just like thermoplastics (Figure 6).¹⁴

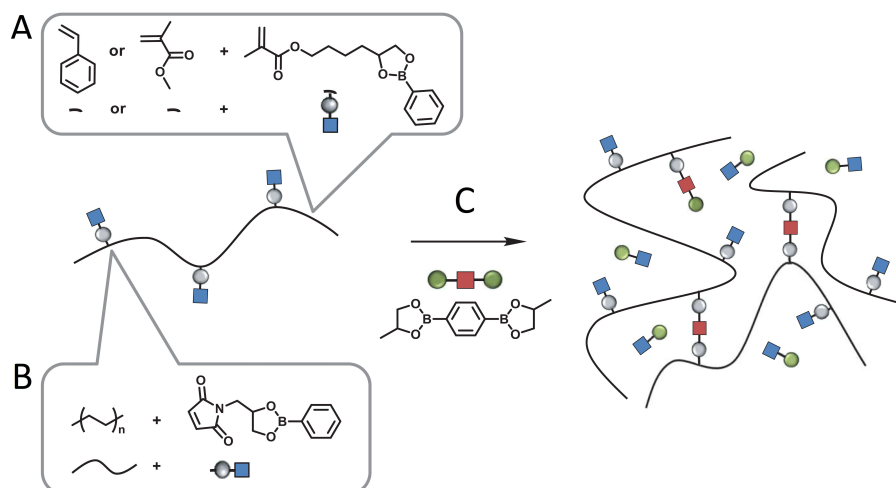


Figure 6. **A:** Synthesis of copolymers containing pendant boronic esters from functional monomers. **B:** Grafting of boronic esters onto thermoplastic polymers by means of reactive processing. **C:** Cross-linking of functional polymers containing pendant boronic ester units by means of metathesis with a diboronic ester.

Nishimura *et al.* introduced silyl ethers as a dynamic covalent crosslinker into polystyrene matrix (Figure 7). The silyl ether exchange rate was accelerated by almost three orders of magnitude using a neighboring amino moiety within the crosslinker itself. This work provided the first experimental observation of viscosity temperature dependence transition from WLF behavior to Arrhenius behavior since a special case of T_v (47 °C) \ll T_g (125 °C) was created, which supports the vitrimers theory of topology freezing through molecular kinetic arrest.⁸

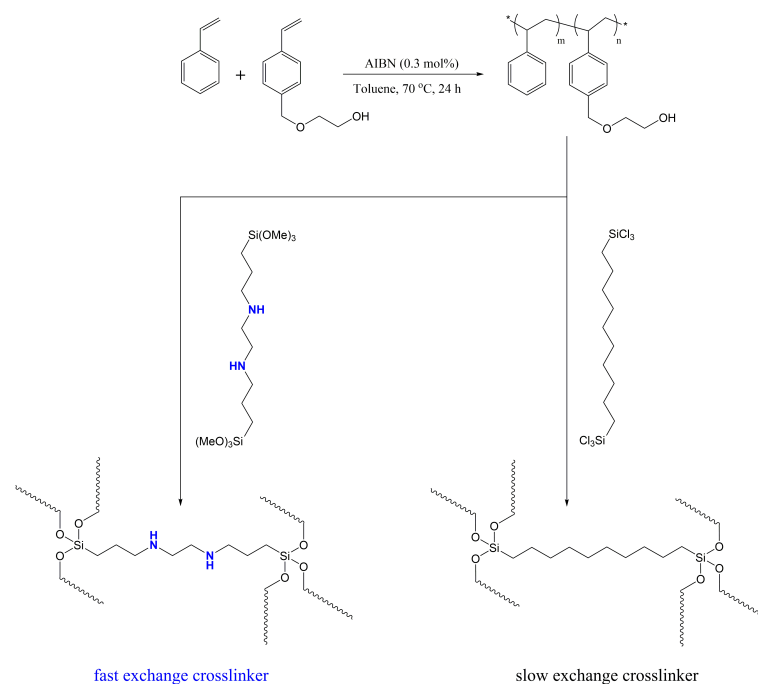


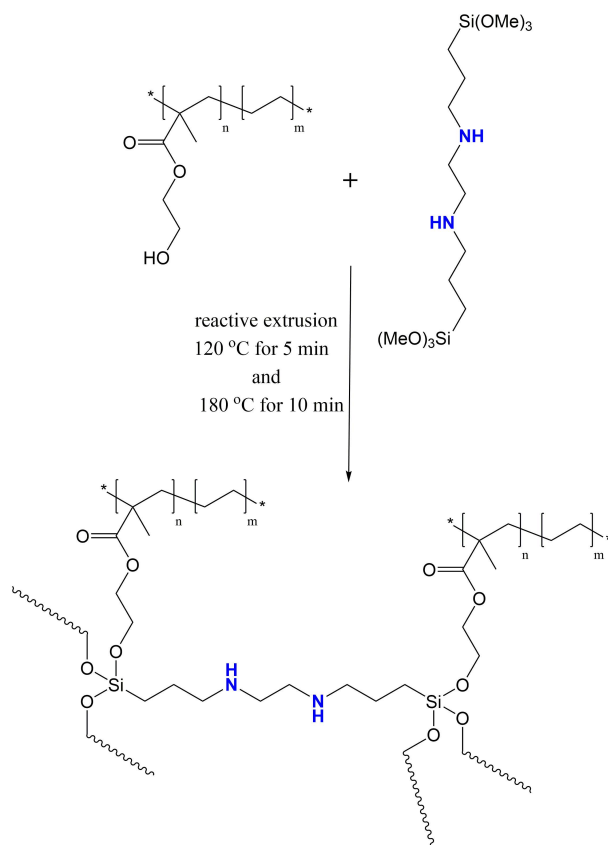
Figure 7. Preparation of silyl ether vitrimers.⁸

Other literature reports on vitrimers include olefin metathesis^{15, 16} siloxane-silanol exchange,^{17, 18} hydroxy mediated transcarbamoylation,¹⁹⁻²¹ transalkylation of triazolium²² and sulfonium salts,²³ and thiol-disulfide exchange or disulfide metathesis.²⁴⁻³⁰ However, most of those vitrimers have major drawbacks like complicated and costly synthetic procedures and reduced thermal or hydrolytic stability limiting their applications. Having hydroxy functionalized PE in hand, we demonstrate here the dynamic crosslinking of PE directly *via* reactive extrusion using commercially available TMSPEDA silyl ether.⁸ Synthesis and characterization of this new, semicrystalline PE vitrimers are presented in this chapter.

5.2 Results and discussion

5.2.1 Crosslinking of PE-HEMA with TMSPEDA dynamic crosslinker *via* reactive extrusion.

TMSPEDA was selected as a dynamic crosslinker to connect the PE-HEMA pendant hydroxy groups (Scheme 1). Following this approach, PE-based vitrimers were directly produced *via* reactive extrusion using PE-HEMA and the desired amount of TMSPEDA crosslinker. Extrusion was performed in a 15 mL twin screw micro compounder at 120 °C for 5 min and at 180 °C till the constant torque was reached (Figure appx 1). The process allowed to produce 10 g of PE vitrimer in around 10-15 min which is a great improvement in comparison to previously reported lengthy solution process.⁸ In addition, the use of costly or toxic solvents is avoided by performing the crosslinking directly in the melt, which makes the process environmentally friendly and easy to upscale. Theoretical crosslink density was varied from 3 to 9 crosslinks per chain (X/C) assuming that all 6 methoxy groups of TMSPEDA can undergo the reaction. Table 1 lists the amount of the crosslinker, the number of crosslinks per chain (X/C), melting (T_m) and beta transition (T_β) temperatures as well as degree of crystallinity (X_{cr}). Thermal properties did not change significantly after the crosslinking which suggests that TMSPEDA is excluded from the PE crystalline phase (Figure appx 4).³¹ Functional group content, melting (T_m) and beta transition (T_β) temperatures, degree of crystallinity (X_{cr}) as well as molecular weight and the molecular weight distribution (\mathcal{D}_M) of PE-HEMA are listed in Table appx 1.



Scheme 1. Preparation of PE silyl ether vitrimers (PE-TMSPEDA) *via* reactive extrusion.

Table 1. TMSPEDA crosslinker content, melting temperatures (T_m), β transition temperatures (T_β) and degrees of crystallinity (X_{cr}) of PE vitrimers.

Vitrimer	PE-HEMA [g]	TMSPEDA [g]	X/C ^a	Maximal reacted	T_m^c [°C]	T_β^d [°C]	X_{cr}^e [%]
				-OH ^b [%]			
1	10	0.66	3	34.7	72.4	4,9	1.8
2	10	0.88	4	46.3	72.1	4,4	2.0
3	8	1.06	6	69.5	71.0	4.0	2.0
4	7	1.39	9	104.2	69.7	1.9	2.2

^aTheoretical number of crosslinks per chain (X/C) was calculated based on M_n of PE-HEMA and the amount of TMSPEDA used, assuming that all 6 methoxy groups of TMSPEDA can undergo the reaction with PE-HEMA hydroxy groups. ^bMaximal % of reacted hydroxy groups was calculated from the mol ratio of HEMA and TMSPEDA assuming that all 6 methoxy groups of TMSPEDA can undergo the reaction with PE-HEMA hydroxy groups. ^cMelting temperatures (T_m) were determined by DSC from the second heating scan. ^d β transition temperatures (T_β) were determined by DMTA from the maximum of $\tan \delta$. ^eDegrees of crystallinity (X_{cr}) were calculated dividing the melting enthalpy of 100 % crystalline PE (286.2 J/g)³² by melting enthalpy of a vitrimer determined by DSC from the second heating scan.

All prepared vitrimers are not completely soluble in xylene at 100 °C for 24 h, demonstrating improved solvent resistance in comparison to PE-HEMA which dissolved completely under the same conditions (Table appx 2). Dynamic silyl ether exchange enabled processability and recyclability of this system using industrially relevant techniques like injection and compression molding (Figure appx 2 and Figure appx 3). Even after reprocessing for 4 times, no decrease in the mechanical performance was observed (Figure 8), showcasing robustness of TMSPEDA crosslinks.

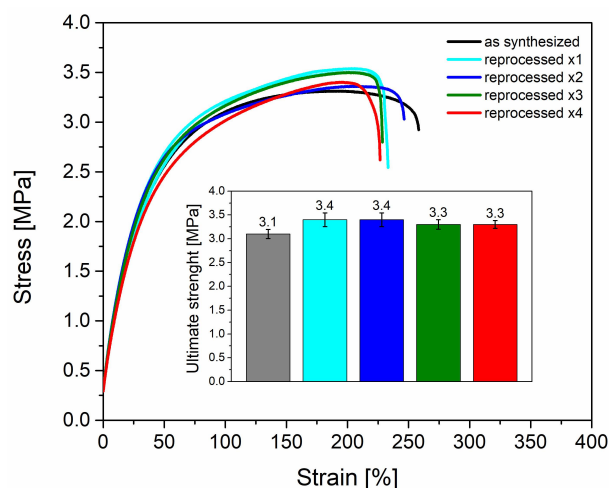


Figure 8. Representative tensile curves and ultimate strength (inset) of vitrimer 2 tested as synthesized and after up to 4th reprocessing cycle.

Since silyl ethers are prone to hydrolysis,^{33, 34} hydrolytic stability of PE-TMSPEDA was assessed by exposing specimens to water for 24 h at room temperature and subsequently measuring water uptake, gel fraction and tensile properties. All vitrimers showed minimal water uptake (less than 1 %, Table appx 3). Gel fraction (Table appx 4) and tensile properties (Figure appx 6) were not significantly affected by exposure to water. In general, hydrophobic nature of the polymer backbone limits swelling and water uptake into the cross-linked network, protecting silyl ethers from hydrolysis which is of great importance for industrial applications like water pipes and electrical cables isolation.¹³

5.2.2 Rheological characterization.

Rheology measurements were performed to investigate properties of PE vitrimers in the melt (Figure 9). Results indicated that PE-HEMA displays a typical behavior of a low molecular weight polymer melt³⁵ with a strong frequency dependence. No crossover point between storage (G') and loss (G'') modulus was observed and the polymer was more viscous (G'' higher than G') than elastic (G' higher than G'') within the whole studied frequency range. Moreover, PE-HEMA was flowing out from between the plates of the rheometer at lower frequencies demonstrating a very low viscosity. After dynamic crosslinking with TMSPEDA, vitrimers behaved like an elastic solid with frequency independent G' and much lower G'' , which is characteristic of crosslinked materials.^{36, 37} Since relaxation times of those dynamic networks are relatively long (Figure appx 11) compared to the probed time scales, within the tested frequency range, no crossover was observed.⁹ Stress relaxation times of the similar system incorporated into polystyrene are roughly two orders of magnitude shorter which can be caused by the different polymer matrix and amount of crosslinks.⁸ Plateau modulus (G_0) taken at the minimum of G'' increased in a linear fashion with increasing crosslink density (Figure appx 7) and ranged from around $2.8 \cdot 10^3$ (vitramer 1) to around $1.2 \cdot 10^5$ MPa (vitramer 4). While PE-HEMA reached the zero-shear viscosity at around 10 Pas, vitrimers 1-4 had viscosities of a few orders of magnitude higher before they even reached their zero shear viscosities (Figure appx 8).^{38, 39} This result indicates highly improved melt strength which is extremely important for processes like film blowing, blow molding, thermoforming and foaming.³⁷

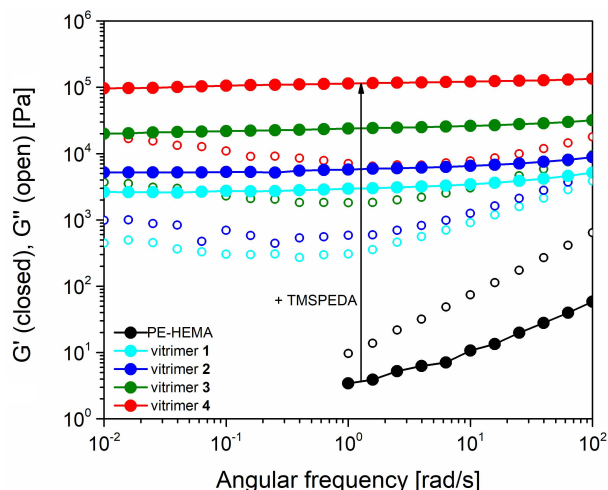


Figure 9. Rheology frequency sweep curves at 180 °C of PE-HEMA and vitrimers 1-4, storage modulus (G') - closed circles, loss modulus (G'') - open circles.

5.2.3 Mechanical properties.

Upon heating, semicrystalline PE usually undergoes three characteristic temperature transitions.^{40, 41} γ transition is observed at around -130 °C, involving rotation of CH_2 groups in the amorphous and crystalline phases, and it is independent of the branching content as well as the degree of crystallinity. β transition, occurring at higher temperatures, can be related to movements involving longer parts of the polymer chains and branch points (T_β). Finally, α transition is associated with a large movement of molecules that arise as the crystalline phase undergoes melting. In the case of PE-HEMA copolymers, an additional transition around -60 °C was observed which most likely results from hydrogen bonds breaking and reforming between hydroxy groups present in the HEMA units.⁴² No influence of dynamic crosslinking on γ transition was observed since this transition is independent of the branching

content. DMTA revealed a linear dependence of crosslink density on β transition (Figure appx 10) since crosslinking creates branched points restricting movement of chains, which increases the temperature of β transitions.^{40, 41} Upon further heating, PE-HEMA and vitrimers **1-4** undergo α transition corresponding to melting of the crystalline phase. While PE-HEMA flows after the melting transition, vitrimers **1-4** display rubbery plateaus with low moduli characteristic of crosslinked materials, which gives also another indication about improved melt strength of those materials. A plateau modulus of vitrimer **4** of around 0.1 MPa was recorded by DMTA however, for softer vitrimers **1-3** with lower crosslink densities, the plateau modulus had to be adapted from rheology temperature sweeps (Figure appx 9) according to Hooke's law $E' = 3G'$ (Figure 10, indicated with arrows).⁴³

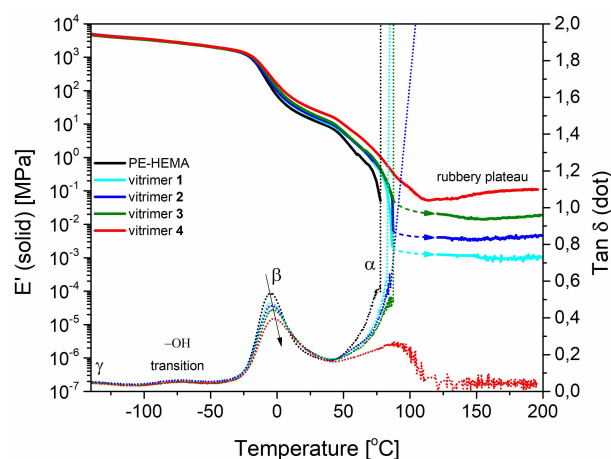


Figure 10. DMTA curves of PE-HEMA and vitrimers **1-4**, storage modulus (E') - solid line, tangent delta ($\tan \delta$) - dot line.

PE-HEMA exhibits tensile properties characteristic of a semicrystalline thermoplastic, displaying an initial elastic deformation before the neck is formed followed by cold drawing and fracture (Figure 11).⁴⁴ Since PE-HEMA has low molecular weight and low crystallinity (Table appx 1), low ultimate strength (2.1 MPa) and Young's modulus (7.4 MPa) were observed. By adding a specific amount of TMSPEDA crosslinker, it was possible to tune tensile properties of PE-HEMA making use of the dynamic crosslinking. As expected, increasing amount of TMSPEDA gradually improved ultimate strength (up to 134 %) and Young's modulus (up to 148 %). On the other hand, vitrimers became more brittle in comparison to PE-HEMA.

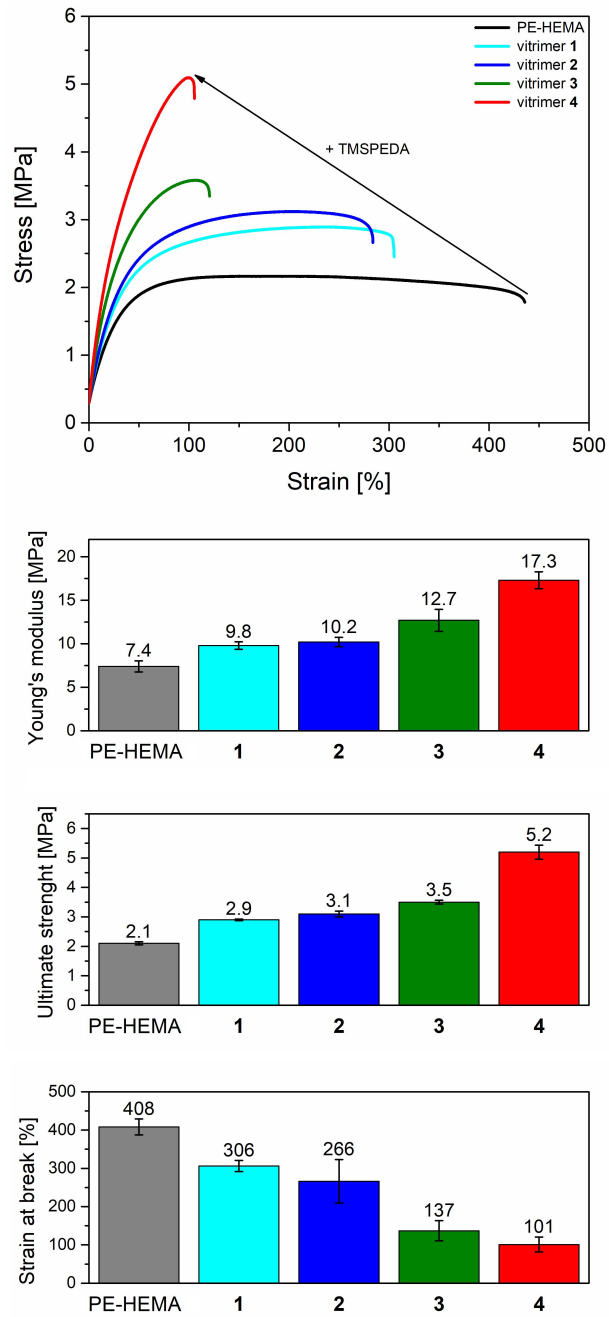


Figure 11. Representative stress-strain curves and Young's modulus, ultimate strength and strain at break of PE-HEMA and vitrimers 1-4.

5.3 Conclusions

PE-based vitrimers were successfully obtained *via* reactive extrusion using commercially available TMSPEDA dynamic crosslinker. This process allowed to produce the vitrimers in a fast and efficient way without using expensive or toxic solvent which makes our process more environmentally friendly and easy to upscale. We demonstrated that thermoplastic PE-HEMA could be transformed into an elastic solid with greatly improved melt strength through the use of dynamic crosslinking. This enhanced property is crucial for processes like film blowing, blow molding, thermoforming and foaming, where permanent covalent crosslinking is often used to achieve the same performance. Additionally, mechanical properties could be tuned by varying the amount of TMSPEDA crosslinker. A gradual improvement of ultimate strength (up to 134 %) and Young's modulus (up to 148 %) was obtained by increasing crosslink density. All prepared vitrimers were insoluble in xylene and were not affected by moisture demonstrating excellent solvent and hydrolysis resistance. Dynamic silyl ether exchange enabled processability and recyclability of this system using industrially relevant techniques like injection and compression molding. Our PE based vitrimer system has a great potential to facilitate the use of vitrimers for commercial applications.

5.4 Experimental section

Materials

Xylene, 1,2-dichlorobenzene (*o*DCB), deuterated chloroform (CDCl₃), deuterated tetrachloroethene (TCE-*d*₂) and Irganox 1010 (98 %) were purchased from Sigma-Aldrich. N,N'-Bis[3-(trimethoxysilyl)propyl]ethylenediamine (TMSPEDA, 95 %,) was purchased from BOC Sciences. PE-HEMA copolymer was kindly provided by SABIC. All materials were used as received unless otherwise stated.

Typical procedure for reactive extrusion of PE-HEMA with TMSPEDA dynamic crosslinker.

PE-HEMA, TMSPEDA and Irganox 1010 (1000 ppm) were mixed in a metal cup and subsequently fed into a 15 mL corotating twin-crew micro extruder. The reaction mixture was processed at 120 °C for 5 min and at 180 °C until the constant viscosity was reached (5-10 min) with a screw speed of 100 RPM after which the discharge valve was opened. The amount of TMSPEDA was determined from the weight ratio of the PE-HEMA and TMSPEDA fed into the extruder.

Measurements

The molecular weight and dispersity were studied by size exclusion chromatography (SEC) measurements performed at 150 °C on a Polymer Char GPC-IR® built around an Agilent GC oven model 7890, equipped with

an autosampler and the Integrated Detector IR4. *o*DCB was used as an eluent at a flow rate of 1 mL/min. The SEC data were processed using Calculations Software GPC One®. The molecular weights were calculated with respect to polyethylene standards.

Melting temperatures (T_m) and enthalpies of the transition (ΔH_m) were measured by differential scanning calorimetry (DSC) using a DSC Q100 from TA Instruments. The measurements were carried out at a heating and cooling rate of 10 °C/min from -20 °C to 150 °C. The transitions were deduced from the second heating.

Tensile tests were performed with a Zwick Z100 tensile tester equipped with a 100 N load cell. The tests were performed on compression molded tensile bars. The samples were pre-stressed to 0.3 MPa, then loaded with a constant cross-head speed of 50 mm/min

Rheology was measured using TA Instruments DHR-2 equipped with parallel plate geometry. Compression molded discs with diameter of 25 mm and thickness of 1 mm were injection molded at 180 °C. Frequency sweeps were measured from 100 to 0.01 rad/s (strain amplitude of 0.4 %) at a temperature of 180 °C. Stress relaxation measurements were performed at 170 °C, 190 °C and 210 °C, applying a step strain of 1 %, then monitoring the stress for 20 000 s.

Dynamical mechanical thermal analysis (DMTA) was measured using TA Instruments Q800 in tensile mode. The specimens were compression molded at 180 °C. Samples were measured from -140 to 200 °C with a heating speed of 3 °C/min and a fixed oscillation (amplitude 10 μ m, frequency 1 Hz).

5.5 Appendix

Table appx 1. Functional group content, melting temperature, degree of crystallinity as well as molecular weight and the molecular weight distribution (\mathcal{D}_M) of PE-HEMA.

Polymer	HEMA content [mol %] ^a	T_m ^b [°C]	T_β ^c [°C]	X_{cr} ^d [%]	M_n ^e [g/mol]	\mathcal{D}_M ^e
PE-HEMA	12.0	73.9	-6,5	1.7	2 900	2.2

^a Functional group content was calculated from the ^1H NMR (120 °C, TCE-*d*₂). ^b Melting temperature (T_m) was determined by DSC from the second heating scan. ^c β transition temperatures (T_β) were determined by DMTA from the maximum of $\tan \delta$. ^d Degrees of crystallinity (X_{cr}) were calculated dividing the melting enthalpy of 100 % crystalline PE (286.2 J/g)³² by melting enthalpy of a vitrimer determined by DSC from the second heating scan. ^e Molecular weight and dispersity were determined by SEC in *o*DCB at 150 °C with respect to polyethylene standards.

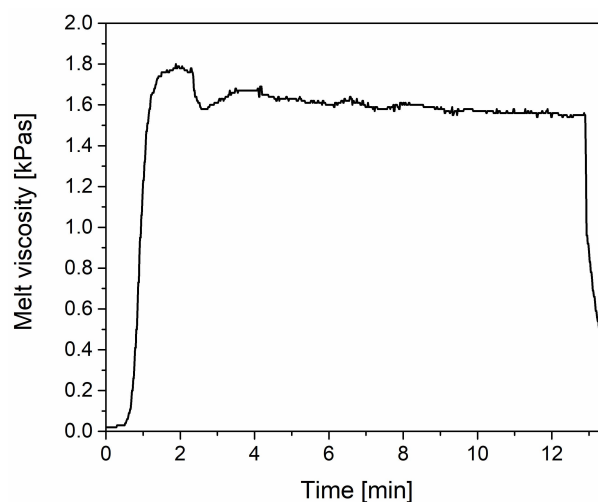


Figure appx 1. Representative melt viscosity changes recorded during the reactive extrusion of vitrimer 2.

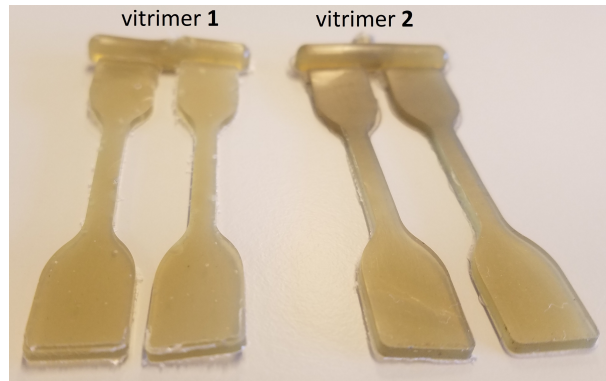


Figure appx 2. Injection molded dog bones of vitrimer 1 and 2, melt temperature 180 °C, mold temperature 80 °C, pressure 10 bar, injection time 10 s.

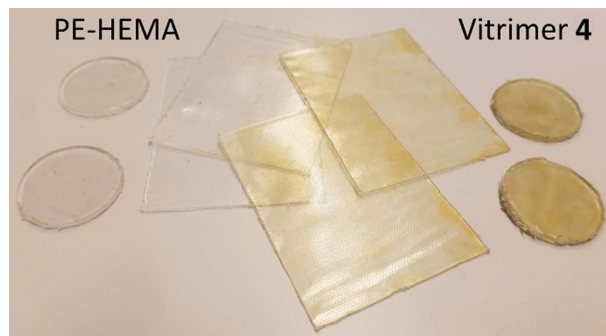


Figure appx 3. Compression molded films and discs for rheology measurement of PE-HEMA and vitrimer 4.

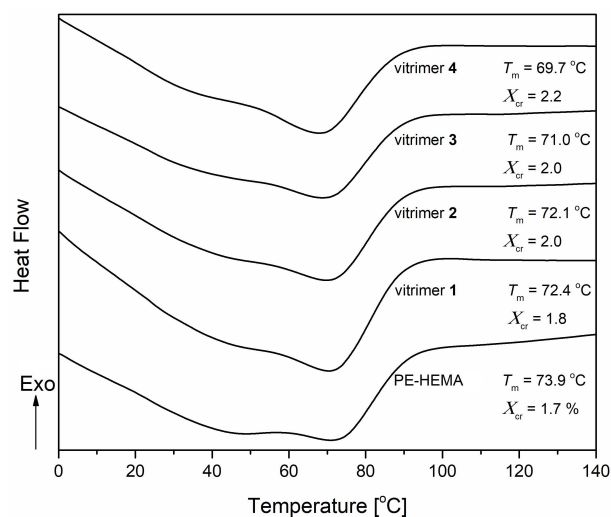


Figure appx 4. DSC second heating curves of PE-HEMA and vitrimers 1-4.

Determination of gel fraction

A small piece (~200 mg) of cross-linked polymers was weighed and placed in a vial to which around 200 mL of xylene was added. The vial was closed and heated at 100 °C for 24 h. After that, the xylene was removed and the remaining undissolved polymer was washed with acetone, dried under vacuum at 80 °C for 24 h and weighed again. Gel fraction was calculated from the mass ratio of the polymer after and before heating in xylene.

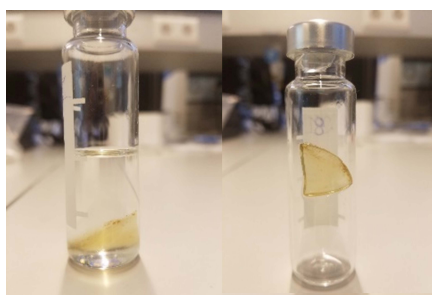


Figure appx 5. Sample of vitrimer 1 after heating in xylene at 100 °C for 24 h before (left) and just after (right) the xylene was removed from the vial.

Table appx 2. Gel fraction of PE-HEMA and vitrimers 1-4.

Polymer	X/C ^a	Before [g]	After [g]	Gel fraction [%]
PE-HEMA	0	0.224	0	0
vitramer 1	3	0.208	0.039	19
vitramer 2	4	0.242	0.061	25
vitramer 3	6	0.242	0.068	28
vitramer 4	9	0.248	0.1	40

^aTheoretical number of crosslinks per chain (X/C) was calculated using M_n of PE-HEMA and the amount of TMSPEDA used assuming that all 6 methoxy groups of TMSPEDA can undergo the reaction with PE HEMA hydroxy groups.

Reprocessability

After the initial tensile test, the tensile bars of vitramer 2 were cut into pieces and compress molded again 4 times. After each reprocessing step tensile test was repeated to evaluate mechanical properties deterioration. Tensile curves of all the samples look very similar and ultimate tensile strength was maintained even after 4th reprocessing cycle.

Resistance to moisture

To investigate the water uptake of PE-HEMA-TMSPEDA vitrimers, samples of around 200 mg were weighed and submerge in deionized water for 24 h. Subsequently, the samples were dried with a paper towel and weighed again. Water uptake was calculated by dividing the initial mass by the mass of absorbed water which was minimal (below 1 %)

Table appx 3. Water uptake of PE-HEMA and vitrimers 1-4.

Polymer	X/C ^a	Before [g]	After [g]	Water uptake [%]
PE-HEMA	0	0.262	0.263	0.38
vitramer 1	3	0.226	0.228	0.88
vitramer 2	4	0.24	0.242	0.83
vitramer 3	6	0.41	0.243	0.83
vitramer 4	9	0.253	0.255	0.79

^aTheoretical number of crosslinks per chain (X/C) was calculated using M_n of PE-HEMA and the amount of TMSPEDA used assuming that all 6 methoxy groups of TMSPEDA can undergo the reaction with PE-HEMA hydroxy groups.

Resistance to hydrolysis was evaluated by measuring gel fraction of samples previously used for water uptake experiment. Gel fraction was not affected by exposure to water.

Table appx 4. Gel fraction of PE-HEMA and vitrimers 1-4 after exposure to water for 24 h at room temperature.

Polymer	X/C ^a	Before [g]	After [g]	Gel fraction [%]	Gel fraction as synthesized [%]
PE-HEMA	0	0.262	0	0	0
vitramer 1	3	0.226	0.043	19	19
vitramer 2	4	0.24	0.061	25	25
vitramer 3	6	0.241	0.07	29	28
vitramer 4	9	0.253	0.104	41	40

^aTheoretical number of crosslinks per chain (X/C) was calculated using M_n of PE-HEMA and the amount of TMSPEDA used assuming that all 6 methoxy groups of TMSPEDA can undergo the reaction with PE-HEMA hydroxy groups.

Additionally, tensile bars of PE-HEMA and vitrimers 1-4 were submerged in deionized water for 24 h at room temperature and subsequently, tensile test of the sample was performed. Mechanical properties remained almost unaltered after submerging samples in water demonstrating excellent moisture resistance. In general, hydrophobic nature of the polymer backbone prohibits swelling and water uptake into the cross-linked network, protecting silyl ethers from hydrolysis.

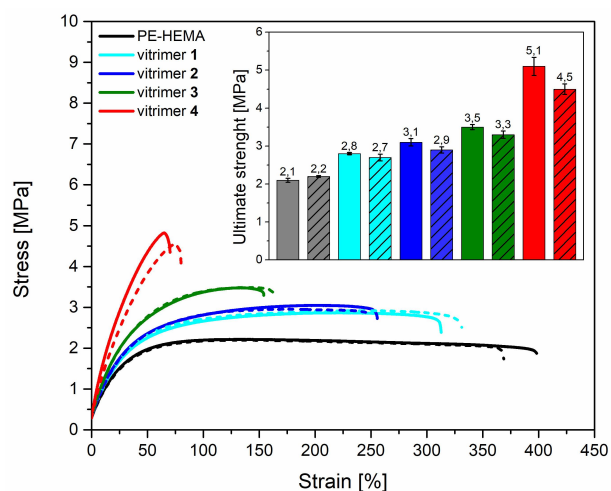


Figure appx 6. Representative tensile curves and ultimate strength (inset) of PE-HEMA and vitrimers 1-4 before and after submerging in water for 24 h at room temperature.

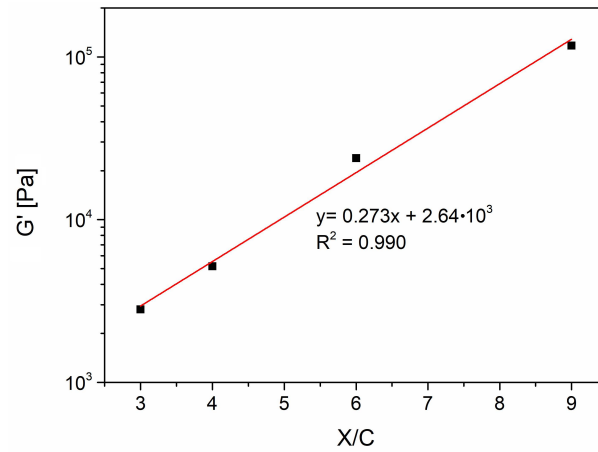


Figure appx 7. Linear relationship between plateau modulus and crosslink density determined by rheology frequency sweep.

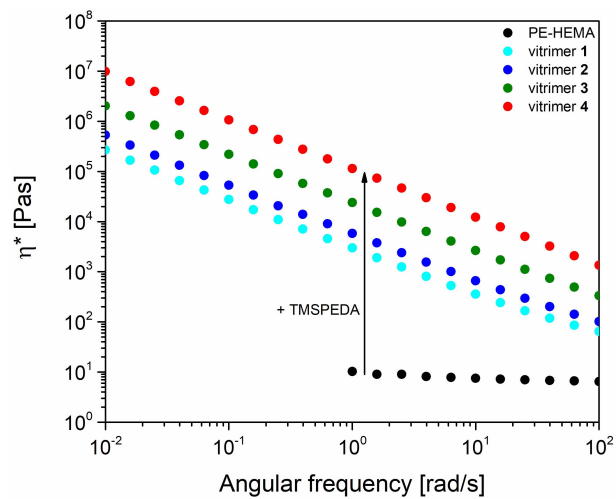


Figure appx 8. Complex viscosity (η^*) dependence on frequency of PE HEMA and vitrimers 1-4 determined by rheology frequency sweeps.

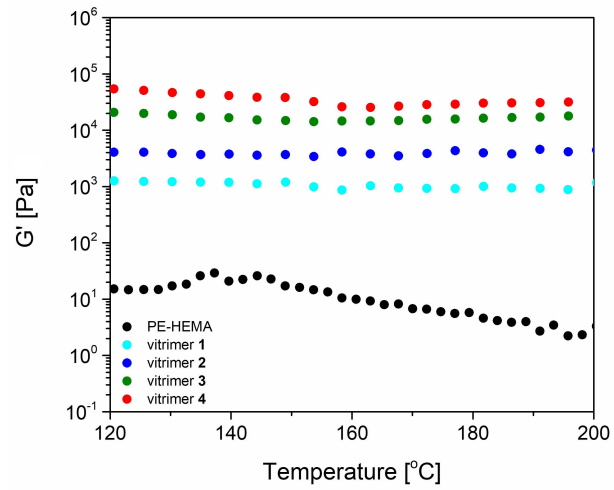


Figure appx 9. Rheology temperature sweep curves at 180 °C of PE-HEMA and vitrimers 1-4.

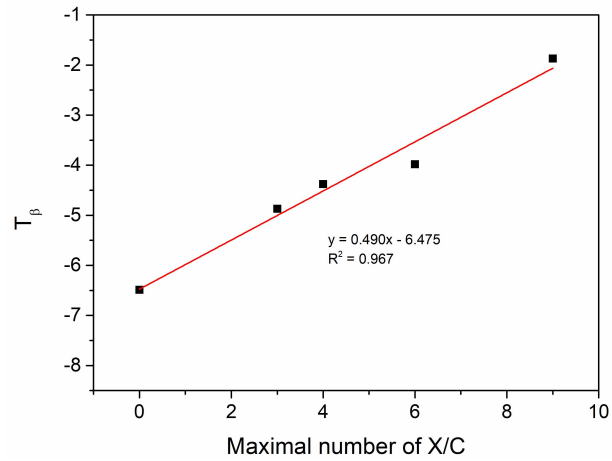


Figure appx 10. Linear relationship between β transition temperature and crosslink density determined by DMTA.

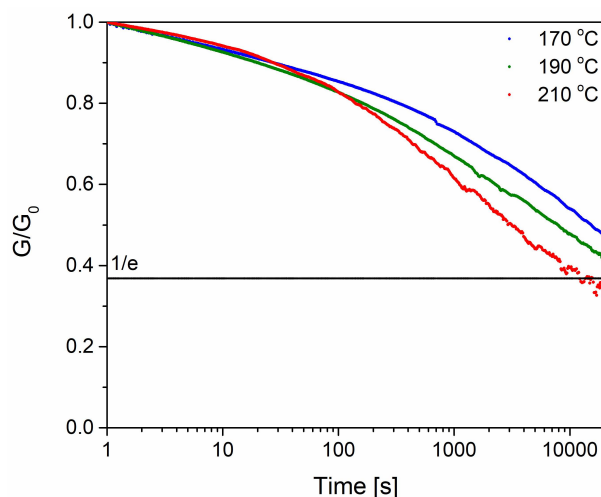


Figure appx 11. Stress relaxation curves of vitrimer 2.

5.6 References

1. Montarnal, D.; Capelot, M.; Tournilhac, F.; Leibler, L. Silica-Like Malleable Materials from Permanent Organic Networks. *Science* **2011**, *334*, 965-968.
2. Capelot, M.; Unterlass, M. M.; Tournilhac, F.; Leibler, L. Catalytic Control of the Vitrimer Glass Transition. *ACS Macro Lett.* **2012**, *1*, 789-792.
3. Denissen, W.; Rivero, G.; Nicolaÿ, R.; Leibler, L.; Winne, J. M.; Du Prez, F. E. Vinylogous Urethane Vitrimers. *Adv. Funct. Mater.* **2015**, *25*, 2451-2457.
4. Denissen, W.; Winne, J. M.; Du Prez, F. E. Vitrimers: Permanent Organic Networks with Glass-Like Fluidity. *Chem Sci* **2016**, *7*, 30-38.
5. Ferry, J. D.; Ferry, J. D., *Viscoelastic Properties of Polymers*. John Wiley & Sons: 1980.
6. Dyre, J. C. Colloquium: The Glass Transition and Elastic Models of Glass-Forming Liquids. *Rev. Mod. Phys.* **2006**, *78*, 953-972.

7. Williams, M. L.; Landel, R. F.; Ferry, J. D. The Temperature Dependence of Relaxation Mechanisms in Amorphous Polymers and Other Glass-Forming Liquids. *J. Am. Chem. Soc.* **1955**, *77*, 3701-3707.
8. Nishimura, Y.; Chung, J.; Muradyan, H.; Guan, Z. Silyl Ether as a Robust and Thermally Stable Dynamic Covalent Motif for Malleable Polymer Design. *J. Am. Chem. Soc.* **2017**, *139*, 14881-14884.
9. Zhou, Y.; Goossens, J. G. P.; Sijbesma, R. P.; Heuts, J. P. A. Poly(Butylene Terephthalate)/Glycerol-Based Vitrimers Via Solid-State Polymerization. *Macromolecules* **2017**, *50*, 6742-6751.
10. Demongeot, A.; Groote, R.; Goossens, H.; Hoeks, T.; Tournilhac, F. o.; Leibler, L. Cross-Linking of Poly (Butylene Terephthalate) by Reactive Extrusion Using Zn (Ii) Epoxy-Vitrimer Chemistry. *Macromolecules* **2017**, *50*, 6117-6127.
11. Denissen, W.; Dreesbeke, M.; Nicolay, R.; Leibler, L.; Winne, J. M.; Du Prez, F. E. Chemical Control of the Viscoelastic Properties of Vinylogous Urethane Vitrimers. *Nat. Commun.* **2017**, *8*, 14857.
12. Stukenbroeker, T.; Wang, W.; Winne, J. M.; Du Prez, F. E.; Nicolay, R.; Leibler, L. Polydimethylsiloxane Quenchable Vitrimers. *Polym. Chem.* **2017**, *8*, 6590-6593.
13. Cromwell, O. R.; Chung, J.; Guan, Z. Malleable and Self-Healing Covalent Polymer Networks through Tunable Dynamic Boronic Ester Bonds. *J. Am. Chem. Soc.* **2015**, *137*, 6492-6495.
14. Rottger, M.; Domenech, T.; van der Weegen, R.; Breuillac, A.; Nicolay, R.; Leibler, L. High-Performance Vitrimers from Commodity Thermoplastics through Dioxaborolane Metathesis. *Science* **2017**, *356*, 62-65.
15. Lu, Y. X.; Tournilhac, F.; Leibler, L.; Guan, Z. Making Insoluble Polymer Networks Malleable Via Olefin Metathesis. *J. Am. Chem. Soc.* **2012**, *134*, 8424-8427.

16. Lu, Y. X.; Guan, Z. Olefin Metathesis for Effective Polymer Healing Via Dynamic Exchange of Strong Carbon-Carbon Double Bonds. *J. Am. Chem. Soc.* **2012**, *134*, 14226-14231.
17. Zheng, P.; McCarthy, T. J. A Surprise from 1954: Siloxane Equilibration Is a Simple, Robust, and Obvious Polymer Self-Healing Mechanism. *J. Am. Chem. Soc.* **2012**, *134*, 2024-2027.
18. Schmolke, W.; Perner, N.; Seiffert, S. Dynamically Cross-Linked Polydimethylsiloxane Networks with Ambient-Temperature Self-Healing. *Macromolecules* **2015**, *48*, 8781-8788.
19. Fortman, D. J.; Brutman, J. P.; Cramer, C. J.; Hillmyer, M. A.; Dichtel, W. R. Mechanically Activated, Catalyst-Free Polyhydroxyurethane Vitrimers. *J. Am. Chem. Soc.* **2015**, *137*, 14019-14022.
20. Zheng, N.; Fang, Z.; Zou, W.; Zhao, Q.; Xie, T. Thermoset Shape-Memory Polyurethane with Intrinsic Plasticity Enabled by Transcarbamoylation. *Angew. Chem. Int. Ed. Engl.* **2016**, *55*, 11421-11425.
21. Fortman, D. J.; Brutman, J. P.; Hillmyer, M. A.; Dichtel, W. R. Structural Effects on the Reprocessability and Stress Relaxation of Crosslinked Polyhydroxyurethanes. *J. Appl. Polym. Sci.* **2017**, *134*, 44984.
22. Obadia, M. M.; Mudraboyina, B. P.; Serghei, A.; Montarnal, D.; Drockenmuller, E. Reprocessing and Recycling of Highly Cross-Linked Ion-Conducting Networks through Transalkylation Exchanges of C-N Bonds. *J. Am. Chem. Soc.* **2015**, *137*, 6078-6083.
23. Hendriks, B.; Waelkens, J.; Winne, J. M.; Du Prez, F. E. Poly(Thioether) Vitrimers Via Transalkylation of Trialkylsulfonium Salts. *ACS Macro Lett.* **2017**, *6*, 930-934.
24. Canadell, J.; Goossens, H.; Klumperman, B. Self-Healing Materials Based on Disulfide Links. *Macromolecules* **2011**, *44*, 2536-2541.
25. Pepels, M.; Pilot, I.; Klumperman, B.; Goossens, H. Self-Healing Systems Based on Disulfide–Thiol Exchange Reactions. *Polym. Chem.* **2013**, *4*, 4955-4965.

26. Martin, R.; Rekondo, A.; Ruiz de Luzuriaga, A.; Cabañero, G.; Grande, H. J.; Odriozola, I. The Processability of a Poly(Urea-Urethane) Elastomer Reversibly Crosslinked with Aromatic Disulfide Bridges. *J. Mater. Chem. A* **2014**, *2*, 5710-5715.
27. Rekondo, A.; Martin, R.; Ruiz de Luzuriaga, A.; Cabañero, G.; Grande, H. J.; Odriozola, I. Catalyst-Free Room-Temperature Self-Healing Elastomers Based on Aromatic Disulfide Metathesis. *Mater. Horiz.* **2014**, *1*, 237-240.
28. Lei, Z. Q.; Xiang, H. P.; Yuan, Y. J.; Rong, M. Z.; Zhang, M. Q. Room-Temperature Self-Healable and Remoldable Cross-Linked Polymer Based on the Dynamic Exchange of Disulfide Bonds. *Chem. Mater.* **2014**, *26*, 2038-2046.
29. Imbernon, L.; Oikonomou, E.; Norvez, S.; Leibler, L. Chemically Crosslinked yet Reprocessable Epoxidized Natural Rubber Via Thermo-Activated Disulfide Rearrangements. *Polym. Chem.* **2015**, *6*, 4271-4278.
30. Gao, W.; Bie, M.; Liu, F.; Chang, P.; Quan, Y. Self-Healable and Reprocessable Polysulfide Sealants Prepared from Liquid Polysulfide Oligomer and Epoxy Resin. *ACS Appl. Mater. Interfaces* **2017**, *9*, 15798-15808.
31. Rutkowski, S.; Zych, A.; Przybysz, M.; Bouyahyi, M.; Sowinski, P.; Koevoets, R.; Haponiuk, J.; Graf, R.; Hansen, M. R.; Jasinska-Walc, L.; Duchateau, R. Toward Polyethylene–Polyester Block and Graft Copolymers with Tunable Polarity. *Macromolecules* **2016**, *50*, 107-122.
32. Wunderlich, B.; Cormier, C. M. Heat of Fusion of Polyethylene. *J. Polym. Sci., Part A-2: Polym. Phys.* **1967**, *5*, 987-988.
33. Cunico, R. F.; Bedell, L. The Triisopropylsilyl Group as a Hydroxyl-Protecting Function. *J. Org. Chem.* **1980**, *45*, 4797-4798.
34. Parrott, M. C.; Luft, J. C.; Byrne, J. D.; Fain, J. H.; Napier, M. E.; DeSimone, J. M. Tunable Bifunctional Silyl Ether Cross-Linkers for the Design of Acid-Sensitive Biomaterials. *J. Am. Chem. Soc.* **2010**, *132*, 17928-17932.
35. Cogswell, F. N., *Polymer Melt Rheology: A Guide for Industrial Practice*. Elsevier: 1981.

36. Deng, G.; Tang, C.; Li, F.; Jiang, H.; Chen, Y. Covalent Cross-Linked Polymer Gels with Reversible Sol– Gel Transition and Self-Healing Properties. *Macromolecules* **2010**, *43*, 1191-1194.
37. Zhou, Y.; Goossens, J. G.; Sijbesma, R. P.; Heuts, J. P. Poly (Butylene Terephthalate)/Glycerol-Based Vitrimers Via Solid-State Polymerization. *Macromolecules* **2017**, *50*, 6742-6751.
38. Ghijssels, A.; De Clippeleir, J. Melt Strength Behaviour of Polypropylenes. *Int. Polym. Proc.* **1994**, *9*, 252-257.
39. Ghijssels, A.; Ente, J.; Raadsen, J. Melt Strength Behavior of Pe and Its Relation to Bubble Stability in Film Blowing. *Int. Polym. Proc.* **1990**, *5*, 284-286.
40. Sauer, J.; Woodward, A. Transitions in Polymers by Nuclear Magnetic Resonance and Dynamic Mechanical Methods. *Rev. Mod. Phys.* **1960**, *32*, 88.
41. Martín, S.; Vega, J. F.; Expósito, M. T.; Flores, A.; Martínez-Salazar, J. A Three-Phase Microstructural Model to Explain the Mechanical Relaxations of Branched Polyethylene: A Dsc, Waxd and Dmta Combined Study. *Colloid. Polym. Sci.* **2011**, *289*, 257-268.
42. Pathmanathan, K.; Johari, G. Dielectric and Conductivity Relaxations in Poly (Hema) and of Water in Its Hydrogel. *J. Polym. Sci., Part B: Polym. Phys.* **1990**, *28*, 675-689.
43. Varga, Z.; Filipcsei, G.; Zrínyi, M. Magnetic Field Sensitive Functional Elastomers with Tuneable Elastic Modulus. *Polymer* **2006**, *47*, 227-233.
44. Xu, M.-m.; Huang, G.-y.; Feng, S.-s.; McShane, G. J.; Stronge, W. J. Static and Dynamic Properties of Semi-Crystalline Polyethylene. *Polymers* **2016**, *8*, 77.

Chapter 6

Conclusions and outlook

The objective of this thesis was to explore properties and potential applications of PE crosslinked using reversible supramolecular or dynamic adaptable covalent crosslinkers.

As an example of supramolecular crosslinker, ureidopyrimidinone quadruple hydrogen bonding was incorporated into various PEs bearing hydroxy groups. Reactive extrusion process was developed allowing to significantly shorten the reaction time, eliminate the use of solvents and catalysts and make upscaling and commercial production feasible. Incorporation of UPy physical crosslinks into PE matrix changed the rheology of a typical entangled thermoplastic melt to that of an elastic crosslinked system. Significantly increased melt strength was observed, which is extremely important for processes like film blowing, blow molding, thermoforming and foaming. Moreover, greatly improved toughness and ultimate tensile strength were achieved without sacrificing elongation at break or Young's modulus. Identified thermal stability limit of those materials allowed for a safe processing, using techniques like compression molding and extrusion. To the best of our knowledge this is the first example of improving mechanical properties of polyethylene utilizing supramolecular interactions and it has a great potential for expanding applications of this commodity thermoplastic even further.

Pyrene π - π stacking was introduced into high density and very low density polyethylene-*graft*-maleic anhydride in an efficient and practical way by means of reactive extrusion. Both polymers functionalized with pyrene showed pronounced fluorescence changes under stress which could be correlated to their different tensile properties. For high density polyethylene containing pyrene, around 50 % drop of the excimer content (I_E/I_M) was observed when the elongation exceeded 50 % which could be related to a neck formation. In contrast, very low density polyethylene containing pyrene showed no necking and a linear decrease of the excimer content (I_E/I_M) with elongation up to 1100 %. Moreover, the resulting strain-reporting PE retains similar mechanical, thermal and rheological properties to that of the starting PE-MAH materials. The results demonstrate a significant potential for the development of a strain-reporting PE directly *via* reactive extrusion which can allow for detection of microcracks and fatigue possible making PE more reliable.

Oxygen and water vapor permeability of PE samples functionalized with UPy and pyrene were analyzed. Both UPy quadruple hydrogen bonding and MIP π - π stacking were able to improve oxygen and water vapor barrier up to 40 %. Despite the achieved improvements, the samples performed worse than commercial multilayer solution. The poor performance can be explained by decreased crystallinity when polyethylene is functionalized. As a consequence, diffusivity through more amorphous polyethylene is increased compromising both oxygen and water vapor barrier properties. This effect is only partially compensated by the increase cohesive interactions between the PE chains thanks to the hydrogen bonding of UPy or π - π

interactions of MIP. Nevertheless, achieved improvements give hope that it is indeed possible to develop a single layer packaging material with high oxygen barrier properties that is not sensitive to humidity. It is of great importance from the environmental point of view to enable recycling of packaging materials and extend shelf life of food which prevents wastage.

PE vitrimers were successfully obtained *via* reactive extrusion using commercially available TMSPEDA dynamic crosslinker. This process allowed to produce PE vitrimers in a fast and efficient way without the need to use expensive or toxic solvents, which makes it environmentally friendly and easy to upscale. Dynamic crosslinking transformed thermoplastic PE into an elastic solid with greatly improved melt strength which is extremely important for processes like film blowing, blow molding, thermoforming and foaming. Mechanical properties could be tuned by varying the amount of TMSPEDA crosslinker. Increasing crosslink density gradually improved ultimate strength and Young's modulus however, the materials became more brittle. All prepared vitrimers were not completely soluble in xylene and were not affected by moisture, demonstrating crosslinked character and improved solvent and hydrolysis resistance which is of great important for industrial applications like water pipes and electrical cables insulation. Despite the crosslink nature, dynamic silyl ether exchange enabled processability and recyclability of this system using industrially relevant techniques like injection and compression molding. This process is applicable not only for PE but also for any thermoplastic bearing hydroxy functional groups.

In general, crosslinking both *via* supramolecular and dynamic covalent interactions gives PE unique properties not available otherwise for this

commodity thermoplastic. All aforementioned solutions have a great potential to find commercially relevant applications and expand the PE market.

Acknowledgements

I would like to thank the European Union and Horizon 2020 Maria Skłodowska-Curie action for founding my PhD. I would like to thank all the people that helped me during my PhD study and contributed to this thesis. My supervisor from SABIC Jerome Vachon for great mentoring, advices, new ideas and discussions, help with manuscripts, that he always had time for me and of course for the football matches. Prof. Enrico Dalcanale and Prof. Roberta Pinalli from the University of Parma for the supervision, advices, discussions, help with manuscripts and managing of the SupraBarrier project. My colleague from the SupraBarrier project Jonathan Tellers for discussions, exchange of ideas, two tough months in India and that there was always someone to complain to. My brother Mateusz for proofreading the thesis. My master student Alice Verdelli for a great amount of experimental work performed during her master project. Maria Soliman, Estelle Poulet, Deliani Lovera for the managing and support of the Suprabarrier project at SABIC. Peter Neuteboom, Diego Castaneda, Jan Duchateau from LDPE team for providing PE-HEMA and PE-MAH polymers. Brian Marwi, Maurice Wijers, Maurice Dohmen, Jos Verhaeren from the processing laboratory. Analytical team from BOZ for NMR, IR, TGA and elemental analysis. Dhanabalan Anantharaman, Abbas Shaikh, Sunil Erath, Rukmini Khatokar and the whole team from STC Bangalore. Group of Prof. Oren Scherman for two months at the University of Cambridge. Group of Prof. Rint Sijbesma for two Months at Technical University Eindhoven.

Curriculum Vitae

Arkadiusz Zych was born on the 2nd of December 1989 in Gdańsk, Poland. In 2014 he graduated from Gdańsk University of Technology in Poland with Bachelor Degree of Engineer in chemistry followed by Master degree in Chemical technology with specialization in Organic Technology. He completed the master project funded by Foundation for Polish Science (Homing Plus Program), on renewable polyamides. Results of this project have been presented at the European Polymer Congress in Pisa, Italy and published in Polymer chemistry journal. During the final year of his master he performed an internship at the Technology and Innovation Center of SABIC in Geleen, the Netherlands. The research project was directed to the synthesis and characterization of novel polyolefins with special properties and resulted in one publication in Macromolecules and two patent applications. In 2015 he started Maria Skłodowska-Curie industrial PhD at the University of Parma, Italy and SABIC, Geleen, the Netherlands including two months secondments at Eindhoven Technical University, the Netherlands, University of Cambridge, England and SABIC research center in Bangalore, India. The main results obtained during this PhD are presented in this thesis.



List of publications and patents

So far, this thesis has resulted in the following publications:

Peer-reviewed journal publications:

A. Zych, A. Verdelli, M. Soliman, R. Pinalli, A. Pedrini, J. Vachon, E. Dalcanale, Strain-reporting pyrene-grafted polyethylene, Strain-reporting pyrene-grafted polyethylene, *Eur. Pol. J.*, **2019**, 111, 69-73.

A. Zych, A. Verdelli, M. Soliman, R. Pinalli, J. Vachon, E. Dalcanale, Reactive extrusion of ureidopyrimidinone functionalized polyethylene with enhanced mechanical properties, *submitted to Polym. Chem.*

A. Zych, A. Soliman, R. Pinalli, J. Vachon, E. Dalcanale, Reactive extrusion of polyethylene vitrimers based on silyl ether exchange, *to be submitted.*

Patent applications:

Zych, J. Tellers, M. Soliman, R. Pinalli, J. Vachon, E. Dalcanale, Gas barrier film, 16POLY0166

Zych, J. Tellers, M. Soliman, R. Pinalli, J. Vachon, E. Dalcanale, Silyl ether vitrimers, patent application in preparation.

Other peer-reviewed journal publications related to the author:

S. Rutkowski, A. Zych, M. Przybysz, M. Bouyahyi, P. Sowinski, R. Koevoets, J. Haponiuk, R. Graf, M. R. Hansen, L. Jasinska-Walc, Toward

Polyethylene-Polyester Block and Graft Copolymers with Tunable Polarity. *Macromolecules* **2017**, *50* (1), 107-122.

A. Wroblewska, A. Zych, S. Thiyagarajan, D. Dudenko, D. van Es, M. R. Hansen, C. Koning, R. Duchateau, L. Jasinska-Walc, Towards sugar-derived polyamides as environmentally friendly materials. *Polym. Chem.* **2015**, *6* (22), 4133-4143.

Other patent applications related to the author:

L. Jasinska-walc, M. Bouyahyi, R. Duchateau, L. S. Rutkowski, A. Zych, Process for the preparation of a block copolymer comprising a first polyolefin block and a second polymer block and the products obtained therefrom, US20170349710A1.

L. Jasinska-walc, R. Duchateau, M. Bouyahyi, L. S. Rutkowski, S. V. Kulangara, A. Zych, A process for the preparation of a graft copolymer comprising a polyolefin main chain and one or a multiple polymer side chains and the products obtained therefrom, US20170320989A1.